Genetic and Molecular Basis of Encapsulation and Capsule Diversity in *Kingella kingae*

by

Kimberly Freeland Starr

Department of Molecular Genetics and Microbiology
Duke University

Date:_____

Approved:

_____
Joseph W. St. Geme III, Co-Supervisor

_____
Patrick C. Seed, Co-Supervisor

_____
Raphael H. Valdivia

_____
Margarethe J. Kuehn

_____
Jörn Coers

Dissertation submitted in partial fulfillment of
the requirements for the degree of Doctor
of Philosophy in the Department of
Molecular Genetics and Microbiology in the Graduate School
of Duke University

2016

ABSTRACT

Genetic and Molecular Basis of Encapsulation and Capsule Diversity in *Kingella kingae*

by

Kimberly Freeland Starr

Department of Molecular Genetics and Microbiology
Duke University

Date:_____
Approved:

_____
Joseph W. St. Geme III, Co-Supervisor

_____
Patrick C. Seed, Co-Supervisor

_____
Raphael H. Valdivia

_____
Margarethe J. Kuehn

_____
Jörn Coers

An abstract of a dissertation submitted in partial
fulfillment of the requirements for the degree
of Doctor of Philosophy in the Department of
Molecular Genetics and Microbiology in the Graduate School of
Duke University

2016

Abstract

Kingella kingae is a bacterial pathogen that is increasingly recognized as an etiology of septic arthritis, osteomyelitis, bacteremia, and endocarditis in young children. The pathogenesis of *K. kingae* disease starts with bacterial adherence to the respiratory epithelium of the posterior pharynx. Previous work has identified type IV pili and a trimeric autotransporter protein called Knh (*Kingella* NhhA homolog) as critical factors for adherence to human epithelial cells. Additional studies established that the presence of a polysaccharide capsule interferes with Knh-mediated adherence. Given the inhibitory role of capsule during adherence we sought to uncover the genes involved in capsule expression to understand how capsule is elaborated on the cell surface. Additionally, this work aimed to further characterize capsule diversity among *K. kingae* clinical isolates and to investigate the relationship between capsule type and site of isolation.

We first set out to identify the carbohydrates present in the *K. kingae* capsule present in the prototype strain 269-492. Glycosyl composition and NMR analysis of surface extractable polysaccharides demonstrated two distinct polysaccharides, one consisting of GalNAc and Kdo with the structure →3)-β-GalpNAc-(1→5)-β-Kdop-(2→ and the other containing galactose alone with the structure →5)-β-Galf-(1→.

To discern the two polysaccharides we disrupted the *ctrA* gene required for surface localization of the *K. kingae* polysaccharide capsule and observed a loss of GalNAc and Kdo but no effect on the presence of Gal in bacterial surface extracts. In contrast, deletion of the *pamABCDE* locus involved in production of a reported galactan exopolysaccharide eliminated Gal but had no effect on the presence of GalNAc and Kdo in surface extracts. These results established that *K. kingae* strain KK01 produces a polysaccharide capsule with the structure →3)-β-GalpNAc-(1→5)-β-Kdop-(2→ and a separate exopolysaccharide with the structure →5)-β-Galf-(1→.

Having established that *K. kingae* produces a capsule comprised of GalNAc and Kdo, we next set out to identify the genetic determinants of capsule through a transposon mutagenesis screen. In addition to the previously identified *ctrABCD* operon, *lipA*, *lipB*, and a putative glycosyltransferase termed *csaA* (capsule synthesis region A gene A) were found to be essential for the production of surface-localized capsule. The *ctr* operon, *lipA, lipB,* and *csaA* were found to be present at unlinked locations throughout the genome, which is atypical for gram-negative organisms that elaborate a capsule dependent on an ABC-type transporter for surface localization. Through examining capsule localization in the *ctrA*, *lipA*, *lipB,* and *csaA* mutant strains, we determined that

the *ctrABCD*, *lipA*/*lipB,* and *csaA* gene products respectively function in capsule export, assembly, and synthesis, respectively. The GalNAc transferase and Kdo transferase domains found in CsaA further support its role in catalyzing the synthesis of the GalNAc-Kdo capsule in the *K. kingae* prototype strain.

To investigate the capsule diversity that exists in *K. kingae* we screened a panel of strains isolated from patients with invasive disease or healthy carriers for the *csaA* capsule synthesis locus. We discovered that *Kingella kingae* expresses one of 4 capsule synthesis loci (csa, csb, csc, or csd) associated with a capsule consisting of Kdo and GalNAc (type a), Kdo and GlcNAc (type b), Kdo and ribose (type c), and GlcNAc and galactose (type d), respectively. Cloning of the *csa*, *csb*, *csc,* or *csd* locus into the empty flanking gene region in a non-encapsulated mutant (creation of an isogenic capsule swap) was sufficient to produce either the type a, type b, or type c capsule, respectively, further supporting the role of these loci in expression of a specific polysaccharide linkage. Capsule type a and capsule type b accounted for 96% of invasive strains. Conversely, capsule type c and capsule type d were found disproportionately among carrier isolates, suggesting that capsule type is important in promoting invasion and dissemination.

In conclusion, we discovered that *Kingella kingae* expresses a polysaccharide capsule and an exopolysaccharide on its surface that require distinct genetic loci for surface localization. Further investigation into genetic determinants of encapsulation revealed the loci *ctrABCD*, *lipA*/*lipB*, and a putative glycosyltransferase are required for capsule expression, with the gene products having roles in capsule export, assembly, and synthesis, respectively. The putative glycosyltransferase CsaA was determined to be a bifunctional enzyme with both GalNAc-transferase and Kdo-transferase activity. Furthermore, we discovered a total of 4 capsule types expressed in clinical isolates of *K. kingae*, each with a distinct capsule synthesis locus. The variation in the proportion of capsule types found between invasive strains and carriage strains suggest that capsule type is important in promoting invasion and dissemination. Taken together, this work expands our knowledge of the capsule types expressed among *K. kingae* carrier and invasive isolates and provides insights into the common genetic determinants of capsule expression. These contributions may lead to selecting clinically relevant capsule types to develop into a capsule based vaccine to prevent *K. kingae* colonization.

Dedication

I dedicate this work to my husband, George (Joey), and my son, Jacob, the two most important people in my life.

Contents

List of Tables

List of Figures

Acknowledgements

I first need to thank my advisor and mentor Dr. Joseph St. Geme III for providing me the opportunity to join his wonderful lab and complete my graduate work. He was always my biggest supporter and made me feel like I could do great things. He not only encouraged me to conduct rigorous scientific research, but also to focus on publishing and presenting whenever possible. His optimism never wavered and was a much needed during difficult experiments. Even from a distance, he was always there when I need advice or encouragement. Next I have to thank Eric Porsch for getting me to see the joys of working with *Kingella*. He was a great mentor, teacher, and a constant sounding board to bounce ideas off of pertaining to science or an AMC television series. I learned a lot about drafting manuscripts due to his critical eye for writing and editing. A special thanks to Sue Grass, Jessica McCann, and Brad Kern for being great lab mates and contributing a wonderful working environment where we challenged one another scientifically but also had fun doing it. Thanks to Katherine Rempe for going through this Graduate School journey with me and being my committee meeting buddy. Thanks to the Seed Lab members for a great lab environment in which I loved coming to work every day. I'd also like to thank our collaborators at the Complex Carbohydrate Research Center for their

intellectual contributions to our publications and for all the things I learned from them.

My committee members, Dr. Pat Seed, Dr. Raphael Valdivia, Dr. Meta Kuehn, and Dr. Jörn Coers provided valuable insight and suggestions for my work in our frequent committee meetings. I would like to thank Dr. St. Geme for sacrificing his time to fly to NC to attend every single one. I would also like to thank Dr. Seed for taking on an increasingly active mentoring role during the second half of my studies. I want to also thank the DSMM mentors for selecting me to participate in the Duke Scholars in Infectious Diseases Program. This program opened my eyes to a new way of looking at important problems and identifying new ways to tackle them. I'd like to thank Dr. Kevin Hazen for his valuable career advice and answering my endless questions about the world of clinical microbiology.

I would like to thank my parents who always encouraged me to set goals and attain them, while never doubting my determination. I would last like to thank my husband for the patience and encouragement he has shown me through this process.

1. Introduction

1.1 Kingella history and classification

Kingella kingae was first isolated by Elizabeth King at the Centers for Disease Control and Prevention in 1960. Initial studies suggested that this organism was a novel *Moraxella* species but further investigation warranted reclassification and renaming to *Kingella kingae* in 1976 (Bovre et al. 1974, Henriksen et al. 1976). Using traditional culture based techniques, *K. kingae* was rarely isolated from sites of disease, but the arrival of novel culture based techniques in the 1990s and subsequent culture-independent techniques resulted in an increase in reported cases of *K. kingae* infection among young children (Yagupsky et al. 1995). Numerous studies using PCR based diagnostics have demonstrated the presence of *Kingella kingae* present in bone and joint fluid from suspected cases of osteomyelitis and septic arthritis that were culture negative by traditional culture based diagnostics (Stahelin et al. 1998, Yagupsky 1999, Cherkaoui et al. 2009). More recent studies support that *K. kingae* is a leading cause of bone and joint infections in young children age 6-48 months of age. Currently *K. kingae* is recognized as a leading cause of septic arthritis and

osteomyelitis in young children, with a similar rate of infection as *Staphylococcus aureus (Chometon et al. 2007)*.

1.2 Microbiology

K. kingae is a gram negative, β-hemolytic bacterium in the family Neisseriaceae. It is a small bacillus that usually appears in pairs or short chains (Henriksen et al. 1968). It is facultatively anaerobic and grows best on blood and chocolate agar with the addition of 5-10% CO2. When grown on chocolate agar, *K. kingae* exhibits 3 colony morphologies: spreading/corroding, non-spreading/non-corroding, and domed (Kehl-Fie et al. 2010). The spreading/corroding colony type develops a peripheral fringe around the small central raised colony and is associated with a high level of piliation. The non-spreading/non-corroding colony has a smaller fringe with a large, flat, central colony and is associated with low levels of piliation. The domed colony produces no fringe and lacks pili (Kehl-Fie et al. 2010).

1.3 Epidemiology

1.3.1 Clinical manifestations

K. kingae is a human commensal that colonizes the posterior pharynx asymptomatically, prior to spreading to the bloodstream to cause invasive disease in a subset of children. *K. kingae* is an increasingly common cause of bone and joint infections, bacteremia, and endocarditis (Yagupsky et al. 2011). Cases of *K. kingae* septic arthritis typically present in large joints, including the shoulder, hip, or knee, but may also include the smaller metacarpophalangeal, sternoclavicular, and tarsal joints (Yagupsky et al. 2002, Yagupsky 2004, Dubnov-Raz et al. 2008). Similarly, cases of osteomyelitis caused by *K. kingae* typically affect the long bones, including the femur, the tibia, and the humerus. Other important sites of infection include the clavicle, sternum, calcaneus, and talus (Yagupsky et al. 2002, Dubnov-Raz et al. 2008). Less frequently, *K. kingae* is seen in cases of diskitis, absesses, and meningitis (Morrison et al. 1989).

1.3.2 Carriage and transmission

The first step in the pathogenesis of disease is believed to be asymptomatic colonization of the posterior pharynx. Isolates recovered from the bloodstream as well as the site of invasive disease have been found to be genotypically identical to the strain recovered from the pharynx, supporting the hypothesis that colonization of the pharynx is the first step in pathogenesis (Yagupsky et al. 2009). However, the presence of *K. kingae* in the pharynx is almost nonexistent before 6 months of age, and is only present in approximately 1.5% of healthy children at 6 months. At 12 months of age the rate of carriage increases to 9.6% and remains stable between 10.4% and 12.0% during the second year of life, before decreasing significantly to 5.3% at 30 months (Amit et al. 2014). The timeline of peak colonization is inversely correlated with the lowest levels of IgG and IgA against *K. kingae* surface epitopes in serum (Slonim et al. 2003). As children age, the carriage rate decreases, suggesting that a maturing immune system may mediate clearance of *K. kingae* from the pharynx. The persistence and dissemination of respiratory organisms such as *K. kingae* are dependent on person-to-person transmission (Yagupsky 2015). *K. kingae* spreads easily through large droplet transmission among young children with typical

hygienic habits who share toys contaminated with respiratory secretions or saliva in locations including households and daycare centers (Yagupsky 2015).

1.3.3 Daycare attendance

Several studies have concluded that daycare center attendance is associated with an increased risk of *K. kingae* transmission (Slonim et al. 1998, Kiang et al. 2005, Yagupsky et al. 2006). Yagupsky et al. reported a longitudinal surveillance study performed over an 11-month period that found 73% of children age 6-42 months attending daycare carried *K. kingae* at least once, and 6-35% of children were colonized with *K kingae* in the pharynx at any given time throughout the study (Yagupsky et al. 1995). Molecular methods confirmed the genotypic similarities between circulating strains, suggesting person-to-person transmission among daycare attendees. A further study into the relatedness of pharyngeal isolates from a large cohort of young healthy carriers revealed geographic clustering of related isolates in households and neighborhoods, indicating transmission of *K. kingae* between siblings and playmates (Yagupsky et al. 2009). Colonization is described as a dynamic process, with a given strain colonizing a child for months, followed by frequent turnover of colonizing

strains. A subset of isolates found in healthy colonized children were identical to isolates taken from patients with invasive disease, suggesting that colonizing strains can persist among communities and are potentially virulent (Yagupsky et al. 2009).

1.3.4 Population structure of *Kingella kingae*

K. kingae exhibits genetic heterogeneity (Yagupsky et al. 2009). However, it has been observed that a limited number of distinct clones cause the majority of invasive infections and exhibit genetic stability, long-term persistence, and wide geographic dispersal. The dynamics of carriage of *K. kingae* have been studied in longitudinal studies in which the target population is sampled over a prolonged period of time, and the isolates are analyzed using highly discriminative typing methods (Yagupsky 2014). Significant clustering of genotypic clones in households and neighborhoods has been observed, indicating person-to-person transmission through intimate contact. One study of the *K. kingae* population structure found distinctions between the clones found in healthy carriers making up two ethnic communities in Israel. This study also discovered that the isolated

organisms were identical to historical isolates recovered over the last 15 years from carriers or patients with invasive disease (Yagupsky et al. 2009).

Analysis of the clonal groups associated with invasive disease revealed an association between clonal groups and specific clinical syndromes. Recently a study in Israel looking at PFGE analysis of 181 strains collected over a 21-year period established that a limited number of distinct clones cause the majority of invasive infections. This study, which assessed the relative frequency and invasiveness of various strains, found a total of 32 different *K. kingae* clones identified by PFGE, of which 5 (B, H, K, N, and P) caused 72.9% of all invasive infections. *K. kingae* strains collected over this period in this region showed significant association with specific clinical syndromes, including bacteremia, skeletal system infections, and endocarditis. Clone K was significantly associated with bacteremia, clone N was associated with skeletal system infections, and clone P was associated with bacterial endocarditis (Amit et al. 2012).

1.4 Pathogenesis of K. kingae infection

Pathogenesis begins with asymptomatic colonization of the posterior pharynx. Following attachment, the bacterium breaches the respiratory epithelium and gains access to the bloodstream, likely through the action of an

RTX toxin (Kehl-Fie et al. 2007). After entering the bloodstream, *Kingella* can disseminate to the joints, bones, or endocardium to cause invasive disease. Attachment to host cells is influenced by the interrelationship of Knh, Type IV pili, and a capsule polysaccharide. Knh (Kingella NhhA homolog) is a trimeric autotransporter that is required for full adherence to epithelial cells (Porsch et al. 2012). It has been shown that *K. kingae* expresses a polysaccharide capsule that masks the adherence conferred by Knh in the absence of pili (Porsch et al. 2012). Type IV pili are long adhesive fibers that reach beyond the length of capsule, bind to their host cell receptor, and retract, bringing the bacterium into close contact with the epithelial cell (Porsch et al. 2012). These fibers can have numerous functions, including adherence, natural competence, twitching motility, gliding motility, and microcolony formation. The pilus is made of multimers of the major pilin subunit, PilA1, and these fibers can reach 5-9 nm diameter and several micrometers in length (Strom et al. 1993, Porsch et al. 2012).

Attachment is thought to be a two-step process. The first step is mediated by type IV pili that adhere to the epithelial surface and engage their host cell receptor. Pilus retraction brings the bacterium in close contact with the host cell, causing a displacement of capsule. Once the capsule is displaced, Knh is

unmasked and binds its host receptor, initiating a secondary binding event. It has been shown that type IV pili are important to overcome the polysaccharide capsule and facilitate Knh-mediated adherence when the retraction machinery PilT/PilU are present (Porsch et al. 2012).

1.5 Extracellular polysaccharides

Bacterial cells express two types of polysaccharides near the cell surface: capsule and exopolysaccharide. These extracellular carbohydrate polymers are expressed by both gram-positive and gram-negative bacteria and can vary in structure, linkage, synthesis, and function. Extracellular polysaccharides are produced by many pathogenic bacteria and function as important virulence factors (Nizet et al. 2009). These polysaccharides can be categorized generally as surface-anchoredcapsular polysaccharides or excreted exopolysaccharides.

1.5.1 Capsule polysaccharides

Capsule is a layer of surface-associated polysaccharides that is the outermost covering of bacteria cells. Capsules are responsible for producing the

mucoid appearance to bacterial colonies grown on laboratory solid agar media (Allegrucci et al. 2007). Capsular polysaccharides are lipid-anchored outer membrane-associated carbohydrates and are involved in protection from host immune mechanisms, including phagocytosis and complement-mediated killing (Roberts 1996, Corbett et al. 2010). The capsule also functions as a shield to mask underlying cell surface structures as seen in *Neisseria* species and *Kingella kingae* (Criss et al. 2012*)*. Capsule has been shown to reduce both the assembly and effectiveness of the membrane attack complex and the level of opsonization (Wilson et al. 2011). While capsules function to shield the bacterial cell from innate defenses (Merino et al. 2001), there is increasing evidence that capsular polysaccharides may possess immunomodulatory activities, including modulating the local inflammatory response of epithelial cells in order to maximize bacterial colonization and prevent immune system activation (Dasgupta et al. 2010, Rose et al. 2011, Maue et al. 2013). Polysaccharide capsules exhibit a large degree of variation within a single bacterial species, with examples including *Escherichia coli*, *Streptococcus pneumoniae, and Klebsiella pneumoniae* (Orskov et al. 1977, Riser et al. 1981, Kalin 1998). In select cases, a

specific capsule type can be associated with increased virulence potential, as highlighted by *Haemophilus influenzae* type b (Turk 1984, Jacobs et al. 1998).

In recent work, we identified a polysaccharide capsule in *K. kingae* strain 269–492 that influences adhesive interactions with host cells and is dependent upon the *ctrABCD* ABC-type capsule export operon for surface localization similar to the export operon of *N. meningitidis* (Porsch et al. 2012). The genetic organization of the meningococcal capsule locus is shown in Figure 1.

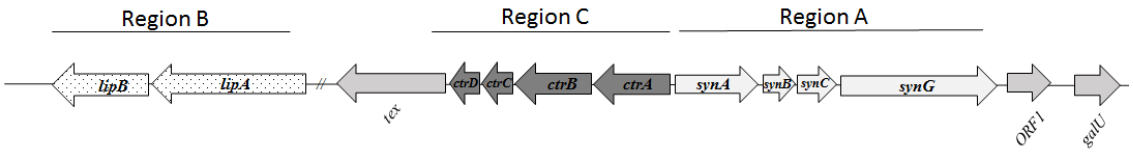

Figure 1: Genetic organization of the meningococcal W-135 capsule locus.

The genes in region A encode enzymes for biosynthesis of the capsular polysaccharide, and the genes in regions B and C are implicated in the translocation of the high molecular weight polysaccharides to the cell surface. Figure adapted from (Harrison et al. 2013)

The *ctrABCD* locus in *Kingella kingae* is also homologous to the capsule gene complexes of other bacteria expressing group 2 capsules, including *E. coli* and *H. influenzae*. The genetic organization of group 2 capsules are made up of three functional regions, which have been thoroughly characterized in *E. coli*. In *E.coli*, Regions 1 and 3 containing the genes involved in capsule export and

assembly are conserved between organisms expressing the group 2 capsule and flank Region 2, which encodes species- and serotype-specific biosynthesis genes (Roberts 1996, Clarke et al. 1999, Whitfield 2006). A model for biosynthesis and assembly of group 2 capsules in *E. coli* is shown in Figure 2.

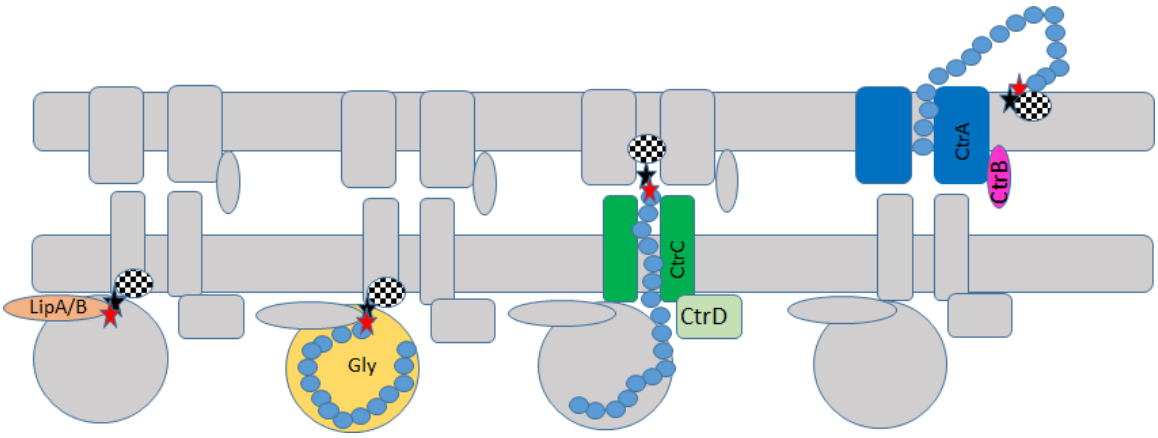

Figure 2: A model for biosynthesis and assembly of group 2 capsules

A Kdo residue (represented by the black star) is added to diacylglycerophosphate (checkerboard pattern circle) by LipB. Several Kdo residues are then added by LipA (red star). The polymer is extended by glycosyltransferases (yellow circle), adding residues to the nonreducing terminus of the chain. The polymer is exported via the ABC transporter (CtrABCD). Figure adapted from (Whitfield 2006, Willis et al. 2013)

Initiation of group 2 capsule synthesis begins with the addition of an initial kdo residue to diacylglycerophosphate by LipB, a retaining-kdo transferase (Willis et al. 2013). Additional (2-7) Kdo residues are then added by LipB. Capsule-type-specific glycosyltransferases add repeating units of the

capsule backbone, before export through the CtrABCD capsule export machinery.

1.5.2 Exopolysaccharides

Bacterial polysaccharides synthesized and secreted into the external environment are referred to as exopolysaccharides. Exopolysaccharides differ from capsule polysaccharides in that they are not membrane anchored or directly surface associated (Kumar et al. 2007, Nwodo et al. 2012). Exopolysaccharides play a variety of roles, including modulation of adherence and modulation of biofilm formation. In a biofilm setting, exopolysaccharides function to modulate adhesion, bacterial cell aggregation, and water retention. They also provide a protective barrier against host defenses during infection, the harmful effects of oxygen, and antimicrobial agents (Kumar et al. 2007, Nwodo et al. 2012).

The diversity of bacterial exopolysaccharides allows for categorization based on chemical structure, functionality, molecular weight, and linkage bonds. In addition, exopolysaccharides are categorized into two groups: homopolysaccharides and heteropolysaccharides (Nwodo et al. 2012). Homopolysaccharides contain only one type of monosaccharide, while heteropolysaccharides are composed of repeating units, varying in size from

disaccharides to heptasaccharides. Exopolysaccharide categories are complex, and homopolysaccharides are further clustered into four groups based on linkages and the nature of the monomeric units: α-d-glucans, β-d-glucans, fructans, and polygalactan. The composition of heteropolysaccharides typically includes repeating units of glucose, galactose, rhamnose, and, in a some instances *N*-acetylglucosamine (GlcNAc), *N*-acetylgalactosamine (GalNAc), or glucuronic acid (GlcA) (Nwodo et al. 2012).

1.6 Capsule diversity among bacterial pathogens

The capsular polysaccharides expressed by a given species can exhibit a great range of diversity. The presence of multiple capsule types is well-documented in species including *S. pneumoniae*, *N. meningitidis*, and *K. pneumoniae*, in which some capsule types are associated with carriage or invasive disease. For example *S. pneumoniae* expresses at least 90 different capsular types, but 23 of these account for more than 90% of invasive pneumococcal disease worldwide (Feldman et al. 1997, Weinberger et al. 2009). In *N. meningitidis* only 6 of the 13 characterized serotypes are responsible for 90% of invasive strains

worldwide (Peltola 1983, Harrison et al. 2009), and in *K. pneumoniae* there are over 78 capsule types with a correlation between certain capsule types and site of isolation (Riser et al. 1981). Due to the range of capsule diversity expressed by a single pathogen, polysaccharide vaccines often consist of multiple polysaccharides representative of the most virulent strains to increase protection. Capsule diversity can also play a role in the immunogenicity of the polysaccharide. Bacterial capsules composed of hyaluronic acid or sialic acid mimic host tissue polysaccharides and are not immunogenic (Clements et al. 2008).

1.7 Capsule as a vaccine target

Capsular polysaccharides have long been used as effective vaccine immunogens (Goldblatt 2000). Capsule polysaccharides have formed the basis for several successful vaccines against pathogenic bacteria, including *H. influenzae, S. pneumoniae*, and *N. meningitidis*, reducing morbidity and mortality worldwide (Goldblatt 2000, Bilukha et al. 2005, Albrich et al. 2007, Maiden 2013). Capsule polysaccharide-based vaccines as well as polysaccharide-conjugate

vaccines function through eliciting specific antibodies to the polysaccharide capsule (Kelly et al. 2004). Specific antibody increases phagocytosis of bacteria and stimulates a protective immune response. Although polysaccharides are often immunogenic on their own, conjugation of polysaccharides to protein carriers has been used historically to improve immunogenicity. Polysaccharide capsule alone elicits T-independent B-cell activation, which is associated with poor or absent immunogenicity in infants (Siegrist 2008). Without T-cell mediated class switching, only IgM is produced, with no memory response. In the case of *H. influenzae* type b, where the highest rate of disease is seen in the first two years of life, conjugation of polysaccharide to a carrier protein that recruits T-cell help for the polysaccharide immune response results in a vaccine that is protective as early as 6 months of life (Kelly et al. 2004). Carrier proteins can be a protein antigen originating from the pathogen to boost the specific immune response to that pathogen, or a more general immunogenic protein that acts as an adjuvant (Goldblatt 2000).

1.8 Thesis overview

Chapter 2 compares the composition and structure of the capsule polysaccharide and exopolysaccharide expressed by *K. kingae* prototype strain

269-492. Chapter 3 describes the discovery of the genetic and molecular basis of capsular biosynthesis in the *Kingella kingae* prototype strain 269-492, including the genes involved in export, assembly, and synthesis. Chapter 4 examines the capsule diversity that exists among colonizing and invasive isolates of *Kingella kingae.* Finally, Chapter 5 summarizes the future directions and implications of this work.

Select portions of Chapter 2 and Chapter 3 have been published or are in press and are referenced below:

Starr KF, Porsch EA, Heiss C, Black I, Azadi P, St Geme JW 3rd. Characterization of the *Kingella kingae* polysaccharide capsule and exopolysaccharide. PLoS One. 2013 Sep 30;8(9):e75409. doi: 10.1371/journal.pone.0075409. eCollection 2013.

Starr KF, Porsch EA, Seed P, St. Geme III JW. Genetic and molecular basis of *Kingella kingae* encapsulation. Accepted to Infect Immun.

2. Characterization of the *Kingella kingae* polysaccharide capsule and exopolysaccharide

2.1 Introduction

Kingella kingae is a gram-negative bacterium that has emerged as a common cause of septic arthritis, osteomyelitis, and bacteremia in children 6-36 months of age (Yagupsky et al. 2011). Studies using culture-based and molecular-based detection strategies have established that *K. kingae* is a common commensal in the upper respiratory tract in young children (Yagupsky et al. 1992, Dubnov-Raz et al. 2008, Weiss-Salz et al. 2011, Yagupsky et al. 2011). In one report, *K. kingae* colonization of the pharynx was found in approximately 70% of children at some point during the first two years of life (Yagupsky et al. 1995). The pathogenesis of *K. kingae* disease is believed to involve bacterial translocation across the pharyngeal epithelial barrier, entry into the bloodstream, and dissemination to the joints, bones, or endocardium (Weiss-Salz et al. 2011). This pathogenic model is supported by data demonstrating genotypically identical isolates of *K. kingae* from the upper respiratory tract and either the bloodstream or joint fluid from patients with invasive disease (Yagupsky et al. 2009, Bidet et al. 2013).

Extracellular polysaccharides are produced by many pathogenic bacteria and function as important virulence factors. These polysaccharides can be categorized generally as capsular polysaccharides or exopolysaccharides. Capsular polysaccharides are lipid-anchored outer membrane-associated carbohydrates and are involved in protection from host immune mechanisms, including phagocytosis and complement-mediated killing (Roberts 1996, Corbett et al. 2010). These polysaccharides often exhibit a large degree of variation within a single bacterial species, with examples including *Escherichia coli* and *Streptococcus pneumoniae* (Orskov et al. 1977, Kalin 1998, Weinberger et al. 2010). In select cases, a specific capsule type can be associated with increased virulence potential, as highlighted by *Haemophilus influenzae* type b (Turk 1984). Exopolysaccharides are secreted carbohydrate polymers that are not anchored to the bacterial surface and that play a variety of roles, including modulation of adherence and modulation of biofilm formation (Kumar et al. 2007, Donot et al. 2012).

In recent work, we identified a polysaccharide capsule in *K. kingae* strain 269–492 that influences adhesive interactions with host cells and is dependent upon the *ctrABCD* ABC-type capsule export operon for surface localization,

which is similar to the capsule export operon of *N. meningitidis* (Porsch et al. 2012). In the current study, we set out to characterize the composition and structure of this polysaccharide capsule. Glycosyl analysis of bacterial surface extracts by gas chromatography/mass spectrometry and NMR revealed two distinct extracellular polysaccharides, including the polysaccharide capsule and a separate exopolysaccharide. The polysaccharide capsule contains N-acetyl galactosamine (GalNAc) and 3-deoxy-D-manno-oct-2-ulosonic acid (Kdo) and has the structure 3→)-β-Gal*p*NAc-(1→5)-β-Kdo*p*-(2→. In contrast, the exopolysaccharide contains only galactose and has the structure →5)-β-Gal*f*-(1→ Targeted mutagenesis established that the capsular polysaccharide and the exopolysaccharide require separate genetic loci for surface localization.

2.2 Materials and Methods

Bacterial strains.

The strains used in this study are listed in Table 1. *K. kingae* strain 269-492 was originally recovered from the joint fluid of a child with septic arthritis at St. Louis Children's Hospital, St. Louis, MO.

Table 1: Strains used in this study

Strain	Description	Work cited
K. kingae strains		
269-492 (KK01)	Clinical isolate Spontaneous nonspreading, non-corroding colony variant of 269-492	(Porsch et al. 2012)
KK01pamABCDE.	Deletion of pamABCDE	This work
KK01ctrA	Polar insertional mutation resulting in disruption of ctrABCD operon	(Porsch et al. 2012)
KK01ctrApamABCDE.	Polar insertional mutation in ctrA and deletion of pamABCDE	This work
E. coli strains		
DH5α	*E. coli* F− Φ80d*lacZ*Δ*M15* Δ(*lacZYA-argF*)*U169 deoR recA1 endA1 hsdR17*(rK− mK+) *phoA supE441 thi-1 gyrA96 relA1*	(Sambrook et al. 1989)

K. kingae KK01 is a stable sparsely piliated natural variant of strain 269-492 that forms nonspreading, non-corroding colonies and was used in all experiments in this study because of its colony morphology (Kehl-Fie et al. 2010). *K. kingae* strains were grown on chocolate agar plates at 37ºC with 5% CO_2 supplemented with 50 μg/ml kanamycin or 2 μg/ml erythromycin as appropriate. *K. kingae* strains were stored at -80ºC in brain heart infusion with 30% glycerol. *E. coli* strain DH5α was used for construction of gene disruption plasmids. *E. coli*

strains were routinely grown at 37ºC on Luria-Bertani (LB) agar or in LB broth with 100 μg/ml ampicillin, 50 μg/ml kanamycin, or 500 μg/ml erythromycin as appropriate. *E. coli* strains were stored at -80ºC in LB broth with 15% glycerol.

Strain construction.

Targeted gene disruptions in *K. kingae* were generated as previously described (Kehl-Fie et al. 2008, Porsch et al. 2012). Briefly, plasmid-based gene disruption constructs were created in *E. coli*, linearized, and introduced into *K. kingae* strain KK01 via natural transformation. Transformants were recovered by plating on chocolate agar plates containing the appropriate antibiotic. Correct localization of gene disruptions was confirmed by PCR. The *ctrA* disruption was generated as described previously (Porsch et al. 2012) but with the *aphA3* kanamycin resistance cassette as the marker. This disruption had a polar effect on the downstream genes in the *ctrABCD* operon. To delete the *pamABCDE* locus, fragments corresponding to the surrounding 5′ and 3′ regions of the locus were PCR amplified using the primers pam 5′for (GCGAATTCGGCGTTGGTGGAATATCCTG), pam 5′rev (GCGGATCCACCTTCTGGTCGCTGAAATG), pam 3′for

(GCGGATCCTCAAAGGCTGGTATAAACAC), and pam 3'rev (GCAAGCTTCCATATCGCTTTGGCTTTGC), respectively. The resulting fragments were ligated into pUC19, creating puC19*pam* 5'+3'::BamHI. The *ermC* erythromycin cassette from pIDN4 was PCR amplified with flanking BamHI sites and ligated into pUC19*pam* 5'+3', generating pUC19*pam*::*ermC*.

Polysaccharide extraction and purification.

For small scale capsule extractions, bacteria were washed and resuspended in either Tris acetate pH 5 (acid treatment for one hour) or PBS (heat treatment at 55ºC for 1 hour). Cells were removed by centrifugation, and extracts were treated with proteinase K for one hour, and then concentrated as previously described (Porsch et al. 2012).

To prepare strains for extraction of extracellular polysaccharide for purification, lawns of bacteria were grown overnight on chocolate agar plates. Subsequently, bacterial growth was swabbed from plates and resuspended in 50 ml of 1% formaldehyde in PBS to fix cells and allowed to stand for 15 minutes at room temperature. Bacteria were centrifuged at 4,355 x g for 10 minutes and then resuspended in 40 ml of 50 mM Tris acetate pH 5. Following vigorous shaking

for 1 hour at room temperature, bacteria were pelleted by centrifugation at 12,096 x g for 20 minutes. The supernatant was recovered and was then filtered using a 0.22 μm filter. The filtered material was adjusted to pH 7 with 1M Tris pH 9. To remove contaminating DNA, RNA, and protein, the filtered material was treated with 10 units of DNase (Fermentas) and 0.1 mg of RNase (Fermentas) at 37ºC for 5 hours and then with 0.18 mg of proteinase K (Roche) at 55ºC overnight. Samples were concentrated to 500 μl using 100 kDa MWCO filters and extracted once with Tris-saturated phenol pH 7.4 and twice with 100% chloroform. Extracted material was dialyzed extensively overnight in deionized water, flash frozen, and lyophilized. To purify exopolysaccharide galactan, we resuspended bacteria in PBS without formaldehyde, shook for one hour, pelleted the bacteria, and subjected the supernatant to the purification described above.

Staining of polysaccharide

Aliquots of the purified polysaccharide from *K. kingae* derivatives were separated on 10% SDS-PAGE gels. For Alcian blue staining, gels were stained with 0.125% Alcian blue as previously described (Porsch et al. 2012). For silver staining, gels were treated as previously described (Kim et al. 1996).

Chemical analysis

Monosaccharide composition analysis was performed by methanolysis and trimethylsilyl derivatization as previously described (Heiss et al. 2009).

NMR Spectroscopy

The isolated polysaccharide was deuterium-exchanged by lyophilization from D_2O (99.9 %D, Aldrich), dissolved in 270 µl D_2O (99.96 %D, Cambridge Isotope) containing 0.3 µl acetone, and placed in a 5-mm NMR tube with D_2O-matched magnetic susceptibility plugs (Shigemi Inc.). One-dimensional proton and 2-D TOCSY and NOESY NMR spectra with solvent presaturation and gradient-enhanced COSY, HSQC, and HMBC NMR spectra were acquired on a Varian Inova 600 spectrometer at 50 °C, equipped with a cryogenic triple-resonance probe. Spectral width was 2841 Hz in the proton and 18096 Hz in the carbon dimension. Mixing times were 150 ms for TOCSY and 300 ms for NOESY. The number of increments and scans, respectively were 512 and 4 for COSY, 200 and 8 for TOCSY, 200 and 16 for NOESY, 128 and 64 for HSQC, and

200 and 88 for HMBC. Chemical shifts were measured relative to acetone (δ_H=2.218 ppm, δ_C=33.0 ppm) (Wishart et al. 1995).

2.3 Results

2.3.1 Polysaccharide can be extracted and purified from the surface of *K. kingae* strain 269-492 variant KK01.

In order to extract and purify the polysaccharide capsule, we incubated a bacterial suspension of *K. kingae* strain 269-492 variant KK01 in Tris acetate pH 5, aiming to dissociate the polysaccharide capsule from the bacterial surface by the acidic pH. To confirm that our extraction procedure yielded pure polysaccharide material, we examined the material by Alcian blue straining and silver staining (Figure 3). Alcian blue is a cationic dye and has been used previously to demonstrate the presence of the *K. kingae* capsule (Porsch et al. 2012).

As shown in Figure 3, the extracted and purified material from the surface of *K. kingae* KK01 stained prominently with Alcian blue and silver reagents (lane 3), similar to control small scale heat and acid extracts from *K. kingae* KK01 (lanes 1-2).

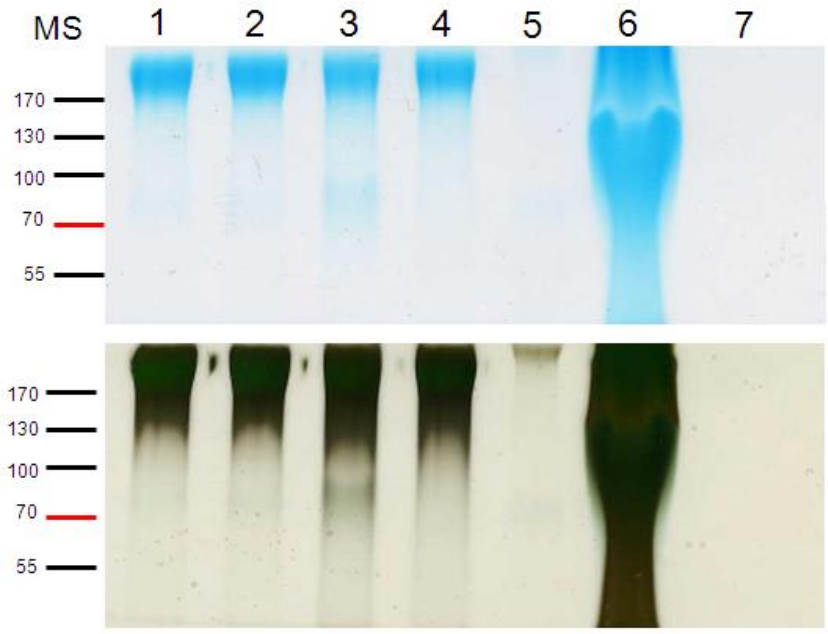

Figure 3: Staining profile and purity of polysaccharide material used for analysis.

Alcian blue staining is shown on the top, and silver staining is on the bottom. Lane 1, extract from KK01 using heat; lane 2, extract from KK01 using Tris acetate; lane 3, purified material from KK01 using Tris acetate; lane 4, purified material from KK01*pamABCDE* using Tris acetate; lane 5, purified material from KK01*ctrA* using Tris acetate; lane 6, purified material from KK01*ctrA* using surface PBS extraction; lane 7, purified material from KK01*ctrA pamABCDE* using Tris acetate. MS= molecular size (in kDa)

The Tris acetate extract from KK01*ctrA* (lacking a functional capsule export locus) failed to stain with either Alcian blue or silver reagents (lane 5), while the PBS surface extract from KK01*ctrA* stained well with Alcian blue and silver reagents (lane 6).

2.3.2 *Kingella kingae* KK01 extracellular polysaccharide contains GalNAc, Kdo, and galactose.

As shown in Table 2, composition analysis of the polysaccharide extracted from *K. kingae* KK01 revealed that the dominant components were GalNAc, Kdo, and galactose in roughly equimolar quantities.

Table 2: Glycosyl composition of extracellular preparations of *K. kingae* strains.

Glycosyl residue	KK01 Tris acetate prep	KK01*pamABCDE* Tris acetate prep	KK01*ctrA* Tris acetate prep	KK01*ctrA* surface PBS extraction	KK01*ctrA pamABCDE* Tris acetate prep
Xylose	0.3 (4.6)	1.0 (14.5)	9.0 (91.1)	0.1 (1.6)	10 (100)
Galactose	2.3 (27.1)	—	0.9 (7.5)	6.2 (64.5)	—
Glucose	0.2 (1.9)	—	0.1 (0.8)	1.8 (18.4)	—
N-Acetyl Galactosamine	3.0 (28.5)	4.2 (41.3)	—	0.1 (1.2)	—
N-Acetyl Glucosamine	0.4 (3.4)	—	—	0.4 (3.4)	—
Kdo*	3.4 (28.8)	4.8 (43.9)	—	0.8 (6.0)	—
Heptose	0.6 (5.6)	—	—	0.5 (4.8)	—

Mass in μg is listed first, and percentage is shown in parentheses. Mass and percentage are per 10 μg polysaccharide material analyzed. *3-Deoxy-D-Manno-oct-2-ulosonic acid

In addition, there were small quantities of xylose, glucose, N-acetyl glucosamine, and heptose, all common contaminants in this kind of preparation. The 1-D proton NMR spectrum of the purified polysaccharide (Figure 4) showed two anomeric signals at 5.18 and 4.70 ppm, with an intensity ratio of 1:3, and two

upfield methylene signals at 2.40 and 1.77 ppm, each of equal intensity with the larger anomeric peak.

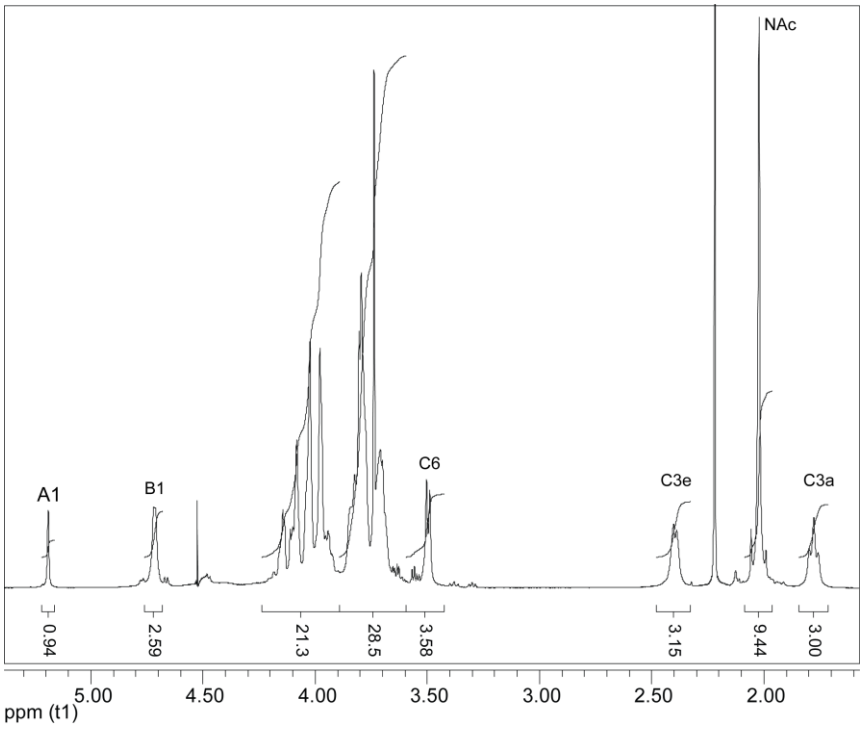

Figure 4: 1-D proton NMR spectrum of the polysaccharide.

The integration values show the relative molar ratio of the two polysaccharides, A_m and $(B\text{-}C)_n$ of about 1:3. For numbering, see Table 3 (C3e and C3a designate the equatorial and axial proton, respectively, of the C-3 methylene group).

The HSQC spectrum (Figure 5) showed that the signal at 5.18 ppm was associated with a carbon chemical shift of 109.4 ppm, implying that this residue was a furanose.

Table 3: Complete chemical shift assignment of the isolated polysaccharides.

No.	Residue	Chemical shift								NOE
		1	2	3	4	5	6	7	8	HMBC
A	5-β-Galf	5.18	4.15	3.94	4.15	4.10	3.82/3.82			
		109.4	84.1	78.5	84.1	**79.2**	62.1			A-5
B	3-β-GalpNAc	4.70	3.97	3.97	4.03	3.70	3.82/3.80			C-5
		105.2	53.6	**77.5**	70.5	77.1	63.5			C-5
C	5-β-Kdop	-	-	1.77/2.40	3.83	4.08	3.50	4.03	3.79/3.70	B-3
		174.3	**104.5**	37.2	70.0	**76.1**	76.1	71.9	65.8	

Chemical shift assignment of the remaining nuclei (Table 3) demonstrated that the furanose had a galacto- configuration, and a 5.9-ppm downfield displacement of its C-5 chemical shift indicated that it was glycosylated in the 5-position.

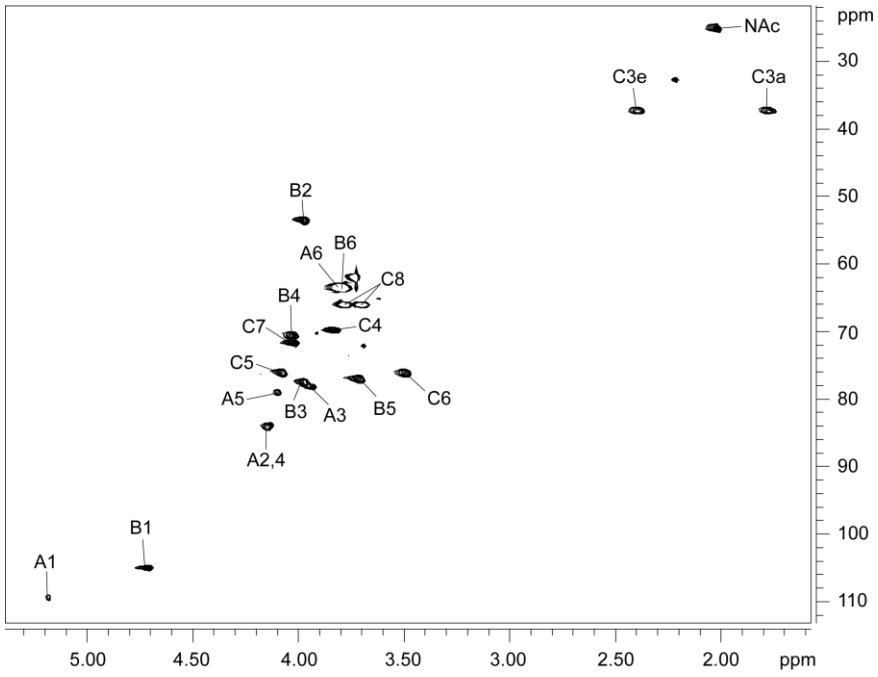

Figure 5: 2-D HSQC NMR spectrum of the polysaccharide with assignments of all the signals of the three major residues.

The further chemical shift assignments, based on 2-D COSY, TOCSY, and HSQC spectra, showed that the anomeric signal at 4.70 ppm belonged to a β-GalNAc residue and the methylene signals at 2.40 and 1.77 ppm belonged to a β-Kdo residue. Downfield shifts of the carbon nuclei involved in glycosidic linkages indicated that GalNAc was 3-linked and Kdo was 5-linked (Table 3). Beside these major residues, small amounts (~5 %) of non-reducing end GalNAc and reducing end 5-α-Kdo were also detected and are likely the result of cleavage of some of the very acid labile Kdo glycosidic bonds during isolation. The NOESY spectrum (Figure 6) revealed NOE contacts between H-1 of GalNAc and H-5 of Kdo and between both H-3s of Kdo and H-3 of GalNAc. The Gal*f* anomeric signal gave NOE contacts only to its own protons. HMBC showed a correlation between H-1 of GalNAc and C-5 of Kdo.

Taken together, these results demonstrated that the sample contained two polysaccharides, one composed of a disaccharide repeating unit with the structure →3)-β-Gal*p*NAc-(1→5)-β-Kdo*p*-(2→ and the other a galactofuranosyl homopolymer (galactan) with the structure →5)-β-Gal*f*-(1→(Figure 7).

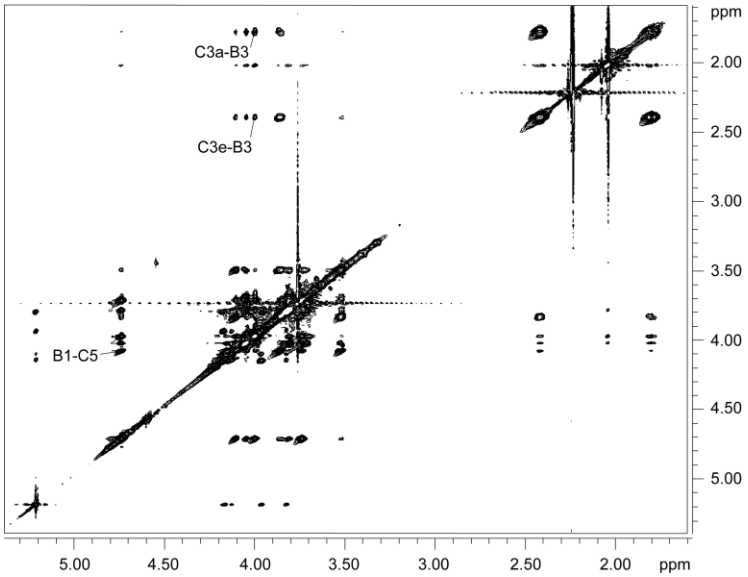

Figure 6: 2-D NOESY NMR spectrum of the polysaccharide. The sequence-determining correlations are labeled.

The galactan homopolymer accounted for the galactose in the composition and methylation analyses and was present at about one-third the molar concentration of the GalNAc-Kdo polymer.

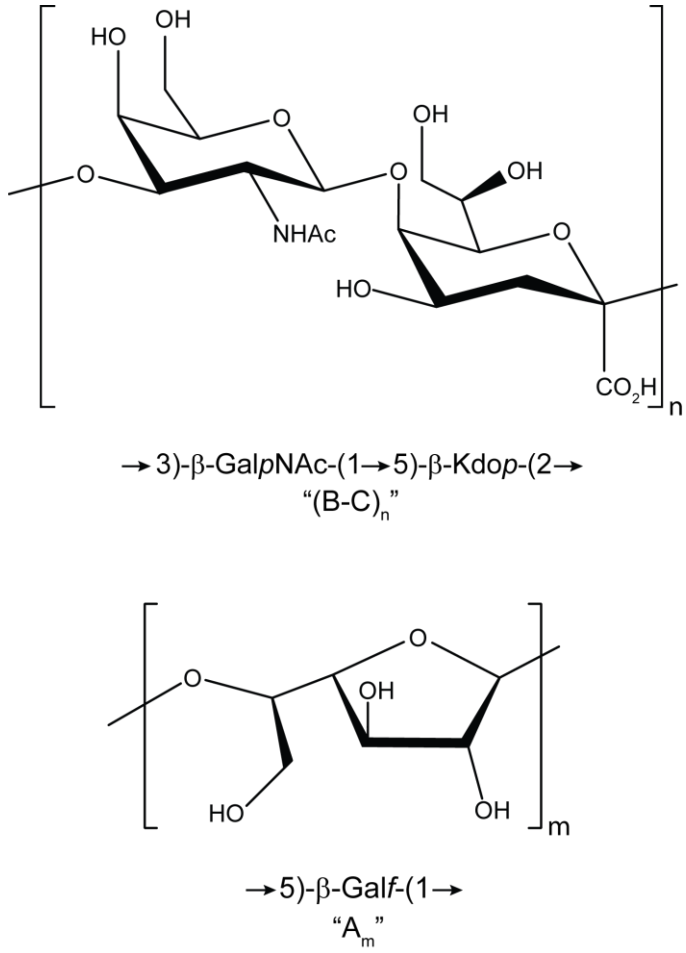

Figure 7: Structure of capsule polysaccharide repeating unit (top) and galactan exopolysaccharide repeating unit (bottom).

2.3.3 The GalNAc-Kdo polymer is the polysaccharide capsule and the galactan homopolymer is an exopolysaccharide.

In a recent report, *K. kingae* strain PYKK181 was found to produce an exopolysaccharide that is a galactan homopolymer and is encoded by the

pamABCDE locus (Bendaoud et al. 2011). To elucidate the relationship between the *K. kingae* polysaccharide capsule and the two distinct polysaccharide structures present in our bacterial surface extracts, we began by creating a derivative of KK01 with a deletion of *pamABCDE.* As shown in Figure 3 (lane 4) and Table 2, the polysaccharide extract from KK01*pamABCDE* stained with Alcian blue, contained large amounts of GalNAc and Kdo, and had only trace quantities of galactose, suggesting that the –5)-β-Gal*f*-(1–homopolymer corresponds to the galactan exopolysaccharide present in *K. kingae* strain PYKK181. As shown in Figure 8, examination of the colony morphology of KK01*pamABCDE* revealed mucoid colonies, indicating encapsulation and suggesting that the GalNAc-Kdo polysaccharide corresponds to the polysaccharide capsule.

To confirm these conclusions, we examined polysaccharide extracts from strain KK01*ctrA*, recognizing that the *ctrA* gene is required for export and surface localization of the polysaccharide capsule. Interestingly, glycosyl composition analysis revealed no GalNAc or Kdo and minimal amounts of galactose compared to the quantities of contaminating xylose and glucose (Table 2), raising

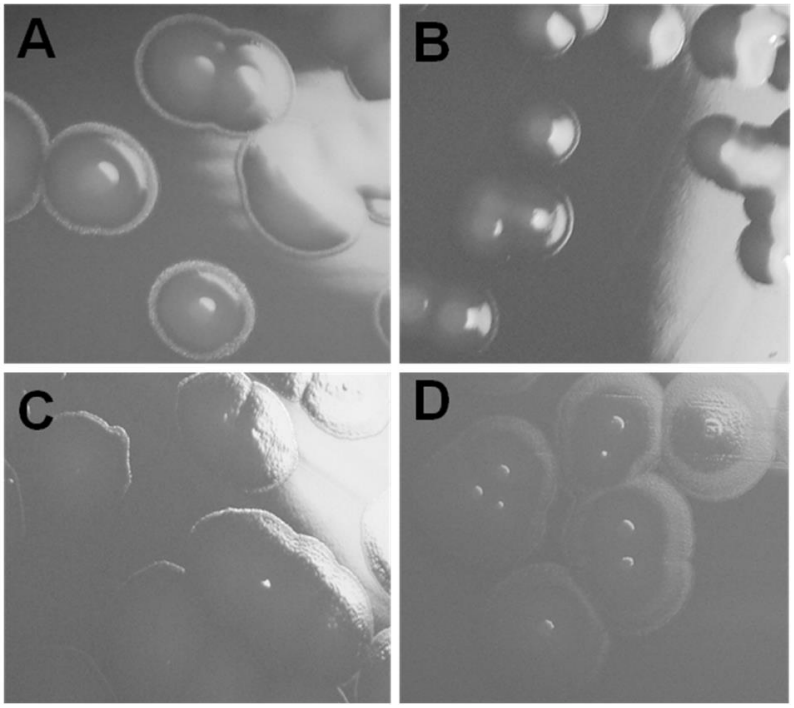

Figure 8: Colony morphology of *K. kingae* strains used in this study.

Strain KK01 (A) and KK01*pamABCDE* (B) form mucoid colonies consistent with encapsulation. KK01*ctrA* (C) and KK01*ctrA pamABCDE* (D) form rough, non-mucoid colonies consistent with loss of encapsulation.

the possibility that either the absence of the GalNAc-Kdo polysaccharide results in free release of the galactan exopolysaccharide or that *ctrA* is essential for surface localization of both the GalNAc-Kdo polysaccharide and the galactan homopolymer. To address these possibilities, we modified the extraction procedure to eliminate both the initial fixation step and the Tris acetate treatment, aiming to recover loosely associated polysaccharide from strain

KK01*ctrA*. Using this technique, a large quantity of galactose was detected in the purified material and only minimal amounts of GalNAc and Kdo were present (probably reflecting some bacterial lysis) (Table 2), indicating that strain KK01*ctrA* localizes the →5)-β-Gal*f*-(1→ polymer but not the →3)-β-Gal*p*NAc-(1→5)-β-Kdo*p*-(2→ polymer on the bacterial surface. Consistent with our previous work, examination of the colony morphology of KK01*ctrA* revealed non-mucoid colonies (Figure 8), indicating lack of a capsule. Analysis of the KK01*ctrA pamABCDE* double mutant revealed no Alcian blue staining material, complete loss of GalNAc, Kdo, and galactose, and non-mucoid colonies (Figure 3, Table 2, and Figure 8). Together these results provide strong evidence that the GalNAc-Kdo polysaccharide is the polysaccharide capsule and that the galactan polymer is an exopolysaccharide.

2.4 Discussion

In previous work we showed that *K. kingae* produces a polysaccharide capsule and contains a capsule export locus designated *ctrABCD* with high homology to the capsule export locus in *N. meningitidis*. In addition, we demonstrated that the *K. kingae* capsule is associated with a mucoid colony

phenotype on chocolate agar and is visible by thin section transmission electron microscopy after staining with cationic ferritin (Porsch et al. 2012). In the present study we set out to characterize the composition and structure of the *K. kingae* polysaccharide capsule. As a first step, we developed a capsule extraction and purification procedure that generated material amenable to analysis by GC/MS and NMR. Examination of the extracted material from *K. kingae* strain KK01 revealed GalNAc, Kdo, and galactose in roughly equimolar amounts. Additional analysis of the extracted material from derivatives of strain KK01 containing targeted mutations in the capsule export locus, the galactan biosynthesis locus, or both loci established that GalNAc and Kdo make up the capsule and that galactose makes up a galactan exopolysaccharide.

In considering our results, it is noteworthy that Bendaoud et al. reported two polysaccharides in the supernatant from *K. kingae* strain PYKK181, including a polysaccharide with the structure →6)-α-D-Glc*p*NAc-(1→5)-β-Kdo*p*-(2→ and a galactan homopolymer with the structure →3)-β-Galf-(1→6)-β-Galf-(1→ that was designated poly-DNA-containing *a*nti-adhesive *m*aterial extract (PAM galactan) and was found to inhibit biofilm formation by a variety of organisms (Bendaoud et al. 2011). In the report by Bendaoud and coworkers, the specific relationship

between these two polysaccharides and the organism was unclear. Based on the results of our mutational studies, we believe that the GlcNAc-Kdo polymer from strain PYKK181 is a polysaccharide capsule and that the PAM galactan is an exopolysaccharide.

It is interesting that the strain KK01 polysaccharide capsule has the structure →3)-β-Gal*p*NAc-(1→5)-β-Kdop-(2→ and the strain PYKK181 polysaccharide capsule has the structure →6)-α-D-Glc*p*NAc-(1→5)-β-Kdo*p*-(2→ (Bendaoud et al. 2011). The fact that the polysaccharide capsules expressed by these strains have different structures raises the possibility that there may be multiple *K. kingae* capsule types, similar to the case with *E. coli, S. pneumoniae, N. meningitidis, H. influenzae,* and a number of other bacterial pathogens (Orskov et al. 1977, Kalin 1998, Virji 2009). Along these lines, it is notable that Amit et al. observed an association between *K. kingae* PFGE clonal types and specific clinical presentations (Amit et al. 2012). In ongoing work, we are examining whether there is variability in capsule type among different clones and conservation of capsule type within a given clone. It is possible that certain capsule types confer greater virulence than others and are associated with specific disease processes.

Both the strain KK01 polysaccharide capsule and the strain PYKK181 polysaccharide capsule contain Kdo, a molecule that is well recognized as an essential component of lipopolysaccharide and is also present in a small number of bacterial polysaccharide capsules. The capsule produced by strain KK01 has the same structure as the capsule produced by *Moraxella nonliquefaciens* strain 3828/60 (Reistad et al. 1993) and has the same composition but different glycosyl linkages compared to the capsules produced by *E. coli* K14 [→6)-β-D-Gal*p*NAc-(1→5)-β-Kdo*p*(2→] (Jann et al. 1983) and *N. meningitidis* serogroup 29E [→3)-α-D-Gal*p*NAc-(1→7)-β-Kdo*p*(2→] (Bhattacharjee et al. 1978). Other examples of bacterial polysaccharide capsules that contain Kdo include the capsule produced by *Actinobacillus pleuropneumoniae* serotype 5a (identical to the capsule produced by *K. kingae* strain PYKK181) (Perry et al. 1990), the capsule produced by *Sinorhizobium meliloti* strain 1021 with the structure →7)-β-Kdo*p*(2→ (Fraysse et al. 2005), and the capsule expressed by *E. coli* K15 with the structure →4)-α-D-Glc*p*NAc-(1→5)-β-Kdo*p*(2→ (Jann et al. 1983).

In considering the genetic determinants of *K. kingae* polysaccharide capsule biosynthesis, it is notable that the *ctrABCD* capsule export locus is not flanked by a capsule synthesis operon, thus differing from the configuration of

capsule genes in most other bacteria that produce a polysaccharide capsule (Roberts 1996, Dolan-Livengood et al. 2003, Corbett et al. 2010). We speculate that genes involved in capsule synthesis and LPS synthesis may have overlapping functions, accounting for the fact that *K. kingae* capsule genes are not clustered in a single location.

Sequence analysis of the PAM locus in *K. kingae* strain KK01 and the PAM locus in *K. kingae* strain PYKK 181 reveals almost complete identity. Despite this sequence conservation, the structures of the galactan homopolymers in these strains are different, with distinct linkages. One possibility is that there are other genes beyond *pamABCDE* involved in biosynthesis of the galactan exopolysaccharides. Alternatively, the limited sequence variation may result in significant changes in enzymatic specificity.

To summarize, in this study we have established that *K. kingae* expresses two extracellular polysaccharides that require distinct genetic loci for surface localization, including a polysaccharide capsule and an exopolysaccharide. In future studies we will examine the contribution of these polysaccharides to the pathogenesis of *K. kingae* disease.

3. Genetic and molecular basis of *Kingella kingae* encapsulation

3.1 Introduction

Kingella kingae is an emerging pediatric pathogen and is a common etiology of septic arthritis, osteomyelitis, and bacteremia in children 6-48 months of age. The pathogenesis of *K. kingae* disease begins with asymptomatic colonization of the posterior pharynx, followed by bacterial translocation across the pharyngeal epithelial barrier, invasion of the bloodstream, and dissemination to distant sites (Yagupsky et al. 2009, Yagupsky et al. 2011). In previous work, our group described a series of surface factors expressed by *K. kingae* that influence adherence to epithelial cells *in vitro*, including type IV pili and a trimeric autotransporter protein called Knh. Adherence by our prototype *K. kingae* strain is impeded by a [→3)-β-Gal*p*NAc-(1→5)-β-Kdo*p*-(2→]$_n$ polysaccharide capsule, which masks the adhesive properties of Knh and is likely displaced when pili bind to the cell surface and retract (Porsch et al. 2012, Starr et al. 2013).

Polysaccharide capsules are often involved in virulence and possess functions that range from masking of bacterial surface antigens and protection

against serum killing to prevention of dessication and phagocytosis. Polysaccharide-conjugate vaccines based on the capsular polysaccharides of *Neisseria meningitidis*, *Haemophilus influenzae* type b, and *Streptococcus pneumoniae* have dramatically reduced childhood morbidity and mortality worldwide (Goldblatt 2000). The development of these vaccines has been among of the most successful public health innovations of the last 25 years (Maiden 2013).

The gene clusters involved in production of the *E. coli* K1 and K5 polysaccharide capsules have been studied extensively and provide the basis for our current understanding of the genetic organization and regulation of so-called group 2 capsules (Roberts 1996). The modular, polycistronic organization of group 2 capsule gene clusters has been well-established and includes Region 1, Region 2, and Region 3 genes in *E. coli* (Roberts 1996). Region 1 and Region 3 are highly conserved across different serotypes, and Region 2 is serotype specific (Clarke et al. 1999). Region 1 encodes components of the export apparatus called KpsF, KpsE, KpsD, and KpsU and also encodes β-Kdo transferases called KpsC and KpsS responsible for synthesizing the poly-Kdo linker between the α-glycerophosphatidic acid capsule membrane anchor and the reducing terminus of the capsular polysaccharide polymer (Roberts 1996). Region 2 encodes the

serotype-specific enzymes required for synthesis of the capsule polymer. Region 3 encodes the energy-dependent components of the ABC-transporter called KpsM and KpsT. *N. meningitidis* also expresses a group 2 capsule and contains all genes involved in capsule biosynthesis at a single locus called the *cps* locus. In *N. meningitidis,* the genes in region A are responsible for synthesis of the capsule polymer, the genes in region B are called *lipA* (*ctrE*) and *lipB* (*ctrF*) and serve the same assembly functions as *E. coli kpsC* and *kpsS*, respectively (Whitfield et al. 1999, Tzeng et al. 2005, Whitfield 2006, Harrison et al. 2013), and the genes in Region C are called *ctrABCD* and encode the ABC-type transporter apparatus.

Given that capsules are classic virulence factors and attractive vaccine antigen candidates, we were interested in defining the machinery required for capsule biosynthesis in *K. kingae*. We have previously shown that *K. kingae* contains a *ctrABCD* capsule export operon that is necessary for capsule surface localization (Porsch et al. 2012). However, unlike the cassette-like organization of most group 2-like capsules, there were no capsule-related genes nearby this *K. kingae* operon, suggesting that capsule genes in *K. kingae* may be unlinked and scattered throughout the genome. In this study we aimed to define the genetic determinants of encapsulation in *K. kingae*, with specific focus on the genes

necessary for synthesis of the GalNAc-Kdo capsular polymer in prototype strain 269-492. Using a transposon library mutagenesis screen and bioinformatic approaches, we identified a *lipA*/*KpsC*-like gene, a *lipB*/*KpsS*-like gene, and a putative glycosyltransferase gene designated *csaA* as the core genes required for encapsulation. Additional analysis demonstrated that the *csaA* gene product (CsaA) is a bi-functional glycosyltransferase essential for synthesizing the GalNAc-Kdo polymer.

3.2 Methods

Bacterial Strains

The strains used in this study are listed in Table 4. *K. kingae* strain 269–492 was isolated from the joint fluid of a child with septic arthritis at St. Louis Children's Hospital in St. Louis, MO and expresses a polysaccharide capsule, as previously reported (Kehl-Fie et al. 2007).

Table 4: Strains and plasmids used in this study.

Strain	Description	Source/Reference
Kingella kingae		
269-492	*K. kingae* isolate from St. Louis Children's Hospital	(Porsch et al. 2012)
KK01	Stable non-spreading/non-corroding derivative of 269-492	(Porsch et al. 2012)
ctrA	KK01 with the *aphA3* (Kan^R) cassette inserted into *ctrA* resulting in inactivation of *ctrABCD*	(Porsch et al. 2012)
lipA	KK01 deletion of *lipA*, containing the *aphA3* cassette	This study
lipB	KK01 deletion of *lipB*, containing the *aphA3* cassette	This study
csaA	KK01 deletion of *csaA*, containing the *aphA3* cassette	This study
lipA(lipA)	Inducible complement of *lipA* in the *lipA* background	This study
lipB(lipB)	Inducible complement of *lipB* in the *lipB* background	This study
csaA(csaA)	Inducible complement of *csaA* in the *csaA* background	This study
lipApilA1	*lipA* with the *cat* (Cm^R) cassette disrupting *pilA1*, resulting in inactivation of *pilA1*	This study
lipBpilA1	*lipB* with a *cat* cassette disrupting *pilA1*, resulting in inactivation of *pilA1*	This study
csaApilA1	*csaA* with a *cat* cassette disrupting *pilA1*, resulting in inactivation of *pilA1*	This study
lipA(lipA)pilA1	*lipA/(lipA)* with a *cat* cassette disrupting *pilA1*, resulting in inactivation of *pilA1*	This study
lipB(lipB)pilA1	*lipB/(lipB)* with a *cat* cassette	This study

	disrupting *pilA1*, resulting in inactivation of *pilA1*	
csaA(csaA)pilA1	*csaA/(csaA)* with a *cat* cassette disrupting *pilA1*, resulting in inactivation of *pilA1*	This study
$CsaA_{D99A}$	Amino acid change in the first D of the DXD motif	This study
$CsaA_{D101A}$	Amino acid change in the second D of the DXD motif	This study
$CsaA_{A99D*}$	Reversion of CsaAD99A to wild type	This study
$CsaA_{A101D*}$	Reversion of CsaAD101A to wild type	This study
$CsaA_{H518A}$	Amino acid change of the H of the HP motif	This study
$CsaA_{P519A}$	Amino acid change of the P of the HP motif	This study
$CsaA_{A518H*}$	Reversion of CsaAH518A to wild type	This study
$CsaA_{A519P*}$	Reversion of CsaAP519A to wild type	This study
E. coli		
DH5α	F– Φ80*lac*ZΔM15 Δ(*lac*ZYA-*arg*F) U169 *rec*A1 *end*A1 *hsd*R17 (rK–, mK+) *pho*A *sup*E44 λ– *thi*-1*gyr*A96 *rel*A1	(Sambrook et al. 1989)
BL21(DE3)	F– *omp*T *hsd*SB(rB–, mB–) *gal* *dcm* (DE3)	(Studier et al. 1986)
Plasmids		
pUC19*ctrA*	*ctrA* disruption construct marked with *aphA3* cassette	(Porsch et al. 2012)
pUC19*lipA*	*lipA* disruption construct marked with the *aphA3* cassette	This study
pTrcCErm*lipA*com	Complementation vector	This study

p	containing full length *lipA*	
pUC19*lipB*	*lipB* disruption construct marked with *aphA3*	This study
pTrcCErm*lipB*com p	Complementation vector containing full length *lipB*	This study
pUC19*csaA*	*csaA* disruption construct marked with *aphA3*	This study
pTrcCErm*csaA*com p	Complementation vector containing full length *csaA*	This study
pTrcCErm	Complementation vector (pUC19) containing the *trc* promoter that targets recombination to complementation locus with homologous flanking regions. Contains the *ermC* (Erm^R) cassette	This study
pCsaA5′	pUC19 containing coding sequence for CsaA N terminus and upstream 5′ sequence	This study
$pCsaA_{D99A}$	pCsaA5′ containing D99A point mutation	This study
$pCsaA_{D101A}$	pCsaA5′ containing D101A point mutation	This study
$pCsaA_{A99D*}$	pCsaA5′ containing A99D reversion	This study
$pCsaA_{A101D*}$	pCsaA5′ containing A101D reversion	This study
pCsaA3′	pUC19 containing coding sequence for CsaA C terminus and downstream 3′ sequence	This study
$pCsaA_{H518A}$	pCsaA5′ containing H518A point mutation	This study
$pCsaA_{P519A}$	pCsaA5′ containing P519A point mutation	This study
$pCsaA_{A518H*}$	pCsaA5′ containing A518H reversion	This study
$pCsaA_{A519P*}$	pCsaA5′ containing A519P	This study

	reversion	
pNtermCsaA	pET-15b containing *csaA* inserted into XhoI/BamHI sites	This study
pIND4	Source of the *ermC* erythromycin resistance gene	(Hamilton et al. 2001)
pACYC184	Source of the *cat* chloramphenicol resistance gene	(Chang et al. 1978)
pFalcon2	Source of the *aphA3* kanamycin resistance gene	(Hendrixson et al. 2001)
pUC19*pilA1*	*pilA1* disruption construct marked with *cat*	(Porsch et al. 2012)

K. kingae strain KK01 is a stable natural variant of strain 269–492 that grows as a non-spreading, non-corroding colony type and was used as the parent strain in this study (Kehl-Fie et al. 2007, Porsch et al. 2012). *K. kingae* strains were grown on chocolate agar (Chocolate II Agar, BD, Franklin Lakes, NJ) at 37°C with 5% CO_2 supplemented with 50 μg/ml kanamycin or 2 μg/ml erythromycin, as appropriate. *K. kingae* strains were stored at -80°C in brain heart infusion broth with 30% glycerol. *E. coli* strain DH5α was used for construction of the gene disruptions and complementation constructs. *E. coli* strains were grown at 37°C on Luria-Bertani (LB) agar or in LB broth with 100 μg/ml ampicillin, 50 μg/ml kanamycin, or 500 μg/ml erythromycin, as appropriate. *E. coli* strains were stored at -80°C in LB broth with 15% glycerol. For expression induction experiments, IPTG was added to a final concentration of 0.1 mM.

Plasmid and strain construction

Targeted gene disruptions and complementation constructs in *K. kingae* were generated as previously described (Kehl-Fie et al. 2009, Porsch et al. 2012). Briefly, plasmid-based gene disruption constructs were created in *E. coli*, linearized, and introduced into *K. kingae* via natural transformation followed by plating on chocolate agar containing the appropriate antibiotics. The gene disruptions and complementation constructs were confirmed by PCR.

The *ctrA* and *pamABCDE* disruptions used in this study were generated previously (Porsch et al. 2012, Starr et al. 2013). To delete the *lipA, lipB,* and *csaA* loci, fragments corresponding to the surrounding 5′ and 3′ regions were PCR amplified using the primers shown in Table 5, and a resistance cassette was ligated between the flanking regions.

To complement the *lipA, lipB, and csaA* deletions, fragments corresponding to the ORFs were PCR amplified using primers specific to each gene (Table 5). The resulting fragments were ligated into a plasmid called ptrcCErm, which is a modified version of the previously described *K. kingae* complementation construct (Porsch et al. 2012) and contains the P_{trc} promoter and the *lacI* operator.

Table 5: Primers used in this study

Primer name	Sequence
lipA 5′for	GCCGAATTCCGTTGTCGCCTTGTCCTATTT
lipA 5′rev	GCGGGATCCCAAGCAGCCTGCACTTTTTG
lipA 3′for	GCGGGATCCAATGTGCAGGCTGCTTTTTA
lipA 3′rev	GCGAAGCTTCCGAAGGTTACGGCAATTTC
lipB 5′for	ACGTGAATTCTTGCGATTGTGGCCCACAGTTG
lipB 5′rev	ACGTGGATCCGGGCGATACGGAGTCATACAAATGG
lipB 3′for	ACGTGGATCCGCACCCACATCAACGGCTATTACTAC
lipB 3′rev	ATGCAAGCTTCCAGCGAAGACTATCCCATTGGC
csaA 5′for	GCGGAATTCGCTGCTTTGGTGCAAAATCG
csaA 5′rev	GCGGGATCCTCGCAACAACAAGTGTTCTG
csaA 3′for	GCGGGATCCAAAAGTCGGTAAGTAGTGCG
csaA 3′rev	GCGAAGCTTCAGCCTGCACTTTTTTGTTG
TrcFor	GCAGGTCGACTTCACCGTCATCACCGAAAC
TrcRev	GCAGGTCGACGCTCGAATTCCATGGTCTGT
lipAFor	GCATGGATCCTATGACATCATAATACATTG
lipARev	GCATGGATCCGCACATTGGATAAACAAGTG
lipBFor	GCATGGATCCCGGATAGTTTGGTTCATGAT
lipBRev	GCATGGATCCCATTTGTATGACTCCGTATC
CsaA5′mutFor	GCATGGATCCGAGATTAAATTCAATTTATT
CsaA5′mutRev	GCATGGATCCGTTTCACTAAAAAATAACCA
CsaA3′mutFor	ACGTGAATTCTTGCAAGGCGACAAACAAGC
CsaA3′mutRev	ACGTGAATTCTTAAAGTGCAGGCTGCTTTTATGG
CsaAD99AFor	CGAGCGGTAAGTTTTTTAGCCGTAGATTTGCGTGTTG C
CsaAD99ARev	GCAACACGCAAATCTACGGCTAAAAAACTTACCGC TCG
CsaAD101AFor	CGGTAAGTTTTTTAGACGTAGCGTTGCGTGTTGCGCC TGATTT
CsaAD101ARev	AAATCAGGCGCAACACGCAACGCTACGTCTAAAAA ACTTACCG
CsaAA99/101DFor	GGTAAGTTTTTTAGACGTAGATTTGCGTGTTGCGCCT GAT
CsaAA99/101DRev	ATCAGGCGCAACACGCAAATCTACGTCTAAAA

CsaAH518AFor	TGGGTTGTATTGTGTAAGAAGGCACCGCTAGAAACCGAAGTACCC
CsaAH518ARev	GGGTACTTCGGTTTCTAGCGGTGCCTTCTTACACAATACAACCCA
CsaAP519AFor	CTTCGGTTTCTAGCGCATGCTTCTTACACAATACAAC
CsaAP519ARev	GTTGTATTGTGTAAGAAGCATGCGCTAGAAACCGAAG
CsaAA518HFor	GCGGGTACTTCGGTTTCTAGCGGATGCTTCTTACACAATACAACCCAG
CsaAA518HRev	CTGGGTTGTATTGTGTAAGAAGCATCCGCTAGAAACCGAAGTACCCGC
CsaAA519PFor	GCGGGTACTTCGGTTTCTAGCGGATGCTTCTTACACAATACAACCCAG
CsaAA519PRev	CTGGGTTGTATTGTGTAAGAAGCATCCGCTAGAAACCGAAGTACCCGC
CsaAXho1For	GCATCTCGAGATGTATGCCTTATCTGTCAT
CsaABamH1Rev	GCATGGATCCTCTACGGTTATTTAGCTTAC
ARB1	GGCCACGCGTCGACTAGTACNNNNNNNNNNGATAT*
ARB6	GGCCACGCGTCGACTAGTACNNNNNNNNNNACGCC*
Solo5′Arb#1	GCCCGGGAATCATTTGAAGGTTG
Solo3′Arb#1	CGCGTCGCGACGCGTCAATTCGAGG
Solo3′outN	CGCTCTTGAAGGGAACTATGTTG
Solo5′outN	AATATGCATTTAATACTAGCGACGCC
ARB2	GGCCACGCGTCGACTAGTAC

To introduce site-directed mutations in *csaA*, we generated separate plasmids containing coding sequence for the glycosyltransferase N-terminal region with 5′ flanking sequence and coding sequence for the C-terminal region

with 3′ flanking sequence, using primers CsaA5′mutFor/CsaA5′mutRev and CsaA3′mutFor/CsaA3′mutRev, respectively. The resulting plasmids called pCsaA5′ and pCsaA3′ were used as the templates for the mutagenesis reactions. The QuikChange II XL Site-Directed Mutagenesis Kit (Agilent Technologies, Santa Clara, CA) was used to change the targeted amino acids in the DXD and HP motifs in the respective plasmids. The primers used in the mutagenesis and reversion reactions are listed in Table 5. Nucleotide sequencing was used to confirm that only the desired mutation was introduced.

Transposon screen

DNA was purified from *K. kingae* strain KK01 using the Wizard Genomic DNA Kit (Promega, Madison, WI) according to the manufacturer's instructions. To create the transposon library, chromosomal DNA from *K. kingae* KK01 was mutagenized using the Himar1 transposase and pFalcon2 as the source of the *mariner* transposon derivative containing an *aphA3* kanamycin resistance cassette as previously described (Kehl-Fie et al. 2007). Following transposition, the transposed genomic DNA was dialyzed and transformed into *K. kingae* KK01 followed by recovery in BHI+16% horse serum for 2 hours at 37°C. The reaction

mixtures were then plated onto chocolate agar containing kanamycin for selection. To identify mutants lacking polysaccharide capsule, we screened colonies by assessment of colony morphology and by alcian blue staining of colony blots. To obtain the colony blots, circular nitrocellulose membranes were applied to agar plates for 30 seconds and were then lifted, stained with alcian blue for one hour, and destained with 40% ethanol/5% acetic acid overnight. Following confirmation of nonencapsulated transformants, we sequenced out from the transposon to identify the insertion site using arbitrary PCR as previously described (Kehl-Fie et al. 2007). The initial PCR was performed using arbitrary primer ARB1 or ARB6 and specific primer Solo5′Arb#1 or Solo3′Arb#1 (Table 5). Solo5′Arb#1 anneals at the 5′ end of the Solo transposon, and Solo3′Arb#1 anneals at the 3′ end of the Solo transposon. In the second round of amplification we utilized ARB2, which anneals to the 5′ end of ARB 1 and ARB 6, and Solo5′outN or Solo3′outN, which are external to Solo5′Arb#1 and Solo3′Arb#1, respectively. The PCR products from the second round of amplification were gel purified and sequenced (Eton Bioscience, San Diego, CA) using either Solo5′outN or Solo3′outN, as appropriate.

Polysaccharide Capsule Extraction

In preparation for capsule extraction, bacteria were grown overnight on chocolate agar. Subsequently, bacteria were resuspended in PBS, washed once with PBS, and then resuspended in 50 mM Tris acetate pH 5. After agitation for one hour, bacteria were removed by centrifugation. The bacterial supernatants were collected and concentrated using an Amicon Ultra centrifuge filter with a 10,000 molecular weight cutoff and were then treated with proteinase K at 55°C for one hour.

Thiobarbituric Acid (TBA) Assay

To quantify capsule extracted from the bacterial cell surface or present in whole bacterial lysates, samples were examined using the thiobarbituric acid (TBA) assay as previously described (Warren 1959, Straus et al. 1990). Briefly, capsule material was hydrolyzed by the addition of strong acid (1.12 μl of 24% H_2SO_4 per 50 μl sample). A 50 μl sample of extracted polysaccharide was added to 25 μl of 25 mM periodate solution. The tubes were inverted to mix and allowed to incubate at 37°C for 30 minutes. A 20 μl aliquot of 2% sodium arsenite in 0.5 N HCl was added, and the tubes were allowed to sit at room temperature

until the yellow color disappeared. Subsequently, 200 μl of 0.1 M thiobarbituric acid solution was added to the clear solution, and the tubes were placed in a boiling water bath for 7.5 minutes. Following boiling, the tubes were placed on ice for 5 minutes and then extracted with 700 μl butanol. After centrifugation at 6000 x g, the top organic layer, consisting of a bright pink color, was measured for absorbance at 549 nm.

Staining of Polysaccharide

Aliquots of the capsule polysaccharide from *K. kingae* derivatives were separated on 7.5% SDS-PAGE gels and were stained with 0.125% alcian blue as previously described (Porsch et al. 2012, Starr et al. 2013).

Glycosyltransferase Characterization

Full-length N-terminal His-tagged glycosyltransferase protein was induced in *E. coli* DH5α from the plasmid pNtermCsaA. The induced protein was insoluble in inclusion bodies, which were harvested by centrifugation and separated on an SDS-PAGE gel. The major protein band corresponding to full-length CsaA was excised from the gel and sent to Cocalico Biologicals, Inc.

(Reamstown, PA) for injection into a guinea pig and generation of a polyclonal antiserum (DUGP#115).

The full-length glycosyltransferase was detected in total membranes by Western blot analysis. Total membranes were recovered by centrifugation of cleared bacterial sonicates. The total membrane fraction was separated on a 7.5% SDS-PAGE gel, transferred to nitrocellulose, and probed with DUGP#115 at a dilution of 1:5000 followed by an anti-GP-HRP conjugated secondary antibody at a dilution of 1:10000. The blot was developed using a chemiluminescent substrate.

Adherence to Chang cells

Bacterial adherence assays were performed with Chang cells (ATCC CCL-20.2) as previously described (Porsch et al. 2012).

Transmission Electron Microscopy

Samples of bacteria adherent to Chang cell monolayers in 24-well plates were prepared as previously described (Porsch et al. 2012), except that the monolayers were grown on 7.8 mil (199μm) Aclar embedding film inserts cut to

fit the wells. Following incubation of bacteria and monolayers, samples were fixed with 5% glutaraldehyde in cacodylate buffer for 20 minutes at room temperature. The samples were washed once with cacodylate buffer and incubated in cacodylate buffer containing cationic ferritin (Sigma, St. Louis, MO) added to a final concentration of 1 mg/ml for one hour at room temperature. Following incubation, cationic ferritin solution was removed and inserts were fixed in 5% glutaraldehyde for two hours. The fixative was then removed, and the cells were washed 3 times with cacodylate buffer. Subsequently, the Aclar inserts were removed from the 24-well plates and placed in scintillation vials. Inserts were treated with 2% osmium tetroxide for 30 minutes and dehydrated in a graded series of dimethyl formamide (DMF) while progressively lowering the temperature above the freezing point. (DMF is reported to minimize precipitation of polysaccharides (M E Bayer 1985)). The Aclar film was sandwiched in between glass slides, infiltrated with LR white, and polymerized. After polymerization, the cells were mounted on a resin block and sectioned. Thin sections were placed on 200 mesh grids, stained with uranyl acetate and Reynolds lead citrate at room temperature, and examined using a Philips CM-12 electron microscope.

Animal Studies

K. kingae strains were grown on chocolate agar for 17-18 hours, and the bacterial growth was swabbed from plates and resuspended in PBS to a final density of $7.5x10^7$ cfu/100 μl. Groups of eight nursing five-day-old Sprague Dawley rat pups (Charles River Laboratories, Wilmington, MA) were injected via the intraperitoneal route with 100 μl of the appropriate bacterial suspension or 100 μl of PBS alone (control) using a 27½ gauge needle and were then returned to their cage with a lactating dam. The experimental and control groups were housed separately with a lactating dam and were monitored for mortality and signs of illness twice daily for a total of five days. Animals that were found to be moribund were euthanized using CO_2 inhalation followed by secondary decapitation.

Ethics statement: The animal studies were approved by The Children's Hospital of Philadelphia Institutional Animal Care and Use Committee (Protocol IAC 13-001050) and followed all federal and institutional guidelines.

3.3 Results

3.3.1 Capsule biosynthesis genes are not restricted to a single locus

To identify the genetic determinants of encapsulation in *K. kingae* strain 269-492, we generated a random transposon library in strain KK01, a stable non-spreading/non-corroding derivative of 269-492 with a prominent mucoid colony morphology. Non-encapsulated mutants of KK01 were identified based on a non-mucoid colony morphology and lack of staining with alcian blue in colony blots (Austrian 1953, Radke et al. 1971). The resulting mutants were subjected to sequencing of the transposon insertion sites, revealing insertions in the *ctrABCD* capsule export operon that we described earlier (Porsch et al. 2012), a gene with homology to the *N. meningitidis lipA* gene and the *E. coli kpsC* gene involved in capsule assembly, a gene with homology to the *N. meningitidis lipB* gene and the *E. coli kpsS* gene involved in capsule assembly, and a gene encoding a hypothetical protein. Analysis of the homology of the hypothetical protein to other proteins revealed similarity to known and predicted glycosyltransferases, suggesting that this protein is involved in capsule polysaccharide synthesis. Further analysis revealed two distinct domains, including one in the N-terminal region with homology to GalNAc transferases and another in the middle region

with homology to Kdo transferases. With this information in mind, we designated the gene encoding the hypothetical protein *csaA* for *c*apsule *s*ynthesis region *a* gene A.

As shown in Figure 9, the genes identified in our screen involved in capsule export, assembly, and probable synthesis are present in unlinked loci on the *K. kingae* chromosome, thus differing from the organization of capsule genes in *N. meningitidis* (Dolan-Livengood et al. 2003), *E. coli,* and other group 2 encapsulated bacteria.

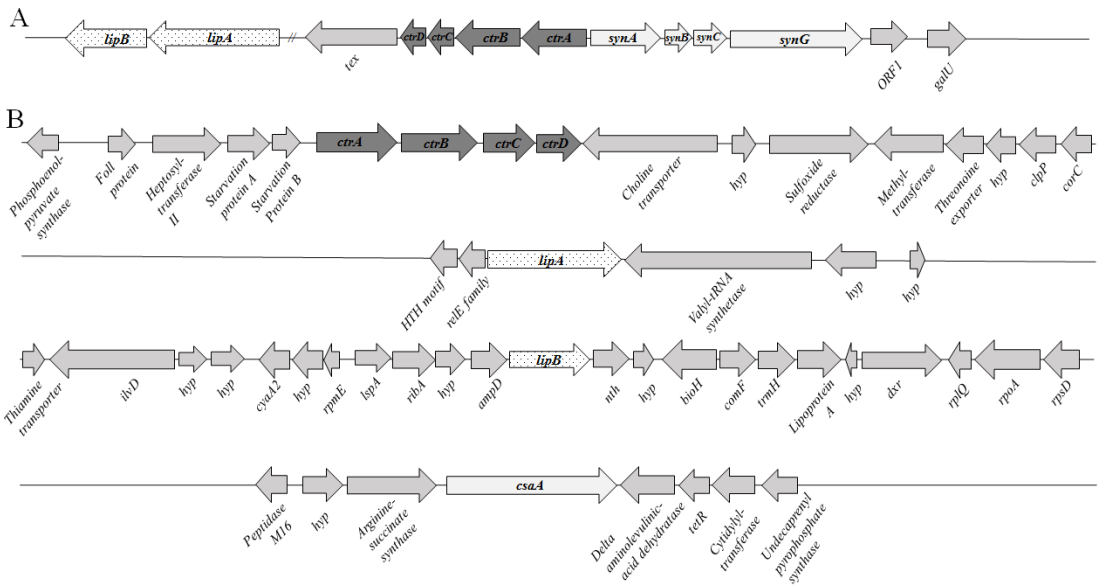

Figure 9: Location of the *K. kingae* capsule export/assembly/synthesis genes reveals an atypical organization.

(A) The *Neisseria meningitidis* serogroup W-135 capsule locus is composed of contiguous region A-D genes, including export (*ctrABCD* in dark gray), assembly (*lipA* and *lipB* in white with stippling), and synthesis (light gray). The homologous genes in *K. kingae* are shown in their disparate genetic locations in the corresponding shades (B).

3.3.2 LipA/LipB affect capsule assembly and CsaA affects polysaccharide synthesis

To confirm that the genes identified in our screen are involved in encapsulation, we generated targeted deletions in *lipA*, *lipB*, and *csaA*. These deletions resulted in loss of the mucoid colony phenotype, consistent with loss of encapsulation. To extend these findings, surface polysaccharides were acid extracted from these mutants, separated on an SDS-PAGE gel, and stained with alcian blue to visualize extractable polysaccharide capsule. As shown in Figure 10, targeted deletion of *lipA*, *lipB*, or *csaA* resulted in loss of alcian blue staining of surface polysaccharide material compared to parent strain KK01, indicating loss of encapsulation, analogous to disruption of the *ctrABCD* operon.

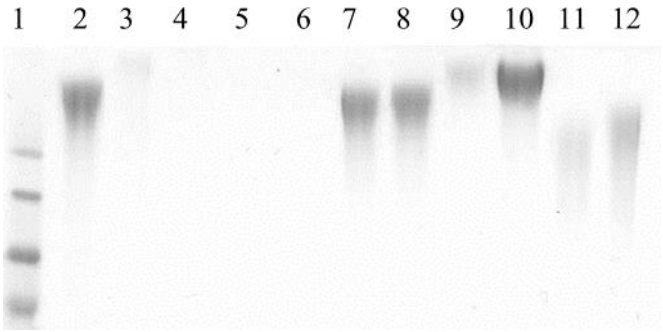

Figure 10: Alcian blue stained gel of purified capsule material

Lane 1, ladder; lane 2, prototype strain KK01; lane 3, *ctrA* mutant; lane 4, *lipA* mutant; lane 5, *lipB* mutant; lane 6, *csaA* mutant; lane 7, *lipA* mutant complemented with intact *lipA [lipA(lipA)]*; lane 8, *lipA* mutant complemented with intact *lipA* induced with IPTG *[lipA(lipA)IPTG]*; lane 9, *lipB* mutant complemented with intact *lipB [lipB(lipB)]*; lane 10, *lipB* mutant complemented with intact *lipB* induced with IPTG *[lipB(lipB)IPTG]*; lane 11, *csaA* mutant complemented with intact *csaA [csaA(csaA)]*; lane 12, *csaA* mutant complemented with intact *csaA* induced with IPTG *[csaA(csaA)IPTG].*

Complementation of the *lipA*, *lipB* and *csaA* deletions at a separate locus on the chromosome restored encapsulation as visualized by colony morphology and alcian blue staining of surface polysaccharide material (Figure 10). Slight differences in mobility and intensity of the bands were observed for the surface extracts from the *lipB(lipB)* and *csaA(csaA)* complemented strains. Capsule material appeared to migrate through the gel slower than KK01 capsule in the *lipB(lipB)* complemented strain and faster than KK01 capsule in the *csaA(csaA)* complemented strain. Mass spectrometry analysis of the capsule material

obtained from the complemented strains confirmed that the polysaccharides contained both GalNAc and Kdo, as expected (data not shown). Other investigators have suggested that altered stoichiometry of LipA/KpsC to other capsule biosynthetic components may result in aberrant capsule chain length (Willis et al. 2013), raising the possibility that altered stoichiometry of capsule synthesis components through complementation at a non-native locus may result in a similar change in capsule chain length.

As another approach to quantify the amount of polysaccharide in the mutant and complemented strains, we measured thiobarbituric acid (TBA) reactivity. The TBA assay relies on measurement of sialic acids and related products, including Kdo, which represents half of the sugar content in the strain KK01 polysaccharide capsule. As shown in Figure 11A, disruption of *ctrA*, *lipA*, or *lipB* resulted in a 90% reduction in TBA reactivity of surface extractable material and a 20-60% reduction in TBA reactivity of whole cell extracts in these

mutants compared to the parent KK01 strain.

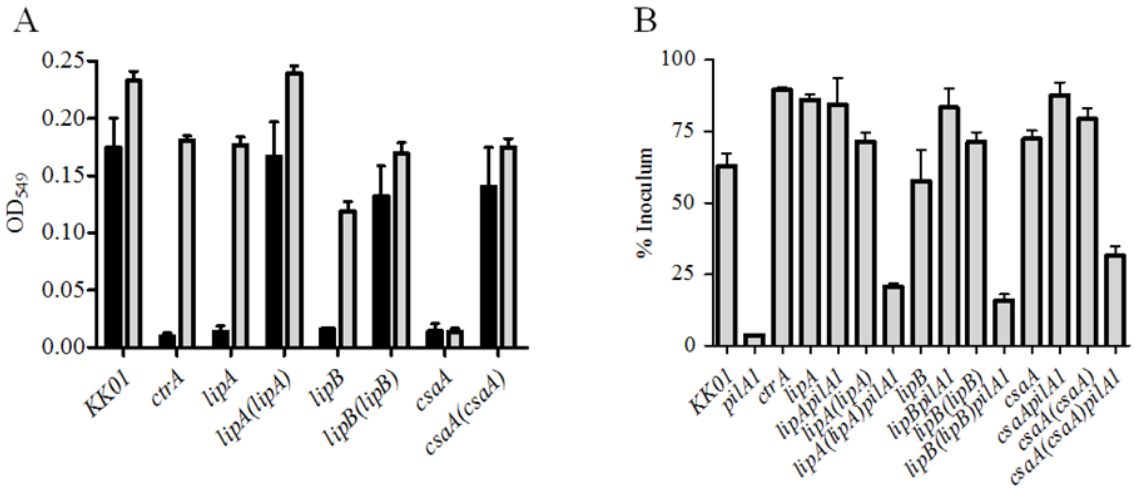

Figure 11: TBA reactivity and adherence as functional readouts of capsule loss and complementation.

(A) TBA reactivity of mutant and complemented strains. Surface extractable values are shown in black, and whole cell reactivity values are shown in gray. (B) Adherence to Chang cells by mutant and complemented strains as a percent of the inoculum. Bars represent the mean and standard error measurements of assays performed in biological and technical triplicate.

Complementation of the *lipA* and *lipB* mutations restored TBA reactivity of surface extracts and whole cell extracts to wild type levels. We were unable to generate a complementation construct for the *ctrA* mutant, as we previously reported (Porsch et al. 2012). Unlike the *ctrA*, *lipA*, and *lipB* mutants, the *csaA* mutant demonstrated a marked reduction in TBA reactivity of both surface extracts and whole cell extracts, suggesting absence of intracellular

polysaccharide pools. TBA reactivity was fully restored by complementation of the *csaA* deletion (*csaA(csaA)*).

In previous work, we established that *K. kingae* encapsulation masks the adhesive properties of the Knh autotransporter protein when type IV pili are absent (Porsch et al. 2012). To create a functional readout of encapsulation in the mutant and complemented strains, we eliminated pili by insertionally inactivating the *pilA1* structural pilin gene and then measured Knh-mediated adherence to Chang epithelial cells. We predicted that mutant strains would be fully adherent and that the complemented strains would produce a capsule that masks Knh-mediated adherence like the capsule in the parent KK01 strain. As shown in Figure 11B, the complemented *lipA(lipA)*, *lipB(lipB)*, and *csaA(csaA)* strains were fully adherent, similar to parent strain KK01. In contrast, the *lipA(lipA)pilA1*, *lipB(lipB)pilA1*, and *csaA(csaA)pilA1* complemented strains were minimally adherent, similar to nonpiliated parent strain KK01, indicating a capsule capable of masking Knh in the absence of pili.

In order to visualize surface-associated capsule, we stained bacteria with cationic ferritin and performed thin-section transmission electron microscopy (Figure 12).

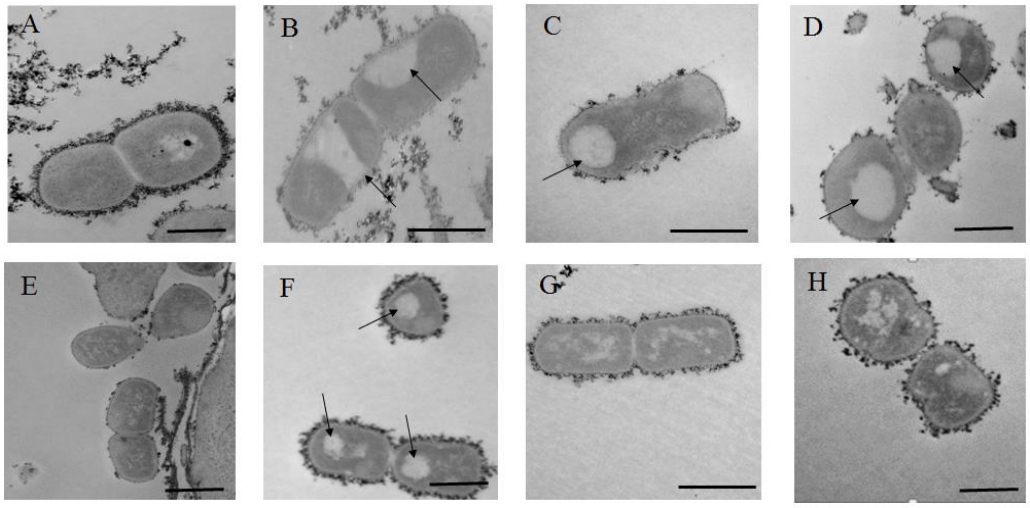

Figure 12: Thin section transmission electron microscopy images of cationic ferritin-stained K. kingae.

(A) KK01 parent (B) *ctrA* mutant (C) *lipA* mutant (D) *lipB* mutant (E) *csaA* mutant (F) *lipA* mutant complemented with intact *lipA [lipA(lipA)]* (G) *lipB* mutant complemented with intact *lipB [lipB(lipB)]* (H) *csaA* mutant complemented with intact *csaA [csaA(csaA)]*. Arrows highlight lacunae. Scale bar represents 500 nm.

As shown in Figure 12A, we observed a layer of cationic ferritin-stained material around parent strain KK01, as evidenced by the enhanced electron density. In the *ctrA* mutant we observed a lack of cationic ferritin-stained surface polysaccharide (Figure 12B). Instead, this mutant had intracellular pools of polysaccharide (lacunae) that appeared to be membrane associated, likely indicating that the intracellular polysaccharide is assembled and lipidated but is unable to be exported. In the *lipA* (Figure 12C) and *lipB* (Figure 12D) mutants,

we also observed a lack of surface capsule and the presence of lacunae. Interestingly, in these mutants the lacunae were in the interior of the cell and were not associated with the inner membrane, suggesting that the intracellular polysaccharide is unable to link to the inner membrane when LipA or LipB is absent, as observed in *E. coli* when KpsS or KpsC is absent [19]. In the *csaA* mutant (Figure 12E), we observed a lack of surface capsule and a lack of lacunae, supporting the conclusion that *csaA* plays a role in capsule synthesis.

All of the complemented strains had a restoration of surface capsule as assessed by cationic ferritin staining of surface polysaccharide, with some strain-to-strain variability in the quantity of capsule. Complementation of *lipA* (Figure 12F) resulted in an even layer of cationic ferritin staining on the cell surface despite some persistence of the intracellular pools. Complementation of *lipB* (Figure 12G) resulted in a layer of cationic ferritin that resembled the parent KK01 and small lacunae. Complementation of *csaA* (Figure 12H) resulted in an interrupted layer of cationic ferritin.

3.3.3 Mutation of the CsaA DXD or HP motif results in loss of polysaccharide capsule

Given the novelty of the CsaA glycosyltransferase, we used BLAST and PHYRE2 to compare its amino acid sequence and predicted protein structure to other known glycosyltransferases. At the N terminus of CsaA we found a GT-A type glycosyltransferase superfamily domain that has homology to the N terminus alpha-n-2 acetylgalactosaminyltransferase-t1, which catalyzes the transfer of alpha-N-acetylgalactosamine from UDP-GalNAc to Ser or Thr residues of core proteins to form the Tn antigen (GalNAc-alpha-1-O-Ser/Thr) in mice, suggesting that CsaA is a GalNAc tranferase (Fritz et al. 2004). In support of this hypothesis, CsaA has Asp residues at positions 99 and 101, similar to the DXD motif in GT-A structural superfamily glycosyltransferases (Breton et al. 2006). To assess whether these Asp residues represent a critical DXD domain, we mutated these residues and examined the effect on encapsulation.

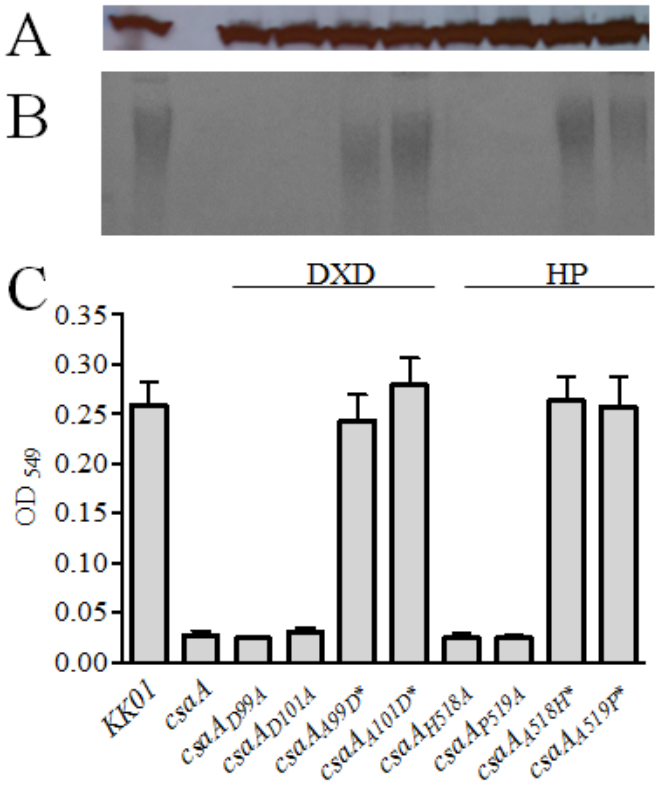

Figure 13: Characterization of the CsaA glycosyltransferase domain mutations.

(A) CsaA Western blot analysis of total membrane preparations from *K. kingae* strains. (B) Alcian blue staining of acid extracted capsule preparations resolved on an SDS-PAGE gel. (C) TBA reactivity of acid extracted capsule preparations. Reversions are noted with an asterisk. DXD refers to the Asp-X-Asp motif, and HP refers to the His-Pro motif.

Mutation of either Asp residue to Ala resulted in a loss of surface-extractable alcian blue staining and TBA reactive material. Reversion of each Ala back to Asp restored capsule production (Figure 13B and C). In the middle region of CsaA we found a capsule synthesis domain with homology to the *Acinetobacter baumannii* WaaA 3-deoxy-d-manno-octulosonic-acid (Kdo)

transferase, which is responsible for the addition of Kdo from the activated CMP-Kdo to the 4′-phosphorylated lipid A precursor (Schmidt et al. 2012, Smyth et al. 2013, Kelley et al. 2015). This domain contains a His residue at position 518 and a Pro residue at position 519, suggesting an HP motif similar to the HP motif present in some sialytransferases and the KpsC/LipA and KpsS/LipB βKdo transferases (Freiberger et al. 2007, Willis et al. 2013). As shown in Figure 13B, mutation of either the His at position 518 or the Pro at position 519 to Ala resulted in loss of encapsulation. Reversion of these mutations restored encapsulation (Figure 13B and C). None of the introduced mutations affected the CsaA protein level as assessed by Western blot analysis (Figure 13A). Together, these results indicate that the N-terminal and middle regions of CsaA likely function together in synthesis of the GalNAc-Kdo polysaccharide capsule.

3.3.4 Capsule is required for *K. kingae* virulence in a juvenile rat infection model

To begin to address the role of capsule in *K. kingae* virulence, we took advantage of the previously described juvenile rat infection model (Basmaci et al. 2012). Five-day-old Sprague-Dawley rats in groups of eight were injected via the intraperitoneal route with $7.5x10^7$ cfu of *K. kingae* strains KK01, *ctrA*, *csaA*, or

csaA(*csaA*) or with PBS only as a control. Among pups infected with an encapsulated strain [KK01 or *csaA*(*csaA*)], all except one succumbed to infection during the five day observation period [7/8 pups infected with KK01 and 8/8 pups infected with *csaA*(*csaA*)] (Figure 14).

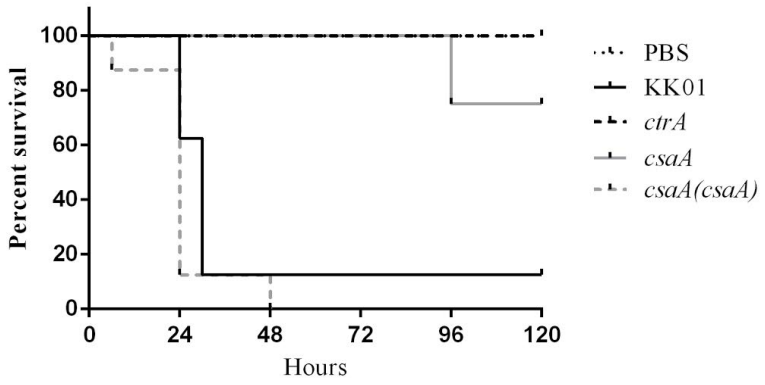

Figure 14: Effect of encapsulation on virulence in the juvenile rat intraperitoneal infection model.

Kaplan-Meyer survival curves of groups of eight 5-day-old Sprague-Dawley rats injected via the intraperitoneal route with 100 µl of PBS (black dotted line) or 7.5x10^7 cfu of strains KK01 (black solid line), *ctrA* (black dashed line), *csaA* (grey line), or *csaA*(*csaA*) (dashed grey line) in 100 µl.

Conversely, among pups infected with a non-encapsulated strain (*ctrA* or *csaA*), only 2 of 16 died (0/8 pups infected with *ctrA* and 2/8 pups infected with *csaA*). The 2 pups that died due to *csaA* succumbed at 96 hrs post-infection, while all of the 15 pups that died due to an encapsulated strain succumbed within 48 hrs of infection (Figure 14). These results indicate that an intact *csaA* and

encapsulation are essential for full *K. kingae* virulence in the juvenile rat infection model.

3.4 Discussion

The pathogenesis of *K. kingae* disease is believed to begin with asymptomatic colonization of the upper respiratory tract, mediated via type IV pili and a trimeric autotransporter adhesin called Knh. In prototype *K. kingae* strain 269-492, we have demonstrated that Knh is masked by a polysaccharide capsule with the structure: [→3)-β-Gal*p*NAc-(1→5)-β-Kdo*p*-(2→]$_n$. Given this unusual structure and the likely role of the capsule in *K. kingae* virulence, we set out to characterize the determinants of capsule biosynthesis. In the current study, we used a transposon screen and identified genes involved in the synthesis, assembly, and export of the *K. kingae* polysaccharide capsule. Targeted gene deletion and complementation studies established that the *csaA* polysaccharide synthesis gene, the *lipA* and *lipB* capsule assembly genes, and the *ctrABCD* capsule export genes are required for encapsulation. Point mutations in *csaA* established that the CsaA glycosyltransferase is a novel bifunctional enzyme that

creates a polymer of GalNAc and Kdo and is essential for creating both the β-Gal*p*NAc-(1→5)-β-Kdo*p* linkage and the β-Kdo*p*-(2→3)-β-Gal*p*NAc linkage.

Our results established that the *csaA, lipA, lipB,* and *ctrABCD* loci are located in four disparate regions of the chromosome and are surrounded by genes with no clear predicted function in capsule expression. While capsule genes are typically clustered together at a single locus on the chromosome, there are reports of atypical genetic arrangements of capsule genes in other bacteria. For example, a transposon screen in *Vibrio vulnificus* identified a region with 4 ORFs essential for capsule expression outside of the central capsule polysaccharide locus (Smith et al. 2003). Similarly, a glycosyltransferase responsible for linking the heparosan backbone in the *Pasteurella multocida* capsule polysaccharide is encoded by a gene outside the capsule biosynthesis locus and is flanked by two metabolic genes with no known role in capsule polymer synthesis (alanine racemase and glucose-6-phosphate isomerase) (DeAngelis et al. 2004). A glycosyltransferase required for encapsulation in *Xanthomonas citri* subsp. citri is encoded by the *gpsX* gene, which is also outside the locus with the other capsule biosynthesis genes (Li et al. 2012). These examples highlight that capsule synthesis genes may reside in distinct regions of

the chromosome and underscore the importance of understanding how the *K. kingae* capsule genes are coordinately regulated.

In recent work, Willis et al. demonstrated that KpsS (LipB) and KpsC (LipA) in *E. coli* and *N. meningitidis* are βKdo transferases that synthesize a poly-βKdo linker onto a phosphatidylglycerol (PG) lipid moiety, serving as the capsule membrane anchor (Willis et al. 2013). KpsS/LipB adds a single βKdo residue to PG, and KpsC/LipA adds a short chain of βKdo residues onto the first βKdo. Current evidence suggests that the capsule polymer is then assembled onto the terminal βKdo residue of the poly-βKdo linker (Willis et al. 2013). Based on alcian blue straining of capsule extracts, TBA analysis, and transmission electron microscopy data, we conclude that LipA and LipB likely serve the same roles in *K. kingae*. The phenotypes of the *lipA* and *lipB* deletion mutants as assessed by TBA assays and transmission electron microscopy are consistent with observations in other organisms (Cieslewicz et al. 1996, Steenbergen et al. 2008, Willis et al. 2013), including the lack of surface capsule and the presence of cytosolic lacunae. It is speculated that these lacunae result from aberrant initiation events, allowing a non-lipidated polymer to form and accumulate in the cytoplasm (Steenbergen et al. 2008, Willis et al. 2013).

Comparison of the *K. kingae lipA* complemented strain with the parent strain revealed no appreciable change in polysaccharide size on SDS-PAGE gels. Interestingly, functional complementation of an *E. coli kpsC* mutation with either *E. coli kpsC* or *N. meningitidis lipA* resulted in a longer polysaccharide. Comparison of the *K. kingae lipB* complemented strain with the parent strain revealed a difference in mobility of the polysaccharide, suggesting that the polysaccharide length might be altered in this strain. However, the *E. coli kpsS* mutation complemented with either *E. coli kpsS* or *N. meningitidis lipB* did not result in a shift in mobility (Willis et al. 2013). One possible explanation for the difference in polysaccharide mobility observed in the *lipB* complemented strain is that the stoichiometry between the polysaccharide synthesis and transporter components may be altered from the wild type state, a factor known to be important for capsule expression (Whitfield et al. 1997). Given that complemented genes were expressed under an IPTG-inducible promoter, competition between synthesis and transport could have affected our complementation strategy. Changes in transcriptional levels or stability could also alter other unknown targets, affecting capsule in subtle ways that we could not appreciate in our assays.

Based on homology analysis, the CsaA glycosyltransferase contains a putative GalNAc transferase domain and a putative βKdo transferase domain. The presence of these two domains suggests that CsaA is a bifunctional enzyme and is essential for synthesizing the GalNAc-βKdo-containing capsule polysaccharide, creating both the β-Gal*p*NAc-(1→5)-β-Kdo*p* linkage and the β-Kdo*p*-(2→3)-β-Gal*p*NAc linkage. Several other examples of bacterial glycosyltransferases with bifunctional activities have been identified over the years. In particular, the *Streptococcus pyogenes* Cap3B synthase (Arrecubieta et al. 1996) and HasA hyaluronan synthase have bifunctional activity (DeAngelis et al. 1994). In addition, the *E. coli* KfiC protein is involved in the biosynthesis of the K5 capsule containing both α- and β-glycosyltransferase activities responsible for the sequential addition of glucuronic acid and N-acetylglucosamine to the growing polysaccharide chain (Griffiths et al. 1998). In *S. pneumoniae*, the Tts β-gludosyltransferase has been suggested to catalyze the 1,2 and 1,3 β-glucosidic capsule linkages (Llull et al. 2001).

The *mariner* transposon mutagenesis strategy used in this study generated approximately 10,000 transposon insertion mutants. A thorough screen of this library identified the *ctrABCD* locus, *lipA*, *lipB*, and *csaA* as the only non-essential

genes required for surface capsule expression in *K. kingae* strain 269-492. Interestingly, most capsule synthesis loci in group 2 *E. coli* contain a gene encoding a putative glycosyltransferase of unknown function (Willis et al. 2013). Willis et al. have speculated that this gene product is a capsule type-specific component of the synthesis machinery necessary to add the first sugar residue onto the terminal βKdo residue of the poly-βKdo linker to serve as an appropriate acceptor for synthesis of the capsular polymer repeating unit (Willis et al. 2013). We speculate that the N-terminal domain of CsaA is able to directly catalyze addition of GalNAc onto the terminal βKdo residue of the poly-βKdo linker, in particular given that the normal acceptor sugar for the GalNAc transferase activity is βKdo, which is added by the middle region domain of CsaA. The possibility that CsaA by itself is sufficient for the synthesis of the capsule polymer onto the poly-βKdo linker as well as polymerization of the repeating unit would explain why we did not identify any other glycosyltransferases in our screen for non-encapsulated mutants. Other genes involved in modulating capsule length or levels of expression may not have been identified in our screen for various reasons, including lethality, redundancy,

compensatory mutations, or partial phenotypes that we could not appreciate using our screening approach.

Most encapsulated bacteria exhibit intraspecies capsule-type diversity, with different strains producing capsules composed of a variety of sugars and glycosidic linkages. This phenomenon has been well-characterized for many human pathogens, including *E. coli*, *N. meningitidis*, *H. influenzae*, and *S. pneumoniae*, among others. Bendaoud et al. reported a different capsule polysaccharide in *K. kingae* strain PYKK181 with the structure [→6)-α-D-GlcNAc*p*-(1→5)-β-Kdo-(2→]$_n$ (Bendaoud et al. 2011), indicating that *K. kingae* expresses at least two distinct capsule types. In future studies, it will be important to examine larger collections of clinical isolates to define the diversity of capsule types in *K. kingae*.

4. Diversity of capsular polysaccharide among colonizing and invasive isolates of *Kingella kingae*

4.1 Introduction

Kingella kingae is being recognized increasingly as an important cause of osteoarticular infections in young children, reflecting more sensitive cultivation techniques and increased availability of molecular-based diagnostic tools. Among the key surface factors expressed by *K. kingae* is a polysaccharide capsule. Capsules are recognized as important virulence factors in many gram-positive and negative-bacteria and have a variety of functions, including inhibiting complement deposition, reducing phagocytosis, and preventing desiccation. Polysaccharide capsules also have served as effective vaccine antigens that have reduced morbidity and mortality worldwide. Widespread use of conjugate capsule vaccines has dramatically reduced the incidence of disease caused by *Streptococcus pneumoniae* (Albrich et al. 2007), *Haemophilus influenzae* type b (Schuchat et al. 1997), and *Neisseria meningitidis* (Bilukha et al. 2005).

In previous work, we described the structure of the capsule expressed by *K. kingae* strain 296-492 as a polymer of →3)-β-Gal*p*NAc-(1→5)-β-Kdo*p*-(2→ and identified the genes essential for capsule synthesis, assembly, and export (Starr et

al. 2013)(Starr et al, submitted). In the course of this work, we established that the CsaA glycosyltransferase contains both a GalNAc-transferase domain and a Kdo-transferase domain and is sufficient for creating both the β-Gal*p*NAc-(1→5)-β-Kdo*p* linkage and the β-Kdo*p*-(2→3)-β-Gal*p*NAc linkage. In addition, the CsaA glycosyltransferase may catalyze addition of β-Gal*p*NAc to the terminal βKdo residue of the poly-βKdo linker (Starr et al, submitted).

Bendaoud et al. recently reported that the structure of the capsule isolated from the surface of another *K. kingae* strain is a polymer of →6)-α-d-GlcNAcp-(1→5)-β-d-OclAp-(2→, suggesting the existence of least at least two different *K. kingae* capsule types. The presence of multiple capsule types is well documented in a variety of bacterial species, with examples including *S. pneumoniae*, *N. meningitidis*, *H. influenzae,* and *K. pneumoniae*. In some cases, specific capsule types are associated more commonly with carriage or more commonly with invasive disease. For example, there are at least 90 different *S. pneumoniae* capsular types, but 23 types account for more than 90% of invasive pneumococcal disease worldwide (Feldman et al. 1997, Weinberger et al. 2009). Similarly, in *N. meningitidis* 6 of the 13 characterized capsule types are responsible for 90% of invasive disease worldwide (Peltola 1983, Harrison et al.

2009). In *K. pneumoniae* capsule types 1, 3, and 4 are associated with infection of the upper respiratory tract, and capsule types 9 and 10 are associated with infection of the urinary tract (Riser et al. 1981).

In this study, we set out to define the genetic and structural basis of capsule diversity in a large collection of *K. kingae* clinical isolates from Israel. In addition, we examined the relationship between specific capsule types and clinical presentations.

4.2 Methods

Bacterial strains and growth conditions

The strains used in this study are listed in Table 6. *K. kingae* strain 269–492 was isolated from the joint fluid of a child with septic arthritis at St. Louis Children's Hospital, St. Louis, MO.

K. kingae strain KK01 is a stable natural variant of strain 269–492 that grows as a non-spreading, non-corroding colony type and was used as the primary strain in this study (Kehl-Fie et al. 2010). *K. kingae* and *E. coli* strains were grown and stored as previously described (Porsch et al. 2012, Starr et al. 2013).

Table 6: Strains used in this study

Strain	Description	Source
269-492	*K. kingae* isolate from St. Louis Children's Hospital	(Kehl-Fie et al. 2010)
KK01	Nonspreading/noncorroding derivative of 269-492	(Kehl-Fie et al. 2010)
PYKK121	Clonal group K isolate from case of bacteremia	Clinical
PYKK89	Clonal group K isolate from case of bacteremia	Clinical
PYKK93	Clonal group P isolate from case of bacteremia	Clinical
PYKK98	Clonal group B isolate from case of bacteremia	Clinical
PYKK060	Clonal group D isolate from case of endocarditis	Clinical
PYKK58	Clonal group N isolate from case of septic arthritis	Clinical
PYKK59	Clonal group N isolate from case of bacteremia	Clinical
D7674	Clonal group R from a healthy carrier	Clinical
E3339	Clonal group F isolate from a healthy carrier	Clinical
D7453	Clonal group G isolate from a healthy carrier	Clinical
BB270	Clonal group U isolate from a healthy carrier	Clinical
KK01*csa*	Contains *csaA* deletion	Starr et al., 2016 in preparation

PYKK58*csb*	Contains capsule synthesis locus *csbABC* deletion	This study
PYKK60*csc*	Contains capsule synthesis locus *cscABC* deletion	This study
BB270*csd*	Contains capsule synthesis locus *csdABC* deletion	This study
KK01*csa(csa)*	Complement of *csa* locus in KK01Δ*csa*	Starr et al., 2016 in preparation
PYKK58*csb(csb)*	Complement of *csb* locus in PYKK58Δ*csb*	This study
PYKK60*csc(csc)*	Complement of *csc* locus in PYKK60Δ*csc*	This study
BB270*csd(csd)*	Complement of *csd* locus in BB270Δ*csd*	This study
KK01SwapEmpty	Contains the capsule synthesis locus flanking genes and a deletion of the *csaA* region.	This study
KK01Swap*csa*	KK01SwapEmpty with *csa* locus recombined at the X site	This study
KK01Swap*csb*	KK01SwapEmpty with *csb* locus recombined at the X site	This study
KK01Swap*csc*	KK01SwapEmpty with *csc* locus recombined at the X site	This study
KK01Swap*csd*	KK01SwapEmpty with *csd* locus recombined at the X site	This study
***E. coli* plasmids**		
pUC19*pam*::*ermC*		(Starr et al. 2013)
pSwapEmpty	Contains the capsule synthesis locus flanking genes and a deletion of the csl variable region	This study
pSwap*csa*	pSwapEmpty with *csa* locus	This study
pSwap*csb*	pSwapEmpty with *csb* locus	This study
pSwap*csc*	pSwapEmpty with *csc* locus	This study
pSwap*csd*	pSwapEmpty with *csd* locus	This study

Clinical isolate strain collection

Kingella kingae isolates were chosen from a large assortment of Israeli strains gathered at the Soroka University Medical Center since the early 1990s. The collection comprises isolates recovered from patients with a variety of invasive infections and organisms isolated from healthy respiratory carriers in the course of epidemiological studies on *K. kingae* carriage and transmission. A total of >200 invasive *K. kingae* strains and >600 carriage strains have been typed by pulsed field gel electrophoresis (PFGE) (Amit et al. 2012), and a sample of the predominant PFGE clones has been further characterized by MLST and *rtx*A gene sequencing (Basmaci et al. 2012). Because PFGE typing is based on a random probing of the entire bacterial genome, including core and accessory genes, whereas MLST explores housekeeping core genes, it was assumed that genotyping data could be employed to guarantee the choice of a representative sample of the *K. kingae* population for capsule analysis.

Based on genotyping results, strains were selected to meet the following study goals while studying a manageable number of strains isolated over more than two decades: inclusion of clones that collectively cause the vast majority of

invasive infections in Israel (Amit et al. 2012), inclusion of clones mostly associated with asymptomatic pharyngeal colonization (Yagupsky et al. 2009), inclusion of clones exhibiting significant statistical association with specific clinical syndromes at the population level (Amit et al. 2012), strains isolated from patients with a variety of clinical syndromes (bacteremia, skeletal system infection, or endocarditis) (Amit et al. 2012), strains associated with clusters of disease in daycare center facilities (Yagupsky 2014).

Molecular methods and strain manipulation

Targeted gene disruptions and complementation constructs in *K. kingae* were generated as previously described (Kehl-Fie et al. 2007, Porsch et al. 2012). Briefly, plasmid-based gene disruption constructs were created in *E. coli*, linearized, and introduced into *K. kingae* using natural transformation. Transformants were recovered by selectively plating on chocolate agar plates with the appropriate antibiotic. Gene disruptions and complementation constructs were confirmed by PCR.

To delete the capsule synthesis locus, we generated plasmid pSwapEmpty. Briefly, fragments of homologous recombination targeting

sequence corresponding to ~1 kb upstream of *csaA* and ~1 kb downstream of *csaA* were PCR amplified from strain KK01 genomic DNA using primers pSwapFor5'/pSwapRev5' and pSwapFor3'/pSwapRev3', respectively, and were cloned into pUC19. A kanamycin resistance cassette was then ligated into the pUC19 KpnI site, which is located between the cloned upstream and downstream homologous recombination targeting sequences, to generate pSwapEmpty. The plasmid was linearized with NdeI and was transformed into strain KK01.

To create the complementation/capsule swap constructs, the capsule synthesis loci were PCR amplified as follows: for the *csa* locus, using genomic DNA from strain KK01 and primers csaswapFor/csaswapRev; for the *csb* locus, using genomic DNA from strain PYKK58 and primers csbswapFor/csbswapRev; for the *csc* locus, using genomic DNA from strain PYKK060 and primers cscswapFor/cscswapRev; and for the *csd* locus, using genomic DNA from strain BB270 and primers csdswapFor/csdswapRev. The *csa* and *csb* locus amplicons were cloned into pSwapEmpty using standard restriction cloning, generating pSwap*csa* and pSwap*csb*, respectively. The *csc* and *csd* amplicons were cloned

into pSwapEmpty using the Gibson Assembly Cloning kit (New England Biolabs), generating pSwap*csc* and pSwap*csd*, respectively.

For capsule swaps we transformed each swap construct (pSwap*csa*, pSwap*csb*, pSwap*csc*, or pSwap*csd*) harboring a kanamycin cassette into the nonencapsulated isogenic strain KK01*csa*(Erm^R) and screened for loss of Erm^R and gain of Kan^R. For capsule synthesis locus complementation, the capsule swap plasmids pSwap*csa*, pSwap*csb*, pSwap*csc*, and pSwap*csd* were transformed into KK01*csa*, PYKK58*csb*, PYKK60*csc*, and BB270*csd*, respectively, using the unmarked transformation protocol described below.

To generate unmarked gene disruptions and complements, we used the following procedure without antibiotic selection. First, *K. kingae* was grown overnight on solid medium, then resuspended in BHI broth containing 50 mM $MgCl_2$ to an OD_{600} of 0.7 and diluted 1:25 in BHI broth. The initial dilution was then serially diluted 1:4 a total of 9 times. From each of the 5^{th}, 6th, 7^{th}, and 8^{th} dilutions, 5 µl of diluted inoculum was transferred to a microfuge tube containing 5 µl of plasmid at a concentration of 50 ng/µl. The 10 µl total mixture was then plated on chocolate plates and allowed to dry in ambient air conditions

(approximately 5 minutes) before placement into the CO_2 incubator at 37°C. Single colonies were screened by PCR for recombination at the locus of interest.

Polysaccharide capsule extraction, purification, and analysis

In preparation for extraction and purification of capsule, the *PAM* locus involved in synthesis of the galactan exopolysaccharide was deleted from the relevant strains (Starr et al. 2013). Extraction and purification of capsule material was performed as previously described, and purified material was sent to the University of Georgia Complex Carbohydrate Research Center in Athens, GA for composition and linkage analysis (Porsch et al. 2012, Starr et al. 2013).

To visualize capsule migration pattern, extracts were run on 7.5% SDS-PAGE gels and stained with alcian blue as previously described (Porsch et al. 2012, Starr et al. 2013).

Genetic screen of capsule synthesis loci

Published *K. kingae* sequence outside of the capsule synthesis locus was used to design flanking primers HemBFor and ArgRev in the *hemB* (delta aminolevulinic-acid dehydratase) and *arg* (arginine-succinate synthase) genes

flanking the glycosyltransferase (Table 7). PCR amplicons were sequenced, and the resulting sequence was the basis for design of interior primers specific for each of the 4 capsule synthesis loci. To screen for presence of each identified locus, we used both universal flanking primers that amplified all capsule loci and locus-specific primers that annealed to the interior portion of each locus. The presence of either *csaA*, *csbABC*, *cscABC* or *csdABC* (the *csa*, *csb*, *csc*, or *csd* capsule synthesis locus) was determined by PCR amplification using interior primers (see Table 7) and confirmed by determining the size and restriction map of the flanking primer amplicon.

Restriction analysis

To obtain restriction digest patterns, PCR products were amplified using the primers HemBFor and ArgRev listed in Table 7 in a total reaction volume of 25 µl. 2.5 µl of 10X digestion buffer and 1 µl of Nru1 enzyme (New England Biolabs) were mixed with PCR products and incubated overnight at 37°C. Digests were resolved on a 1.2% agarose gel and visualized for banding pattern.

Xylanase Pretreatment

Total amount of the sample was digested with endo-1,4-β-Xylanase M1 from *Trichoderma viride* (Megazyme). Digested sample was dialyzed through 10KDa membrane, and the retentate was freeze-dried.

Table 7: Primers used in this study

Gene disruption primers	Sequence
HemBFor	CATTGGCGCAATCCGTCAGG
ArgRev	CTTGGGACGTTTGCTGTATC
csaScreenFor	AAACGAGCCAAATTTTTTAC
csaScreenRev	GCCTTATCTGTCATTATTCC
csbScreenFor	CCTTGGCACGCAAAGCATAG
csbScreenRev	AGCGCTTTATCTACCACCAC
cscScreenFor	AACGAAAGTCATTCTAGATT
cscScreenRev	CAGGGCTTCATTCCAAAGTG
csdScreenFor	CATTGTTACCGATAATCAAATACC
csdScreenRev	AGCGACTATATGCATGCTCC
pSwapFor5′	AGCTGAATTCCAGACGAAGACGACTACAAC
pSwapRev5′	AGCTGGTACCTTATTTAGTTTCCAACTTCGGAATC
pSwapFor3′	ACGTGTCGACTGCAGGCTGCTTTTTATTTATTTG
pSwapRev3′	ACGTAAGCTTGACGAACGCACCAAATTACGC
csaswapFor	ACGTGGTACCTTATCATAGAAAGCATTTCTTACT TTTGTATTATG
csaswapRev	ACGTGGATCCCTTTTTTGTTGAGTTTAAAGTGCAG
csbswapFor	ACGTGGTACCGATTTTTTGAGATGCAAATCAACG TC
csbswapRev	ACGTTCTAGACTTTTTGTTGAGTTTAAAGTGCAG G
cscswapFor	AAATAAGGTACCCGGGATATATAAGATGCGGAT

	ATTTTATATATTAATTTAATATC
cscswapRev	CGGTCGACTCTAGAGACCTTTGCAAAACTACCATG
csdswapFor	AAATAAGGTACCCGGGAACAACATATTCTGAAAATATCAATC
csdswapRev	CGGTCGACTCTAGAGGGGGCTATCCTAGATAAC
lipAscreenFor	ATTGCCCTGCTTGCATTTCG
lipAscreenRev	TCTTCCAACGCCACATACGG
lipBscreenFor	ATACGCCGATTGGTTGCGAG
lipBscreenRev	CCCGACAACGAAACGATAAG
ctrABCDscreenFor	CCGTTATCCAACACCATAGC
ctrABCDscreenRev	CCGTTATCCAACACCATAGC

De-O-Acetylation

The sample solution (~1.5mg/0.5ml) was adjusted to pH 11.0 by addition of 2M ammonium hydroxide solution and kept for overnight at room temperature. Resulting solution was dialyzed through MWCO 3.5KDa membrane to remove salts. The retentate was then deuterium-exchanged for NMR- analysis.

NMR Spectroscopy

The retentate after xylanase digestion (total amount) was deuterium exchanged 2 times by lyophilization in D_2O. Dry residue was re-dissolved in 300 ◎l D2O (99.96%, Cambridge Isotopes) and placed in a 3-mm OD tube. 1-D Proton and 2-D COSY, TOCSY, HSQC, HMBC and NOESY spectra were acquired at 55°C on Varian Inova 600 MHz spectrometer equipped with cryoprobe using standard Varian pulse sequences. Chemical shifts were measured relative to internal acetone peak (δ_H/δ_C =2.22/33 ppm).

Linkage Analysis of the Residues

For glycosyl linkage analysis, the samples were permethylated, depolymerized, reduced, and acetylated; the resultant partially methylated alditol acetates (PMAAs) analyzed by gas chromatography-mass spectrometry (GC-MS) as described by Heiss et al (2009).

Approximately 1 mg of the sample was used for linkage analysis. The samples were suspended in 200 μl of dimethyl sulfoxide and left to stir for 1 day. Permethylation was effected by two rounds of treatment with sodium hydroxide (15 min) and methyl iodide (45 min). Following sample workup, the

permethylated material was hydrolyzed using 2 M TFA (2 h in sealed tube at 121°C), reduced with NaBD4, and acetylated using acetic anhydride/TFA. The resulting PMAAs were analyzed on an Agilent 7890A GC interfaced to a 5975C MSD (mass selective detector, electron impact ionization mode); separation was performed on a 30 m Supelco SP-2331 bonded phase fused silica capillary column.

D and L determination

Sample (1/2 amount of the total sample received) was freeze-dried and hydrolyzed in 2M TFA (500µl) at 120°C for 1.5 hours. The hydrolysate was dissolved in 200µl S-(+)-2-Butanol (Fluka 19025), 15◎l acetyl chloride (Aldrich 236691) was added, and nitrogen gas was bubbled through the solution for 30 seconds. The mixture was capped tightly and incubated at 80°C for 16 hours. After incubation, the mixture was dried down under N2 stream, and then absolute methanol was added to dry again. To the dry sample, 250 µl TMS reagent (Tri-Sil (Pierce) was added and derivatization was carried out at 121ºC for 20 min.

The same procedure was applied to authentic monosaccharide standards. Two sets of standards were derivatized to which either S-(+)-2-Butanol or R-(-)-2-Butanol was added separately. Then the derivatization was carried out as described above for the sample. The derivatized sample and standards were analyzed on Agilent 5975C GC interfaced with 7890A MS detector.

4.3 Results

4.3.1 Four capsule synthesis loci are present in a diverse collection of K. kingae clinical isolates

In initial experiments, we screened a collection of 427 Israeli invasive and carrier isolates for the presence of *csaA*, the capsule synthesis gene in our prototype *K. kingae* strain KK01. Using *csaA*-specific primers and PCR, we found that only 48 percent of all isolates contained the *csaA* gene. We hypothesized that other capsule types exist and that the region containing *csaA* represents the *K. kingae* capsule synthesis locus and differs in genetic content depending on the enzymatic machinery required to synthesize a specific capsular polysaccharide structure. To test this hypothesis, we designed a forward primer annealing to *arg*, the gene upstream of *csaA* in strain KK01, and a reverse primer annealing to *hemB*, the gene downstream of *csaA* in strain KK01, to amplify across the

suspected capsule synthesis locus. As shown in Figure 15A, amplification across this locus in a group of representative isolates in the collection yielded four different amplicon sizes. Restriction mapping of these amplicons with NruI revealed similar banding patterns for strains with the same amplicon size (Figure 15B).

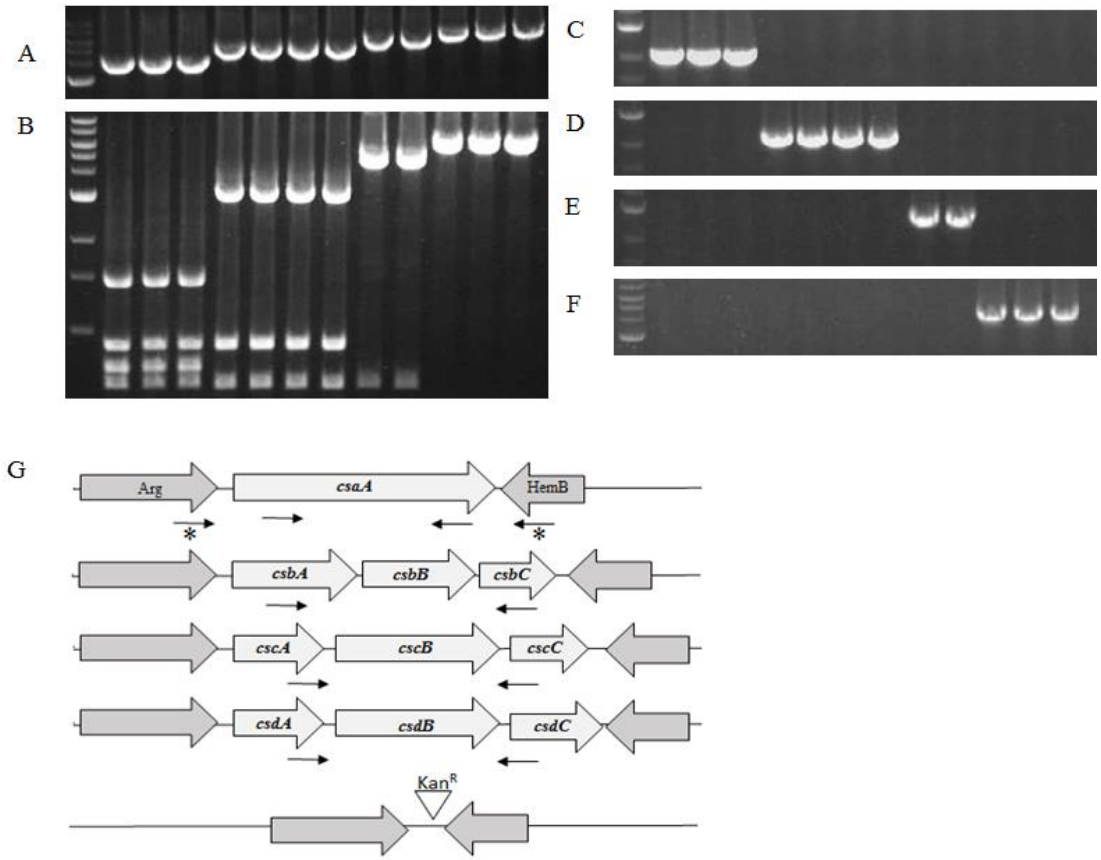

Figure 15: PCR screening of capsule synthesis genes reveals 4 loci

(A) PCR amplification across variable synthesis region using flanking primers produces three sized products. (B) NruI digest of *Arg*/*HemB* amplicon. (C) PCR amplification of *csa* region using internal primers. (D) PCR amplification of the *csb* region using internal primers. (E) PCR amplification of the *csc* region using internal primers. (F) PCR amplification of the *csd* region using internal primers. Lane 1, ladder; lane 2, KK01; lane 3, PYKK98; lane 4, PYKK93; lane 5, PYKK89; lane 6, PYKK121; lane 7, PYKK58; lane 8, PYKK59; lane 9, PYKK60; lane 10, D7674; lane 11, E3339; lane 12, D7453; lane 13, BB270. (G) Illustration of the 4 capsule synthesis loci and the engineered empty locus. Each locus shows the capsule synthesis genes unique to capsule type (light gray) and the highly homologous flanking regions shared among all strains (dark gray). Arrows with asterisks denote screening primers that bind in the homologous flanking regions, used to amplify across the flanking genes irrespective of internal

sequence. Arrows within each synthesis region (A-D) denote sequence specific screening primers unique to each region.

Nucleotide sequencing of the amplicons from multiple strains with the same amplicon size revealed an absolute correlation between the amplicon size and the specific gene or set of genes, indicating that there are four discrete amplicons and four discrete loci (Figure 15G). After determining the predicted open reading frames (ORFs) in each amplicon, we searched for the presence of predicted domains or motifs using BLASTP and PHYRE2. The ~3500 bp amplicon contained only the *csaA* gene (identical to our prototype strain KK01) and was named the *csa* locus. The ~4000 bp amplicon contained a gene encoding a predicted GT-B type glycosyltransferase with homology to a GlcNAc transferase (designated *csbA*), a gene encoding a putative capsule synthesis enzyme with homology to a Kdo transferase (designated *csbB*), and a gene encoding a putative enzyme with homology to an acetyltransferase (designated *csbC*) and was named the *csb* locus. The ~5000 bp amplicon contained two genes encoding putative enzymes with homology to halo-acid dehydrogenases (designated *cscA* and *cscB*) and a gene encoding a predicted glycosyltransferase (designated *cscC*) and was named the *csc* locus. The ~5500 bp amplicon

contained a gene encoding a predicted galactosyltransferase (*csdA*), a gene encoding a predicted GlcNAc transferase (*csdB*), and a gene encoding a predicted GT-A type glycosyltransferase (*csdC*) and was named the *csd* locus. Based on the sequence of the four unique loci, specific internal primer pairs were generated, producing locus specific amplicons, as shown in Figure 15C-F.

4.3.2 Capsule polysaccharide structure is associated with the presence of one of four capsule synthesis loci

To confirm that each of the four capsule synthesis loci is associated with a specific capsule type, we examined the glycosyl composition of purified polysaccharide capsule from representative strains that contain either the *csa*, *csb*, *csc*, or *csd* locus. As a first step, we deleted the *PAM* locus from these strains in order to eliminate contamination by the galactan exopolysaccharide produced by *K. kingae* (Starr et al. 2013). As summarized in Table 8, strains KK01, PYKK98, and PYKK93 harbor the *csa* locus and produce a capsule containing GalNAc and Kdo, which we named capsule type a.

Table 8: Association between capsule locus screening and capsule composition

Clinical isolate	Clinical Syndrome	Clonal group	PCR Result	GalNAC	GlcNAc	Ribose	Galactose	Kdo
KK01	Septic arthritis	H	*csaA*	•				•
PYKK98	Bacteremia/LTB	B	*csaA*	•				•
PYKK93	Bacteremia	P	*csaA*	•				•
PYKK89	Bacteremia	K	*csbABC*		•			•
PYKK121	Bacteremia	K	*csbABC*		•			•
PYKK58	Septic arthritis	N	*csbABC*		•			•
PYKK59	Bacteremia	N	*csbABC*		•			•
PYKK60	Endocarditis	D	*cscABC*			•		•
D7674	Carrier	R	*cscABC*			•		•
E3339	Carrier	F	*csdABC*		•		•	
D7453	Carrier	G	*csdABC*		•		•	
BB270	Carrier	U	*csdABC*		•		•	

Strains PYKK89, PYKK121, PYKK58, and PYKK59 harbor the *csb* locus and produce a capsule that contains GlcNAc and Kdo, which we named capsule type b. Strains PYKK60 and D7674 harbor the *csc* locus and produce a capsule that contains ribose and Kdo, which we named capsule type c. Finally, strains E3339, D7453, and BB270 contain the *csd* locus and produce a capsule that contains galactose and GlcNAc, which we named capsule type d. Considered together, these findings demonstrate complete agreement between the capsule synthesis

locus and capsule glycosyl composition, indicating that genetic screening of the capsule synthesis locus is predictive of capsule type.

4.3.3 Structural analysis reveals 3 distinct capsule structures

In previous work, we reported that the type a polysaccharide capsule is a polymer of →3)-β-Gal*p*NAc-(1→5)-β-Kdo*p*-(2→ (Porsch et al. 2012, Starr et al. 2013). To determine the chemical structure of the *K. kingae* type b, type c, and type d capsules, surface polysaccharide was purified from derivatives of strains PYKK58 (type b), PYKK60 (type c), and BB270 (type d) lacking the *PAM* locus and was analyzed with a combination of 1-D and 2-D NMR spectroscopy.

The type b capsule characteristic peaks in the 1-D proton spectrum included one major anomeric signal at 5.08 ppm, two signals corresponding to the H-3 protons of Kdo, one N-acetyl peak from GlcNAc, and one O-acetyl of unknown origin. Following the connectivities of GlcNAc from H-1 and Kdo from H-3 in the COSY and TOCSY spectra, together with the carbon chemical shifts derived from the HSQC spectrum, led to the complete assignment of the chemical shifts belonging to each residue (Table 9 and Figure 16A)

Table 9: Chemical shift assignments of the type b capsular polysaccharide

No.	Residue	Chemical shift (ppm)								NOE
		1	2	3	4	5	6	7	8	*HMBC*
A	6-α-Glc*p*NAc	5.08	3.99	3.81	3.59	4.26	3.96/3.70			B5
		100.9	*56.9*	*73.6*	*72.8*	*73.2*	***65.9***			*B5*
B	8-OAc-5-β-Kdo	-	-	1.97/2.42	3.83	4.02	3.83	3.91	4.42/4.27	
		175.0	***103.3***	*37.5*	*69.9*	***76.2***	*77.1*	*69.7*	*69.3*	*A6*

Carbon chemical shifts in italics, carbon resonances that are shifted downfield due to glycosylation are in bold

Due to the high molecular weight of the sample, the peaks in the spectra were broad and not suitable to measure proton-proton coupling constants for the determination of the anomeric configurations of GlcNAc and Kdo. However, the proton and carbon chemical shifts of the GlcNAc residue agreed with the α-configuration. Comparison of the chemical shifts of the Kdo residue with literature values (MacLean et al. 2009)showed that Kdo was in the β-configuration. The downfield displacement of carbon chemical shifts GlcNAc-C6 and Kdo-C5 indicated the linkage positions as 6-linked GlcNAc and 5-linked Kdo. The downfield displacement of the proton chemical shifts of Kdo-H8, together with the intensity (3H) and chemical shifts of the O-acetyl signal (2.13/23.1 ppm) indicated acetylation on O-8 of Kdo. Taken together, these NMR

results indicated that the polymer is composed of a disaccharide repeating unit with the structure [6)-α-Glc*p*NAc (1→5)-β-(8-OAc)Kdo*p*-(2→].

The type c capsule characteristic peaks in the 1-D proton spectrum included three anomeric signals at 5.34, 5.29, and 5.18 ppm, two pairs of signals corresponding to the H-3 protons of Kdo, an acetyl methyl signal, and several resonances in the carbohydrate ring region. The presence of two sets of Kdo signals of unequal intensity (ratio 2:3), together with the presence of an acetyl signal with an area three times that of the larger Kdo-H3 peak suggested that 60% of the Kdo residues in the polysaccharide were O-acetylated. To reduce the heterogeneity of the sample, we performed de-O-acetylation. The 1-D proton NMR spectrum of the de-O-acetylated material was simplified compared to the native polysaccharide and displayed only a single set of Kdo H-3 peaks. Following the connectivities of the three anomeric signals from H-1 and of Kdo from H-3 in the COSY and TOCSY spectra, together with the carbon chemical shifts derived from the HSQC spectrum revealed the presence of two 2-linked and one 3-linked β-ribofuranose residues, as well as one 4-linked β-Kdo residue (Table 10 and Figure 16B).

Table 10: Chemical shift assignments of the type c capsular polysaccharide

No.	Residue	Chemical shift (ppm)								NOE
		1	2	3	4	5	6	7	8	*HMBC*
A	3-β-Rib*f*	5.18	4.18	4.28		4.06	3.79/3.57			B2
		110.4	*77.3*	***77.3***		*84.4*	*65.7*			*B2*
B	2-β-Rib*f*	5.34	4.19	4.30		4.02	3.82/3.66			C2
		108.9	***83.5***	*73.1*		*86.0*	*65.4*			*C2*
C	2-β-Rib*f*	5.29	4.12	4.35		3.98	3.80/3.66			D4,5
		107.8	***83.5***	*72.4*		*85.9*	*64.4*			*D4*
D	4-β-Kdo	-	-	2.53/1.85	3.77	4.11	3.66	3.91	3.83/3.77	
		175.9	***104.5***	*35.1*	***77.7***	*67.7*	*76.3*	*71.9*	*66.9*	*A3*
D′	8-OAc-4-β-Kdo	-	-	2.48/1.89	3.80	4.13	3.89	4.05	4.40/4.27	
		175.5	***104.3***	*35.0*	***77.4***	*67.6*	*76.2*	*69.9*	*69.0*	*A3*

Carbon chemical shifts in italics, carbon resonances that are shifted downfield due to glycosylation are in bold

The proton and carbon chemical shifts of the ribose residues clearly indicated β-configuration. Comparison of the chemical shifts of the Kdo residue with literature values (MacLean et al. 2009) showed that Kdo also had the β-configuration. The NOESY and HMBC spectra showed inter-residue cross peaks allowing the determination of the sequence the four monosaccharide residues in the polysaccharide repeating unit. Thus, the three ribose anomeric protons were correlated with their respective non-reducing end neighbors in both NOESY and HMBC spectra, and C-2 of Kdo (and of 8-OAc-Kdo) was correlated in HMBC to H-3 of Residue C. Taken together, these NMR results indicated that the polymer

is composed of a tetrasaccharide repeating unit with the structure [3)-β-Ribf-(1→2)-β-Ribf-(1→2)-β-Ribf-(1→4)-β-Kdop-(2→].

The type d capsule glycosyl composition analysis was performed previously (data not shown) and showed mainly galactose (27 mol %) and GlcNAc (67 mol %). Characteristic peaks in the 1-D proton spectrum included 5 major anomeric signals at 5.39, 5.11, 4.72, 4.68, and 4.62 ppm and N-acetyl peaks from GlcNAc. Doublets at 4.72 and 4.68 ppm were assigned to β-galactosyl residues (Gal, C, C',) and 2 other doublets overlapping ~4.62-4.66 ppm were assigned to β-GlcNAc residues (B, B',). Anomeric configurations of GlcNAc and Gal residues were determined based on the proton-proton coupling constants. Following the connectivities of GlcNAc residues and the Gal from H-1 in the COSY and TOCSY spectra, together with the carbon chemical shifts derived from the HSQC spectrum led to almost complete assignment of the chemical shifts belonging to each residue (Table 11 and Figure 16C).

The downfield displacement of proton chemical shifts GlcNAc-H3 of Residues A and A' indicated that they were 3-linked. The downfield shift of GlcNAc-H3 and H4 signals of Residues B and B' indicated that they are 3,4-linked. The β-Gal chemical shifts indicated that the residue was not further

substituted. Inter-residue linkages were assigned from HMBC and NOESY correlations. An inter-residue NOE was observed between H-1 of Residue A (3-β-GlcNAc) and H-1 of Residue C (t-β-Gal), indicating that anomeric protons of the residues are in close proximity to each other.

The HMBC correlations and NOE between H1 of the B and H3 of A (3-β-GlcNAc) confirm that B (3,4-β-GlcNAc) is glycosidically linked to position 3 of Residue A. From the NOESY and HMBC data it is clear that the terminal β-Gal is 4-linked to B. However, the downfield shifts of H1 of Residue A and of H3 of Residue D were not explained, since no inter-residue linkages were observed in the NOESY and HMBC spectra. The downfield shifts suggested substitution by an electronegative group, such as acetate, sulfate, or phosphate. Therefore desulfation and deacetylation was performed on the sample. However, downfield shifts of H3 signal of residue B and H1 signal of residue A were still observed after treatments ruling out sulfation or acetylation as the cause of the downfield shift. This outcome strongly suggested that H3 of B and H1 of A were O-phosphorylated. To confirm this hypothesis, we acquired 31P NMR, both 1D and 2D-1H-31P-HMQC, which confirmed the presence of phosphate diester and its attachment points to the sugars (Figure 16).

Table 11: Chemical shift assignments of the type d capsular polysaccharide

No.	Residue	Chemical shift (ppm)						NOE
		1	2	3	4	5	6	*HMBC*
A	3-*α*-Glc*p*NAc	5.39	4.03	3.88	3.61	3.85	3.81/3.75	
		96.7	*55.6*	***81.6***	*71.1*	*75.4*	*63.5*	
A'	3-*α*-Glc*p*NAc	5.11	3.96	3.87	3.56	3.85	3.82/3.76	
		93.8	*55.8*	***81.6***	*71.5*	*75.5*	*63.5*	
B	3,4-β-Glc*p*NAc	4.62	4.13	4.30	4.39	3.75	3.84/3.77	A3
		104.1	*54.6*	***77.0***	***76.6***	*76.9*	*63.4*	*A3*
B'	3,4-β-Glc*p*NAc	4.60	4.11	4.28	4.38	3.75	3.84/3.77	A'3
		104.1	*54.6*	***77.0***	***76.6***	*76.9*	*63.4*	*A'3*
C	t-β-Gal*p*	4.68	3.57	3.66	3.91	3.68	3.77/3.75	B4
		106.3	*71*	*75.4*	*71.4*	*77.8*	*63.8*	*B4*
C'	t-β-Gal*p*	4.72	3.58	3.67	3.91	3.68	3.77/3.75	B'4
		106.1	*73.9*	*75.6*	*71.4*	*77.8*	*63.8*	*B'4*

Carbon chemical shifts in italics, carbon resonances that are shifted downfield due to glycosylation are in bold

Taken together, these NMR results strongly indicated that the polymer is composed of a trisaccharide repeating unit with the structure P-(O→3)[β-Gal-

(1→4)]-β-GlcNAc-(1→3)-α-GlcNAc-1-. Linkage and structural data for the type b, c, and d capsules are shown in Figure 16A-C and Table 9-11.

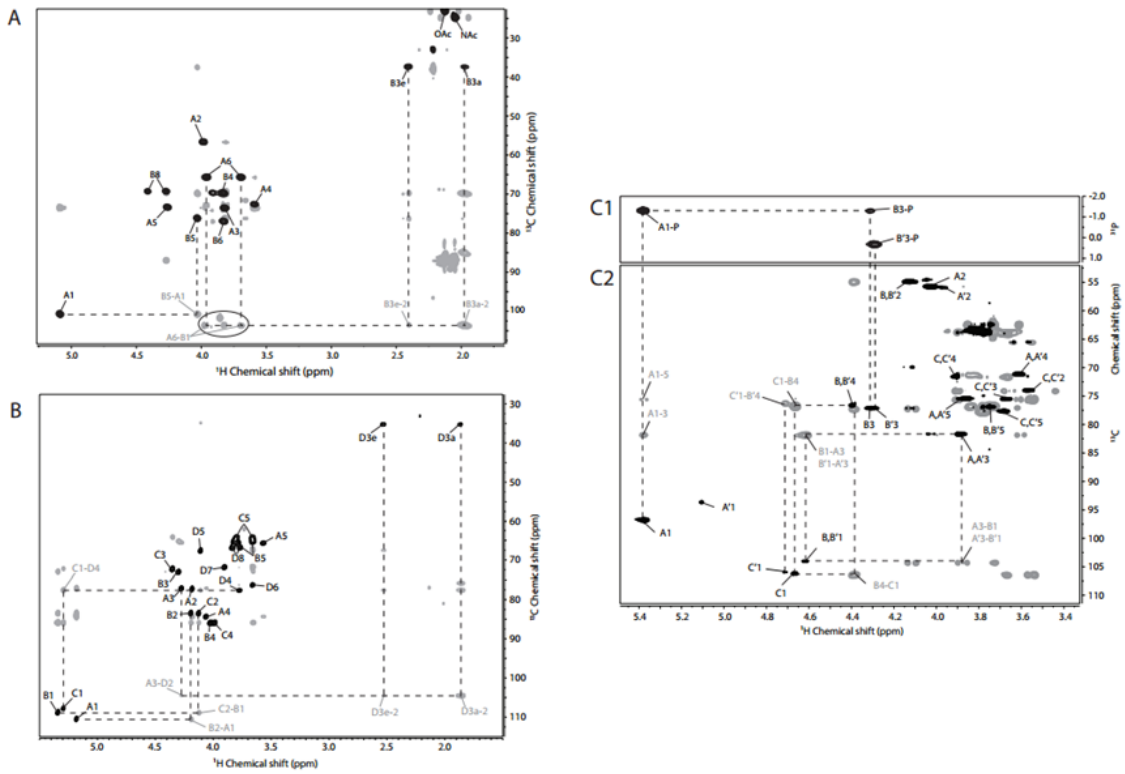

Figure 16: Two-dimensional NMR spectra of the polysaccharides isolated from *Kingella kingae* clinical isolates.

(A) Overlay of 2-D ^{1}H-^{13}C-HMQC (black) and HMBC (gray) NMR spectra of the type b capsule polysaccharide purified from the surface of PYKK58. The circled area is shown at a lower contour level because the peaks in this region were low in intensity. (B) Overlay of 2-D ^{1}H-^{13}C-HSQC (black) and HMBC (gray) NMR spectra of the Type C capsule polysaccharide purified from the surface of PYKK60. Since the Kdo residue does not have an anomeric proton, the HMBC cross peak from H3 to C2 is used to reference the Kdo anomeric carbons in (A) and (B). (C1) ^{1}H-^{31}P-HMQC spectrum of the type d capsule polysaccharide purified from the surface of BB270. This spectrum shows that the polysacccharide consisting of Residues A, B, and C contains a

phosphodiester linking together O-1 of A and O-3 of B and that the sequence consisting of Residues A′, B′, and C′ contains a phosphomonoester attached to O-3 of B′. (C2) Overlay of 2-D ^{1}H-^{13}C-HSQC (black) and HMBC (gray) NMR spectra of the type d capsule polysaccharide purified from the surface of BB270. Dotted lines and gray labels indicate the inter-residue HMBC correlations showing the connections between residues and thus specifying the sequence of the polysaccharide.

Structural analysis revealed that the type b capsule structure is a polymer of [6)-*α*-Glc*p*NAc (1→5)-β-(8-OAc)Kdo*p*-(2→]. The type c capsule structure is a polymer of [3)-β-Rib*f*-(1→2)-β-Rib*f*-(1→2)-β-Rib*f*-(1→4)-β-Kdo*p*-(2→]. The type d capsule structure is a polymer of P-(O→3)[β-Gal-(1→4)]-β-GlcNAc-(1→3)-*α*-GlcNAc-1-. A comparison of the structures of the type a, type b, type c, and type d capsules is shown in Figure 17.

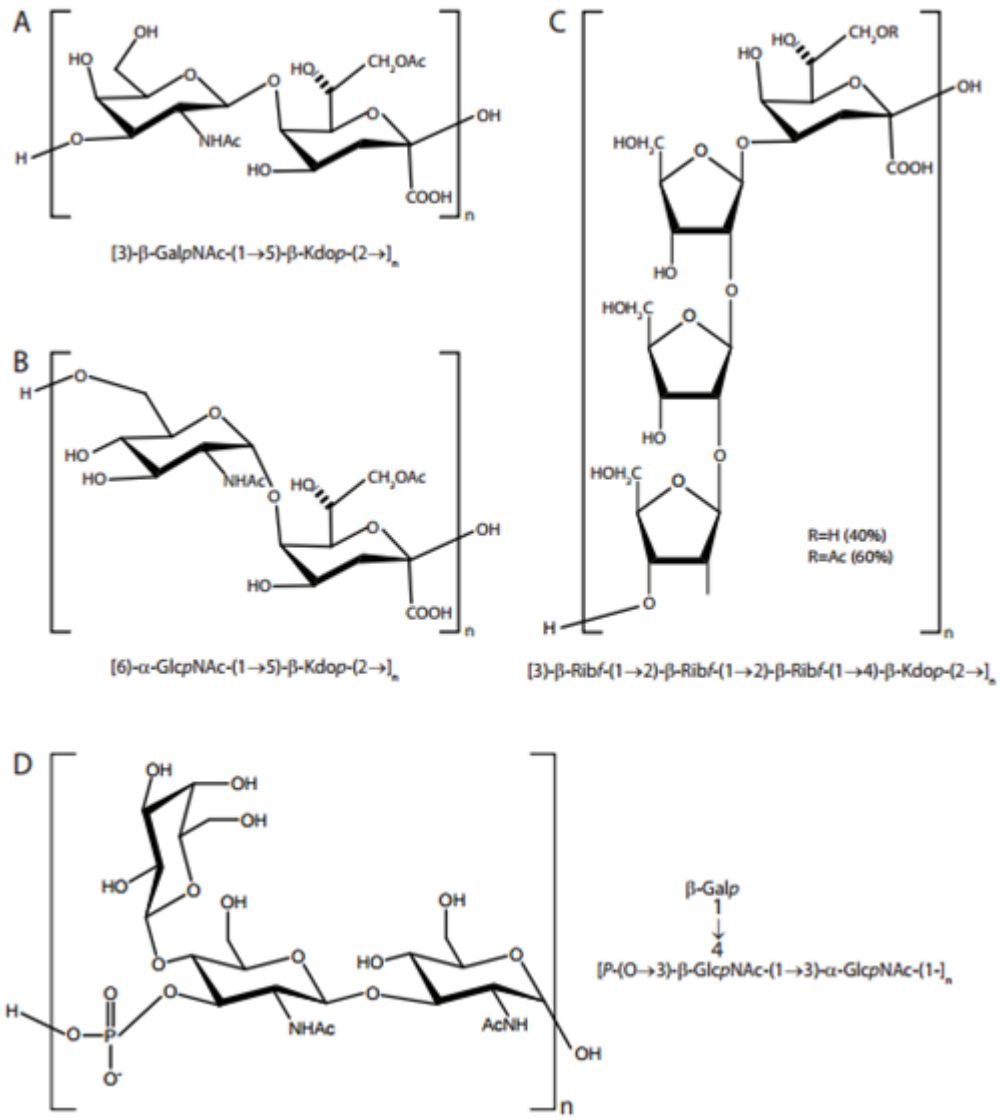

Figure 17: Structure of capsule polysaccharide repeating unit for capsule type a (GalNAc-Kdo, panel A), capsule type b (GlcNAc-Kdo, panel B), capsule type c (Ribose-Kdo, panel C), and capsule type d (galactose-GlcNAc, panel D).

4.3.4. The *csa*, *csb*, *csc*, and *csd* capsule synthesis loci are necessary and sufficient for polysaccharide capsule synthesis

To confirm that the *csa*, *csb*, *csc,* and *csd* loci are essential for production of capsule, we deleted each of these loci and then examined the resulting strains for surface material that stains with alcian blue. As shown in Figure 18, targeted deletion of the *csa*, *csb*, *csc*, or *csd* locus resulted in loss of surface extractable capsule from strains KK01, PYKK58, PYKK60, and BB270, respectively.

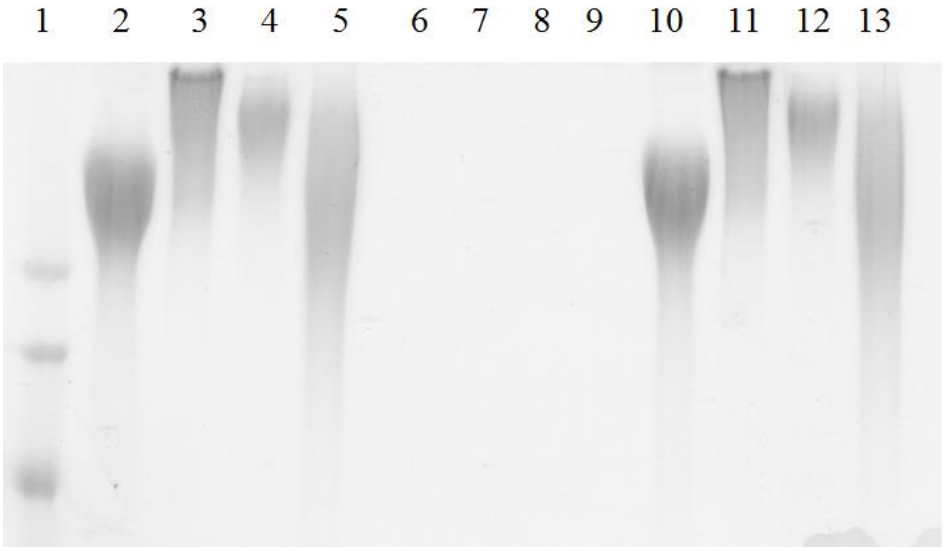

Figure 18: Comparison of capsule migration pattern between capsule types

Alcian blue stained gel depicting the migration pattern of capsule material purified from the surface of the source strains (lanes 2-5), capsule locus deletion mutants (lane 6-9), and the capsule complements (lanes 10-13). Lane 1, ladder; lane 2, KK01; lane 3, PYKK58; lane 4, PYKK60; lane 5, PYKKBB270; lane 6, KK01*csa*; lane 7, PYKK58*csb*; lane 8, PYKK60*csc*; lane 9 PYKKBB270*csd*; lane 10, KK01*csa(csa)*; lane 11 PYKK58*csb(csb)*; lane 12, PYKK60*csc(csc)*; lane 13 PYKKBB270*csd(csd)*.

Chromosomal complementation of each of these regions at the native locus resulted in restoration of encapsulation. These results demonstrate that the capsule synthesis loci are essential for production of capsule in representative type a, type b, type c, and type d *K. kingae* strains.

Table 12: Comparative molar ratio of main glycosyl residues in polysaccharide purified from the surface of capsule swap strains as detected by 1D- Proton NMR.

Sample	b-Ribf	a-GlcNAc	b-GalNAc	Galactose	Kdo
KK01Swap*csa*	---	---	1.23	---	1.0
KK01Swap*csb*	---	1.36	---	---	1.0
KK01Swap*csc*	4.65	---	---	---	1.0
KK01Swap*csd*	---	1.7	---	1.0	---

In additional experiments, we examined the ability of the type a, b, c, and d loci to complement a deletion of the *csa* locus in prototype strain KK01 and produce the corresponding capsule. In performing these studies, we engineered a deletion of *csaA* with no effect on the flanking *arg* and *hemB* genes, producing a strain called KK01Δ*csa*. Subsequently, we generated a plasmid called pSwap, which contains the *arg* and *hemB* genes, a kanamycin resistance marker, and a partial pUC19 multiple cloning site (MCS) (Figure 19A).

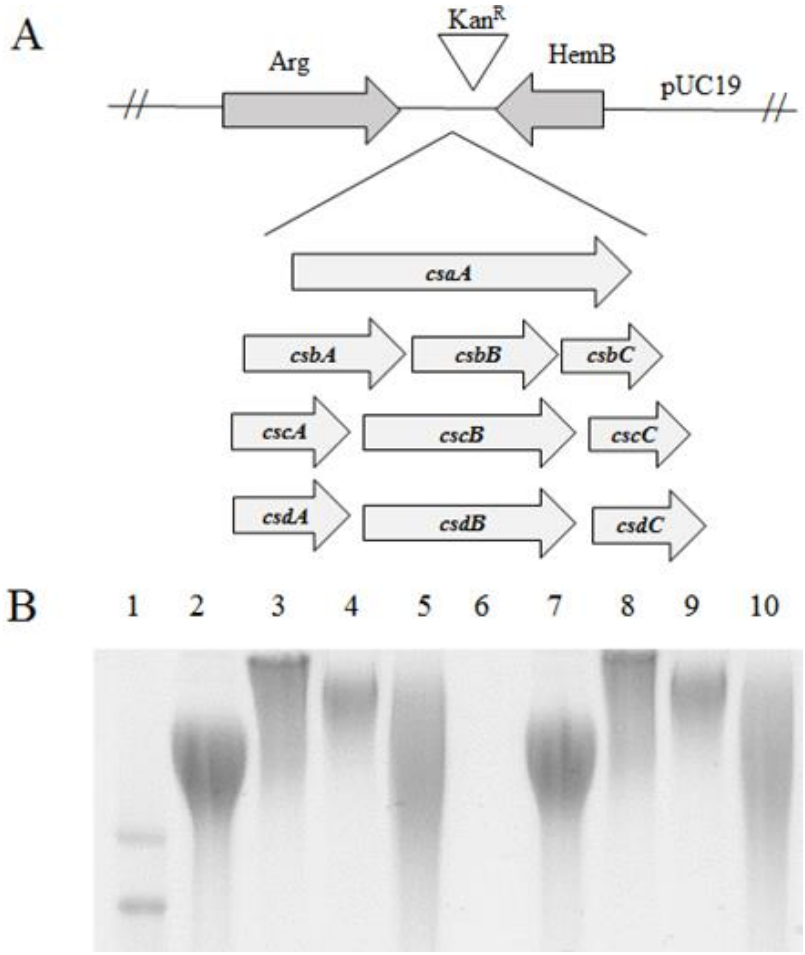

Figure 19: Illustration of the capsule swap vector in pUC19 harboring the *csa*, *csb*, *csc* or *csd* locus with a KanR marker for selection (A). Migration patterns of capsule material from isogenic capsule swaps (B).

Alcian blue stained gel depicting the migration pattern of capsule material purified from the surface of the source strains (lanes 2-5) and the capsule swaps expressed in the isogenic KK01 background (lanes 7-10). Lane 1, ladder; lane 2, KK01; lane 3, PYKK58; lane 4, PYKK60; lane 5, PYKKBB270; lane 6, KK01*csa*; lane 7, *KK01Swapcsa*; lane 8, *KK01Swapcsb*; lane 9, *KK01Swapcsc*; lane 10 *KK01Swapcsd*.

Using this plasmid, we inserted each of the four capsule synthesis loci into the MCS, generating pSwap*csa*, pSwap*csb*, pSwap*csc*, and pSwap*csd*. Each of these plasmids was linearized and transformed into strain KK01Δ*csa*, producing strains KK01Swap*csa*, KK01Swap*csb*, KK01Swap*csc*, and KK01Swap*csd*. As shown in Figure 19B and Table 12, each of these strains produced a capsule as assessed by alcian blue staining of surface extracts.

To confirm that the capsule in each of these strains corresponded to the specific capsule synthesis locus, surface polysaccharide was extracted and examined initially by alcian blue straining. As expected, the alcian blue staining profile of the capsule extracted from the *csa*, *csb*, *csc*, or *csd* swap strains was similar to the profile of the parental capsule locus source strain, suggesting that the capsules produced in a KK01Δ*csaA* background strain retain their native migration pattern (Figure 19B). Glycosyl composition analysis demonstrated that strain KK01Swap*csa* produced the type a capsule, strain KK01Swap*csb* produced the type b capsule, strain KK01Swap*csc* produced the type c capsule, and strain KK01 Swap*csd* produced the type d capsule (Table 12). These results demonstrate that the *csa*, *csb*, *csc*, and *csd* loci encode the synthesis components of the four *K. kingae* capsule types and are functional in an isogenic strain

background containing the capsule export and assembly machinery ((Porsch et al. 2012) Starr et al, submitted).

4.3.5 The type a and type b capsules are enriched in invasive isolates of *K. kingae*.

With our knowledge of the type a, type b, type c, and type d capsule loci in hand, we used a PCR approach to examine our large collection of Israeli *K. kingae* clinical isolates for capsule type. The invasive disease collection contains 189 isolates associated with a variety of clinical disease states, including septic arthritis, osteomyelitis, bacteremia, endocarditis, and others. The carrier collection contains 255 isolates recovered from throat swabs of healthy children. Analysis of these collections revealed that 96% of the invasive isolates express either capsule type a (46%) or capsule type b (50%) (Figure 20A).

Conversely, capsule type c and capsule type d were found disproportionately among carrier isolates (12% compared to 2%, respectively) (Figure 20A). In considering just the invasive isolates, we found a majority of capsule type a and type b across all clinical presentations, with the exception of endocarditis, which also contained the type c capsule (Figure 20B).

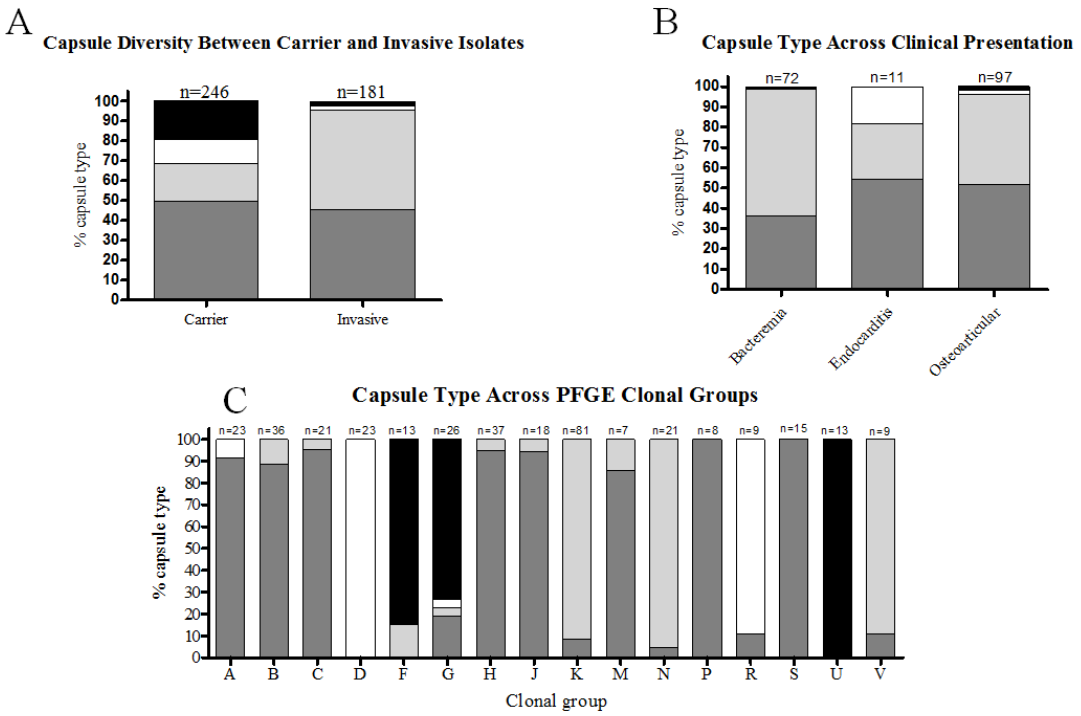

Figure 20: Capsule type diversity

Capsule type diversity among carrier and invasive isolates (A), common *Kingella kingae* clinical presentations (B), and between PFGE clonal groups containing greater than 4 isolates (C). Capsule composition was predicted by PCR screening for each of four glycosyltransferase clusters determining the capsule type. Type a is shown in dark gray, type b in light gray, type c in white, and type d in black.

In assessing the relationship between clonal group and capsule type, we found that clonal groups A, B, C, H, I, J, M, O, P, Q, and S primarily included strains producing a type a capsule, while clonal groups E, K, N, and V primarily included strains producing a type b capsule. Type c and d capsule were found in clonal groups D and R and clonal groups F, G, and U, respectively (Figure 20C).

4.4 Discussion

In this study we examined a large collection of *K. kingae* clinical isolates and established that there are four different *K. kingae* capsule types. In addition, we identified the underlying capsule synthesis genes for each capsule type. Using a combination of mass spectroscopy and NMR, we also determined the structure of the three previously uncharacterized capsule types (type b, type c, and type d), complementing our previous work on the structure of the type a capsule (Starr et al. 2013). Finally, we used a genetic screen to determine the capsule type of invasive disease isolates and healthy carrier isolates and discovered that capsule type a and type b account for 96% of all invasive disease isolates and that capsule type c and type d are disproportionately present among healthy carrier isolates.

We hypothesized that our large collection of *K. kingae* clinical isolates would contain multiple polysaccharide capsule types. Bacterial polysaccharide capsules are traditionally typed using one of two methods: 1) genetically, based on the presence of specific capsule synthesis genes in the capsule locus, or 2) immunologically, based on agglutination reactions using capsule-specific sera.

In this study we used a PCR-based genetic screening method, similar to methods that assess the capsule polysaccharide synthesis region for capsular typing of *K. pneumoniae* (Fang et al. 2005, Chung et al. 2007, Pan et al. 2013), *Pasteurella multocida* (Furian et al. 2014), and *N. meningitidis* (Dolan-Livengood et al. 2003). Using this approach, we established that there are four different capsule types, with each strain containing only one of four distinct capsule synthesis loci. Composition analysis of purified capsule material using a combination of mass spectroscopy and 1D NMR confirmed that capsule type is determined by the gene content of the capsule synthesis locus.

The presence of multiple capsule types in a species is well-documented for a variety of encapsulated pathogens, with examples including *S. pneumoniae* (>90 types), *E. coli* (>80 types), *Klebsiella pneumoniae* (78 types), *N. meningitidis* (12 types), and *H. influenzae* (6 types). Of the four capsule structures that we describe, two have been previously described in other bacteria. In particular, the type a capsule containing →3)-β-Gal*p*NAc-(1→5)-β-Kdo*p*-(2→ is identical to the capsule of *Moraxella nonliquefaciens* strain 3828/60 (Reistad et al. 1993), and the type b capsule expressed by *K. kingae* strains PYKK58, and PYKK181 (Bendaoud et al. 2011) containing 6)-α-Glc*p*NAc (1→5)-β-(8-OAc)Kdo*p*-(2→ is identical to

the *Actinobacillus pleuropneumoniae* serotype 5a capsule (Perry et al. 1990, Bendaoud et al. 2011). In contrast, the type c capsule in strain PYKK60 containing 3)-β-Rib*f*-(1→2)-β-Rib*f*-(1→2)-β-Rib*f*-(1→4)-β-Kdo*p*-(2→ and the type d capsule in strain BB270 containing P-(O→3)[β-Gal-(1→4)]-β-GlcNAc-(1→3)-α-GlcNAc-1- are novel.

Uropathogenic *E. coli* are typically encapsulated with acidic polysaccharides, many of which contain Kdo together with one or two ribose moieties (di- or tri-saccharide) in the repeating unit. For example, the *E. coli* K16-antigen (→2)-β-D-Ribf-(1→3)-β-D-Ribf-(1→5)-α-Kdop-(2→) (Lenter et al. 1990) and the *E. coli* K74 antigen (→3)- β-D-Ribf-(I→2)- β-D-Ribf-(l→6)- βKdo-(2→) (Ahrens et al. 1988) both contain Kdo and ribose in unequal ratios, similar to the type c capsule in *K. kingae*. The Kdo-ribose polysaccharides form a group of closely related but serologically distinct *E. coli* capsular antigens, and the serologic variability is increased by different degrees of O-acetylation at various sites (Jann et al. 1988). We also found acetylation in the *K. kingae* type c capsule, where 60% of the R groups are acetylated. The functional consequence of type c capsule acetylation in terms of serological reactivity remains to be investigated.

The type d capsule described in *K. kingae* strain BB270 has the structure of 3)[β-Gal-(1→4)]-β-GlcNAc-(1→3)-α-GlcNAc-1-P-(O→. While the type c structure appears to be novel, there are examples of polysaccharides containing galactose and GlcNAc as seen in the capsule expressed by *Streptococcus agalactiae* type 1a 4)-[α-d-NeupNAc-(2→3)-β-d-Galp-(1→4)-β-d-GlcpNAc-(1→3)]-β-d-Galp-(1→4)-β-d-Glcp-(1 (Yamamoto et al. 1999).

It is interesting to speculate on the potential for capsule type switching in *K. kingae.* In *N. meningitidis*, capsule switching has been shown to result from recombination of the polysialyltransferase gene (*siaD*) or the capsule biosynthesis operon (Swartley et al. 1997), with evidence for capsule switching between strains implicated in carriage and strains associated with invasive disease (Beddek et al. 2009). Pneumococcal isolates can also undergo capsule switching, with the serotype of a clone changing due to alteration in the capsule biosynthesis locus via mutations or through genetic recombination (Coffey et al. 1998, Wyres et al. 2013, Chaguza et al. 2015). Asymptomatic carriage provides an ideal environment for exchange of genetic loci among bacteria that occupy the same niche (Yazdankhah et al. 2004). The human nasopharynx has been shown to harbor diverse bacteria, including *N. meningitidis*, *H. influenzae*, and *S.*

pneumoniae as well as nonpathogenic *Neisseria* sp. and *Moraxella* sp. Evidence supporting horizontal gene transfer between phylogenetically distant species is seen in the meningococcal genome, which harbors three independent domains of *Haemophilus*-like DNA. Uptake and integration of DNA in the upper respiratory tract is a probable mechanism to explain the capsule diversity observed in *K. kingae* in this study. *Actinobacillus* sp., *Moraxella* sp., and *Kingella* sp. are all found in normal human flora of the upper respiratory tract, providing the opportunity for horizontal gene transfer responsible for the 4 *K. kingae* capsule synthesis loci. *M. nonliquefaciens* has been shown to be present in the respiratory tract of young children (Tønjum et al. 1991, Yi et al. 2014). *A. pleuropneumoniae* is primarily a swine pathogen, but other *Actinobacillus* sp. can be found in humans (Ashhurst-Smith et al. 1998). It is also possible that capsule switching via horizontal gene transfer between 2 *K. kingae* strains occurs, explaining the observation that some *K. kingae* clonal groups are associated with multiple capsule types.

All of the *K. kingae* strains in our collection gave a PCR product for the capsule export and assembly genes *ctrABCD*, *lipA*, and *lipB*, suggesting that these strains all contain the machinery necessary to display a capsule polymer on their surface (Starr et al, submitted). However, out of 427 isolates, two strains

demonstrated atypical PCR capsule typing results. First, strain PYKK56 yielded a *csa* locus PCR product, but the product was smaller than expected. Sequencing of the *csa* locus in this strain revealed a deletion of the 3' end of the *csaA* gene, resulting in a CsaA protein missing 170 amino acids in the C-terminal domain. Alcian blue staining of surface extracts from this strain revealed no capsule, suggesting that the *csaA* mutation resulted in abrogation of capsule expression. Second, strain PYKK183 yielded no capsule locus-specific PCR product and no capsule locus flanking product. Alcian blue staining of surface extracted material revealed that this strain is not encapsulated, indicating that this strain lacks capsule synthesis genes, rather than possessing a unique capsule synthesis locus.

Amit et al determined that *K. kingae* PFGE clonal groups B, H, K, N, and P account for 72.9% of all invasive clones and that PFGE clonal groups A, C, D, F, G, J, R, S, and U are rare among invasive disease isolates (Amit et al. 2012). Interestingly, only capsule types a and b are represented in the B, H, K, N, and P PFGE clonal group isolates. In total, 96% of the total invasive isolate collection expresses either the type a or type b capsule. Conversely, all 4 capsule types are represented in the carrier collection. The type c capsule is most prevalent in PFGE groups D and R, while the type d capsule is most prevalent in PFGE

groups F, U, and G, all of which fall into the subset of rare-disease PFGE clonal groups. An enrichment of particular capsule types among invasive isolates has been documented in other organisms, including *K. pneumoniae***.** *S. pneumoniae*, *N. meningitidis*, and *H. influenzae.* In all of these bacteria, some capsule types are associated more commonly with invasive disease and some are more common among colonizing strains (Riser et al. 1981, Peltola 1983, Feldman et al. 1997, Weinberger et al. 2009). It is also known that not all serotypes of *S. pneumoniae* are equally capable of colonizing the nasopharynx or causing invasive disease. For example, of the more than 90 serotypes , only 23 are responsible for 80 to 90% of invasive pneumococcal infections in the U. S. (1999, Lexau et al. 2005) and only 13 of the clinically important serotypes are targeted by a current vaccine in children. Similarly, of the 12 *N. meningitidis* serogroups, only 5 are responsible for more than 90% of the invasive disease worldwide (Peltola 1983).

Considering the effectiveness of many polysaccharide-conjugate vaccines in reducing childhood morbidity and mortality, it is interesting to speculate that a *K. kingae* capsular polysaccharide-conjugate vaccine may be an effective strategy to prevent *K. kingae* disease. While more studies are needed, the discovery that the capsule repertoire of a diverse collection of *K. kingae* carrier

and invasive disease isolates is represented by only 4 capsule types, with two capsule types accounting for 96% of invasive disease, is an important first step in establishing the feasibility of a vaccine for the prevention of *K. kingae* disease.

5. Conclusions and future directions

5.1 Conclusions

The data presented in Chapters 2-4 establish that *Kingella kingae* expresses a surface polysaccharide capsule and an exopolysaccharide requiring distinct genetic loci for surface localization. Further investigation into the genetic determinants of encapsulation revealed that the *ctrABCD* genes, the *lipA*/*lipB* genes, and a putative glycosyltransferase gene are required for capsule expression, with the gene products having roles in capsule export, assembly, and synthesis, respectively. The putative glycosyltransferase CsaA was determined to be a bifunctional glycosyltransferase with both GalNAc-transferase and Kdo-transferase activity, capable of synthesizing both linkages found in the capsule expressed in our prototype strain: →3)-β-Gal*p*NAc-(1→5)-β-Kdo*p*-(2→. We discovered a total of 4 capsule types expressed in clinical isolates of *K. kingae*, each with a distinct capsule synthesis locus containing capsule-type specific glycosyltransferases. The variation in the proportion of capsule types found between invasive strains and carriage strains suggests that capsule type is important in promoting invasion and dissemination. The future directions

outlined below will allow us to further define the role of capsule type in the pathogenesis of disease.

5.2 Future directions

The future direction will focus on two areas of interest 1) epidemiology and genomics and 2) virulence and host response. We will first expand upon our findings in Chapter 4 to investigate the global distribution of capsule types. To better understand the events responsible for recombination at the capsule synthesis locus, we will look for evidence of capsule switching through sequencing and genome-wide comparisons. Second, to better understand the role of the surface polysaccharides as virulence factors, we will assess the effect of capsule in immune evasion and the humoral response to *K. kingae* capsule types during colonization. In addition, we will optimize the animal model of *K. kingae* to include colonization and invasive disease.

5.3 Epidemiology and genomics

5.3.1 Measure global distribution of capsule types

In the work detailed in Chapter 4 we describe the 4 capsule types produced by *K. kingae* isolates recovered from patients with invasive disease or

individuals who were asymptomatically colonized. The isolates that we characterized were all recovered from individuals in Israel and were provided by Dr. Pablo Yagupsky. To determine whether the capsule types that we detected are also present in other parts of the world, we are collecting strains from the United States, Canada, Paris, Spain, Iceland, and Australia. Preliminary PCR screening of the capsule synthesis locus of a small collection of global isolates reveals the same 4 capsule types without the discovery of new capsule types, as shown in Figure 21.

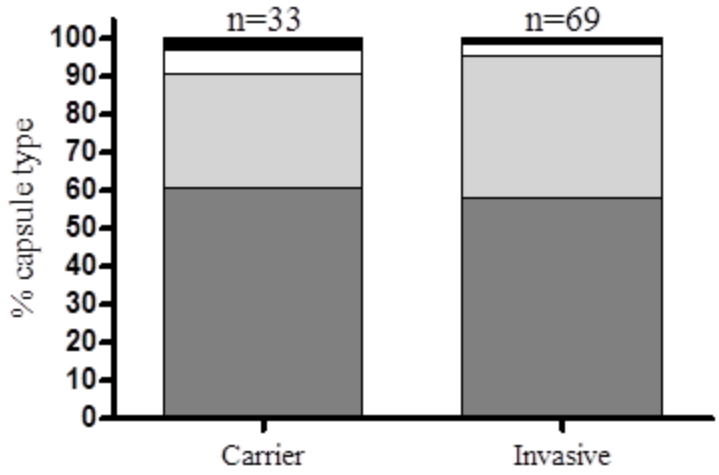

Figure 21: Capsule type diversity among carrier and invasive isolates collected from individuals in the United States, Canada, Paris, Spain, Iceland, and Australia.

Capsule type was determined by PCR screening for each of the four glycosyltransferase clusters determining the capsule type. Type a is shown in dark gray, type b in light gray, type c in white, and type d in black.

We plan to genotype a larger collection of strains to determine if new capsule types exist in *K. kingae* isolates from different regions of the globe. Further expanding our knowledge about the worldwide *K. kingae* capsule type distribution will allow us to determine the most clinically relevant capsule types worldwide, essential information for determining the feasibility of a potential capsule-based vaccine in the future. We will assess the ratio of the 4 capsule types that we described in Chapter 4 to determine if capsule type a and b are overrepresented in invasive strains worldwide. In addition, we will determine which capsule types are most common in carrier strains. If we discover novel capsule types in other countries, we will characterize the structure and prevalence of these polysaccharides as described in Chapter 4.

5.3.2 Investigate recombination of the capsule synthesis locus

K. kingae is naturally competent, and the variable capsule synthesis locus is flanked by regions of nucleotide sequence identity. In other organisms capsule type switching can occur via homologous recombination. Our results reveal the same PFGE groups (clonal groups) with differing capsule synthesis loci,

supporting the theory that the capsule synthesis locus can recombine while leaving the genome at large clonally identical.

We presented evidence in Chapter 4 that capsule types a and b are enriched among invasive isolates, but other *K. kingae* factors beyond capsule are associated with pathogenicity. To investigate whether capsule travels with other virulence factors, we will further investigate the genomic region that undergoes recombination to allow capsule type switching. A large sequencing project is underway in which we will sequence 96 *K. kingae* strains and begin to look for epistasis between capsule type and other gene products that may play a role in virulence such as Knh. We will perform a sequence alignment to compare the homologous regions outside of the capsule synthesis locus to determine other potential gene products that may recombine along with the capsule locus. We will perform sequence comparisons on sequenced genomes from strains with differing PFGE clonal groups and the same or different capsule synthesis loci to define complete region of homology that may be responsible for recombination. Furthermore, we can perform whole genome sequencing to understand horizontal transfer at the capsule locus by looking at strains with similar PFGE typing and different capsule.

5.4 Virulence and host response

5.4.1 Determine the role of capsule and exopolysaccharide in immune evasion

Kingella kingae expresses both a polysaccharide capsule and a galactan exopolysaccharide. We predict that capsule and exopolysaccharide in *K. kingae* also function in immune evasion through limiting neutrophil interaction and dampening the pro-inflammatory cytokine response, similar to extracellular polysaccharides in other bacteria. While it is widely accepted that capsules can prevent complement deposition on the bacterial surface, exopolysaccharides can also offer protection, as described with the Psl exopolysaccharide in *P. aeruginosa* (Mishra et al. 2012). Preliminary data have demonstrated that *K. kingae* is highly resistant to serum killing (up to 50% serum). We plan to investigate the mechanisms by which the capsule and exopolysaccharide affect complement-mediated killing and interactions with phagocytes. Using capsule and exopolysaccharide mutants, we will investigate the role of capsule on complement activity. First, we will use the capsule swap strains, capsule deficient strains, and exopolysaccharide deficient strains in a C3b binding assay

to determine if capsule type plays a role in preventing C3b deposition. C3b is an essential component of complemented mediated killing that is often deposited on the bacterial surface to target it for destruction. We expect to observe a decrease in C3b binding in all strains compared to the unencapsulated strain, indicating that capsule and exopolysaccharide can reduce complement activity by inhibiting C3b binding. We also expect that strains lacking surface polysaccharide will be more susceptible to neutrophil phagocytosis and killing. Phagocytosis assays and neutrophil killing assays will be conducted with neutrophils isolated from fresh human blood. Phagocytosis will be investigated using flow cytometry, fresh human neutrophils, and fluorescent *K. kingae* harboring a chromosomal copy of GFP. Bacteria will be allowed to interact with neutrophils for various timepoints. To calculate neutrophil killing, in a separate experiment we will incubate bacteria with neutrophils for one hour at 37° C and surviving bacteria will be calculated by plating serial dilutions, expressing survival as a percentage of the number of inoculated CFU. If we observe a decrease in phagocytosis or neutrophil killing in type a or type b capsule expressing strains, we will conclude that the capsule types expressed by a majority of invasive strains confer a capacity for survival in neutrophils.

To measure the cytokine response to each capsule type, we will employ THP-1 human macrophage-like cells *in vitro*. Alternative cells lines include Chang conjunctival or A549 lung cells, which support adherence by *K. kingae*. After testing for contaminants including LPS, we will add each of the four purified capsules to a monolayer of cells for two hours before harvesting the cell culture media for released cytokines. We will quantify IL-1B, IL-8, and TNF-α by ELISA to measure the cytokine response to *K. kingae* based on the reported cytokine responses to *Haemophilus influenzae* and *Neisseria meningitidis*, other bacterial pathogens (Naumann et al. 1997, Frick et al. 2000, Zughaier 2011). In addition, we will use the capsule swaps in an isogenic background to look at the cytokine response to viable bacteria expressing different capsule types. We expect to find that capsule type a and b elicit a more modest inflammatory response, given their ability to survive and persist to cause invasive disease. The purified capsule material will likely stimulate these cytokines less than the same capsule expressed on the surface of a whole bacteria expressing other surface proteins and LPS. LPS will be used as a positive stimulation control. PolymyxinB will be included in some assays to ensure that any cytokine response seen from purified capsule is not due to LPS contamination. We will also compare our

findings to an unencapsulated isogenic strain, which we expect will stimulate the cytokine response due to a lack of capsule masking the surface. If the initial cytokines we propose are not changed even with whole bacteria, we will expand our assay to include a larger panel of cytokines.

5.4.2 Measure humoral immunity against *K. kingae* during colonization

In Chapter 4 we describe the association of capsule type a and type b with isolates recovered from patients with invasive disease. It is not known how the host responds to asymptomatic colonizing events. One possibility is that the host responds strongly to type c and type d capsules by eliciting a capsule-specific antibody response. This strong response may explain why these strains exist only as colonizers and rarely overcome the immune system to cause invasive disease. Conversely, type a and type b strains may not elicit a strong antibody response and may thus survive better in the host and have the potential to invade. Currently, there are no data measuring the response to the surface polysaccharides expressed by *K. kingae*. We plan to obtain sera from healthy colonized children and measure serum IgG titers against each capsule type as well as the PAM galactan. As capsule is known to mask surface proteins and is

one of the outermost bacterial factors seen by the immune system, it is possible that capsule type-specific immunity is elicited with each colonization event. To investigate if colonization with one capsule type is protective against secondary colonization with strains expressing the same capsule or a different capsule type, we are collecting sequential isolates taken from healthy carriers at different time points over the course of a year. We have started capsule typing these isolates, and we will look for evidence that colonization with a given capsule type is protective against re-colonization with a strain expressing the same capsule type. In a small sample set we have observed a shift between antigenically distinct strains over time, suggesting colonization with a primary strain elicits an immune response that prevents recolonization with a similar strain. To determine if immunization against colonization is a capsule specific and protective against secondary colonization with a strain expressing the same capsule type, we will determine the capsule type present in primary and secondary colonizing strains from an individual patient. In a small sample set we have already observed colonization and secondary colonization with distinct *K. kingae* strains, both expressing a type a capsule. This observation suggests that colonization with a type a capsule type does not consistently elicit a protective

immune response against secondary colonization with another type a-expressing strain. Intriguingly, we rarely see secondary colonization with type b, c, or d capsule type strains. We hypothesize that primary colonization with capsule types b, c, or d elicits a more protective response, leading solely to recovery of secondary isolates with a different capsule type. Repeated samplings revealing a type a capsule from the same individual support the hypothesis that the type a capsule fails to generate a strong protective immune response. This hypothesis is strengthened by our observation that the type a capsule expressing strains make up roughly half of invasive strains. We will test whether a type a strain fails to elicit a strong immune response by measuring antibody titers.

We hypothesize that a change in capsule type of representative isolates responsible for primary and secondary colonization events is associated with elicitation of a protective immune response against the capsule. To test this hypothesis, we will look at antibody titers against each capsule type over time. We plan to expand on previous work that has measured the immune response to *K. kingae* outer membrane proteins, measuring the immune response to capsule: a factor that likely masks many surface proteins. In a longitudinal study, titers of immunoglobulin G (IgG) antibodies against *K. kingae* outer membrane proteins

were high at 2 months of age, reached a nadir at the age of 6 to 7 months, remained low until the age of 18 months, and increased at the age of 24 months (Slonim et al. 2003). However, exposed epitopes are polymorphic, and the immune response elicited by carriage seems to be incomplete, strain-specific, and unable to prevent colonization by an antigenically different strain (Yagupsky et al. 2005). To investigate the immune response to each capsule type during colonization, we plan to collect serum from patients over several colonization events and look for capsule antibody (IgG and IgA), which would indicate a capsule type-specific protective immune response was generated during colonization. Again, we predict that type a and b capsules will not elicit a strong immune response as measured by antibody titer, and types c and d will elicit the strongest response.

5.4.3 Improve the *K. kingae* animal model of colonization and invasive disease

Previous work from our lab has demonstrated an *in vitro* functional relationship between capsule, type IV pili, and the Knh adhesin (Porsch et al. 2012). Our work has further suggested a relationship between capsule type and site of isolation that we have not been able to test *in vivo*. We have adopted the

previously published juvenile rat model, which involves IP injection of approximately 10^7 *K. kingae* CFU into 5-day-old Sprague-Dawley albino rats and observation for differences in survival and development of necrotic skin lesions (Basmaci et al. 2012). As described in Chapter 3, we were able to detect differences in survival rates for rats inoculated with encapsulated and nonencapsulated (*csaA*) *K. kingae* strains; however, there are several limitations to this IP infant rat infection model that need to be addressed. First, the IP infection route described here does not replicate a natural route of infection, as there is a lack of colonization in the pharynx. The lack of colonization precludes the ability to determine which surface factors (e.g., pili, Knh, capsule, exopolysaccharide) play a role in colonization and the transition from colonization to invasion. Second, the IP rat model with the readout of survival and lesion formation does not accurately portray natural invasive disease caused by *K. kingae*. Furthermore, the infant rat model is not sufficiently sensitive to allow us to detect subtle differences in virulence, as we expect to see when examining specific capsule types. We aim to develop a model that represents stages of infection including colonization and invasive disease.

We discuss here two approaches for development of an animal model. The first model we propose is a macaque model that will be useful for measuring colonization in competitive assays, but will not allow the number of animals needed to compare the phenotypes of mutant strains of *K. kingae* lacking individual or combinations of surface factors. The macaque model is limited in that it does not mimic invasive disease, limiting us to studying virulence factors that affect colonization only. The second model we propose is an optimized mouse/rat model to mimic invasive disease. The ultimate goal is a small animal model that represents both the stages of colonization and invasive disease.

5.4.3.1 Macaque model

If *K. kingae* is truly a human-specific organism like the pathogenic *Neisseria* spp., then non-human primates may be an especially useful animal model to study colonization of the upper respiratory tract. With this idea in mind, we have developed a rhesus macaque colonization model using nasal inoculation and shown that we can achieve colonization of the pharynx for 7 days with *K. kingae* strain KK86 (a carrier isolate). Using this model, we plan to examine the capsule swap strains that we developed in Chapter 4 in colonization competition assays

to assess the influence of capsule type in colonization. We will measure level and duration of colonization by counting bacteria cultured from pharyngeal swabs. We expect that all four capsule types will be capable of colonization, since all four capsule types are found in human carriers. To assess how the immune system responds to the different capsule types, we will measure antibody titers in serum. We expect based on the capsule types present in invasive disease in humans, that capsule types a and b will elicit a weaker immune response than types c and d.

5.4.3.2 Mouse model

Despite the success of the macaque model, a smaller animal colonization model is still needed to increase the number of animals used in each study. While a single model that allows colonization and invasive disease is an ideal model, separate colonization and invasive disease models would still improve our ability to assess the role surface factors and capsule type play during colonization and disease. We aim to refine our rat model to mimic invasive disease, as initial attempts to develop a mouse model using C3/HEN, B6, Swiss, and BalbC tail vein-injected mice have proved unsuccessful in generating

bacteremia or joint involvement. To increase our chances of achieving bacteremia and dissemination to the joints we will expand our model to include the use of immunodeficient RAG-/- rats and mice. Bacteremia and invasive disease in the joints after intranasal inoculation or tail vein injection has been observed with *S. aureus* in mice (Elasri et al. 2002); therefore, we will follow a similar protocol with imunodeficient animals. If we fail to achieve bacteremia in the SCID (RAG-/-) mice due to animal death, we will induce neutropenia, a less severe phenotype, in wild type mice using RB6-8C5 antibody (anti-granulocyte receptor-1) as previously described (Koh et al. 2005). While the role of neutrophils in *K. kingae* infection is not well understood, we predict that by depleting neutrophils, we will be able to achieve bacteremia. This hypothesis is based on the role of neutrophils controlling infections with other respiratory pathogens including *Haemophilus*, *Streptococcus*, and *Klebsiella*, in mice (Garvy et al. 1996, Jeyaseelan et al. 2006, Zola et al. 2009).

As an alternative to traditional mouse lines, the creation a humanized mouse model may allow colonization in a non-human/non-primate animal. To determine the receptors *K. kingae* binds to in cell culture (to be expressed in the mouse), we will develop tagged full length pili and Knh proteins, both surface

adhesins that promote binding to Chang cells. Crosslinking of *K. kingae* will link the adhesins to their host receptors. We will then employ proteomics (Mass Spectroscopy) to determine the host cell proteins bound to Pili and Knh. Negative controls will include addition of a mutant form of the protein that does not facilitate adherence and addition of the tag alone. If we cannot obtain tagged versions we can used pili and Knh antibody bound to beads to pull down our proteins of interest. Determining the host cell receptor will be the first step toward creating a knock-in transgenic mouse line that could potentially allow pharyngeal colonization.

References

(1999). Pneumococcal vaccines. WHO position paper. *Wkly Epidemiol Rec* 74(23): 177-183.

Ahrens, R., B. Jann, K. Jann and H. Brade (1988). Structure of the K74 antigen from *Escherichia coli* O44:K74:H18, a capsular polysaccharide containing furanosidic β-KDO residues. *Carbohydr Res* 179: 223-231.

Albrich, W. C., W. Baughman, B. Schmotzer and M. M. Farley (2007). Changing Ccharacteristics of invasive pneumococcal disease in metropolitan Atlanta, Georgia, after introduction of a 7-Valent pneumococcal conjugate vaccine. *Clin Infect Dis* 44(12): 1569-1576.

Allegrucci, M. and K. Sauer (2007). Characterization of colony morphology variants isolated from *Streptococcus pneumoniae* biofilms. *J Bacteriol* 189(5): 2030-2038.

Amit, U., R. Dagan, N. Porat, R. Trefler and P. Yagupsky (2012). Epidemiology of invasive *Kingella kingae* infections in 2 distinct pediatric populations cohabiting in one geographic area. *Pediatr Infect Dis J* 31(4): 415-417.

Amit, U., S. Flaishmakher, R. Dagan, N. Porat and P. Yagupsky (2014). Age-dependent carriage of *Kingella kingae* in young children and turnover of colonizing strains. *J Ped Infect Dis* 3(2): 160.

Amit, U., N. Porat, R. Basmaci, P. Bidet, S. Bonacorsi, R. Dagan and P. Yagupsky (2012). Genotyping of invasive *Kingella kingae* isolates reveals predominant clones and association with specific clinical syndromes. *Clin Infect Dis* 55(8): 1074-1079.

Arrecubieta, C., R. López and E. García (1996). Type 3-specific synthase of *Streptococcus pneumoniae* (Cap3B) directs type 3 polysaccharide biosynthesis in *Escherichia coli* and in pneumococcal strains of different serotypes. *J Exp Med* 184(2): 449-455.

Ashhurst-Smith, C., R. Norton, W. Thoreau and M. M. Peel (1998). *Actinobacillus equuli* septicemia: an unusual zoonotic infection. *J Clin Microbiol* 36(9): 2789-2790.

Austrian, R. (1953). Morphologic variation in pneumococcus: An anlysis of the basis for morphologic variation in Pneumococcus and description of a hitherto undefined morphologic variant. *J Exp Med* 98(1): 21-34.

Basmaci, R., P. Yagupsky, B. Ilharreborde, K. Guyot, N. Porat, M. Chomton, J.-M. Thiberge, K. Mazda, E. Bingen, S. Bonacorsi and P. Bidet (2012). Multilocus sequence

typing and rtxA toxin gene sequencing analysis of *Kingella kingae* isolates demonstrates genetic diversity and international clones. *PLoS ONE* 7(5): e38078.

Beddek, A. J., M.-S. Li, J. S. Kroll, T. W. Jordan and D. R. Martin (2009). Evidence for Capsule Switching between Carried and Disease-Causing Neisseria meningitidis Strains. *Infection and Immunity* 77(7): 2989-2994.

Bendaoud, M., E. Vinogradov, N. Balashova, D. Kadouri, S. Kachlany and J. Kaplan (2011). Broad-spectrum biofilm inhibition by *Kingella kingae* exopolysaccharide. *J. Bacteriol.* 193(15): 3879-3886.

Bhattacharjee, A., H. Jennings and C. Kenny (1978). Structural elucidation of the 3-deoxy-D-manno-octulosonic acid containing meningococcal 29e capsular polysaccharide antigen using carbon-13 nuclear magnetic resonance. *Biochemistry* 17(4): 645-651.

Bidet, P., E. Collin, R. Basmaci, C. Courroux, V. Prisse, V. Dufour, E. Bingen, E. Grimprel and S. Bonacorsi (2013). Investigation of an outbreak of osteoarticular infections caused by *Kingella kingae* in a childcare center using molecular techniques. *Pediatr. Infect. Dis. J.* doi:10.1097/INF.0b013e3182867f5e.

Bilukha, O. and N. Rosenstein (2005). Prevention and control of meningococcal disease. Recommendations of the Advisory Committee on Immunization Practices (ACIP) MMWR Recomm Rep. 54**:** 1-21.

Bovre, K., S. D. Henriksen and V. Jonsson (1974). Correction of Specific Epithet *kingii* in Combinations *Moraxella kingii* Henriksen and Bovre 1968 and *Pseudomonas kingii* Jonsson 1970 to *Kingae*. *Int J Syst Bacteriol* 24(2): 307-307.

Breton, C., L. Šnajdrová, C. Jeanneau, J. Koča and A. Imberty (2006). Structures and mechanisms of glycosyltransferases. *Glycobiology* 16(2): 29R-37R.

Chaguza, C., J. E. Cornick and D. B. Everett (2015). Mechanisms and impact of genetic recombination in the evolution of *Streptococcus pneumoniae*. *Comput Struct Biotechnol J* 13: 241-247.

Chang, A. C. and S. N. Cohen (1978). Construction and characterization of amplifiable multicopy DNA cloning vehicles derived from the P15A cryptic miniplasmid. *J Bacteriol* 134(3): 1141-1156.

Cherkaoui, A., D. Ceroni, S. Emonet, Y. Lefevre and J. Schrenzel (2009). Molecular diagnosis of *Kingella kingae* osteoarticular infections by specific real-time PCR assay. *J Med Microbiol* 58(Pt 1): 65-68.

Chometon, S., Y. Benito, M. Chaker, S. Boisset, C. Ploton, J. Berard, F. Vandenesch and A. M. Freydiere (2007). Specific real-time polymerase chain reaction places *Kingella kingae* as the most common cause of osteoarticular infections in young children. *Pediatr Infect Dis J* 26(5): 377-381.

Chung, D. R., S. S. Lee, H. R. Lee, H. B. Kim, H. J. Choi, J. S. Eom, J. S. Kim, Y. H. Choi, J. S. Lee, M. H. Chung, Y. S. Kim, H. Lee, M. S. Lee and C. K. Park (2007). Emerging invasive liver abscess caused by K1 serotype Klebsiella pneumoniae in Korea. *Journal of Infection* 54(6): 578-583.

Cieslewicz, M. and E. Vimr (1996). Thermoregulation of *kpsF*, the first region 1 gene in the *kps* locus for polysialic acid biosynthesis in *Escherichia coli* K1. *J Bacteriol* 178(11): 3212-3220.

Clarke, B. R., R. Pearce and I. S. Roberts (1999). Genetic organization of the *Escherichia coli* K10 capsule gene cluster: Identification and characterization of two conserved regions in group III capsule gene clusters encoding polysaccharide transport functions. *J Bacteriol* 181(7): 2279-2285.

Clements, A., F. Gaboriaud, J. F. L. Duval, J. L. Farn, A. W. Jenney, T. Lithgow, O. L. C. Wijburg, E. L. Hartland and R. A. Strugnell (2008). The major surface-associated saccharides of *Klebsiella pneumoniae* contribute to host cell association. *PLoS ONE* 3(11).

Coffey, T. J., M. C. Enright, M. Daniels, J. K. Morona, R. Morona, W. Hryniewicz, J. C. Paton and B. G. Spratt (1998). Recombinational exchanges at the capsular polysaccharide biosynthetic locus lead to frequent serotype changes among natural isolates of Streptococcus pneumoniae. *Mol Microbiol* 27(1): 73-83.

Corbett, D., T. Hudson and I. S. Roberts (2010). Bacterial Polysaccharide Capsules. Prokaryotic Cell Wall Components. C. Konig, Varma, Springer**:** 111-132.

Criss, A. K. and H. S. Seifert (2012). A bacterial siren song: intimate interactions between neutrophils and pathogenic Neisseria. *Nature reviews. Microbiology* 10(3): 178-190.

Dasgupta, S. and D. Kasper (2010). Novel tools for modulating immune responses in the host-polysaccharides from the capsule of commensal bacteria. *Adv Immunol* 106: 61-91.

DeAngelis, P. L. and P. H. Weigel (1994). Immunochemical confirmation of the primary structure of Streptococcal hyaluronan synthase and synthesis of high molecular weight product by the recombinant enzyme. *Biochem* 33(31): 9033-9039.

DeAngelis, P. L. and C. L. White (2004). Identification of a distinct, cryptic heparosan synthase from *Pasteurella multocida* types A, D, and F. *J Bacteriol* 186(24): 8529-8532.

Dolan-Livengood, J. M., Y. K. Miller, L. E. Martin, R. Urwin and D. S. Stephens (2003). Genetic basis for nongroupable *Neisseria meningitidis*. *J Infect Dis* 187(10): 1616-1628.

Donot, F., A. Fontana, J. C. Baccou and S. Schorr-Galindo (2012). Microbial exopolysaccharides: Main examples of synthesis, excretion, genetics and extraction. *Carbohyd. Polym.* 87(2): 951-962.

Dubnov-Raz, G., O. Scheuerman, G. Chodick, Y. Finkelstein, Z. Samra and B. Z. Garty (2008). Invasive *Kingella kingae* infections in children: Clinical and laboratory characteristics. *Pediatrics* 122(6): 1305-1309.

Elasri, M. O., J. R. Thomas, R. A. Skinner, J. S. Blevins, K. E. Beenken, C. L. Nelson and M. S. Smelter (2002). *Staphylococcus aureus* collagen adhesin contributes to the pathogenesis of osteomyelitis. *Bone* 30(1): 275-280.

Fang, F. C., N. Sandler and S. J. Libby (2005). Liver abscess caused by magA+*Klebsiella pneumoniae* in North America. *J Clin Microbiol* 43 (2): 991-992.

Feldman, C. and K. Klugman (1997). Pneumococcal infections. *Curr Opin Infect Di* 10: 109-115.

Fraysse, N., B. Lindner, Z. Kaczynski, L. Sharypova, O. Holst, K. Niehaus and V. Poinsot (2005). *Sinorhizobium melliloti* strain 1021 produces a low-molecular-mass capsular polysaccharide that is a homopolymer of 3-deoxy-D-manno-oct-2-ulosonic acid harboring a phospohlipid anchor. *Glycobiology* 15(1): 101-108.

Freiberger, F., H. Claus, A. Günzel, I. Oltmann-Norden, J. Vionnet, M. Mühlenhoff, U. Vogel, W. F. Vann, R. Gerardy-Schahn and K. Stummeyer (2007). Biochemical characterization of a *Neisseria meningitidis* polysialyltransferase reveals novel functional motifs in bacterial sialyltransferases. *Mol Microbiol* 65(5): 1258–1275

Frick, A. G., T. D. Joseph, L. Pang, A. M. Rabe, J. W. St. Geme and D. C. Look (2000). *Haemophilus influenzae* stimulates ICAM-1 expression on respiratory epithelial cells. *J Immun* 164(8): 4185-4196.

Fritz, T. A., J. H. Hurley, L.-B. Trinh, J. Shiloach and L. A. Tabak (2004). The beginnings of mucin biosynthesis: The crystal structure of UDP-GalNAc:polypeptide α-N-acetylgalactosaminyltransferase-T1. *Proc Natl Acad Sci U S A* 101(43): 15307-15312.

Furian, T., K. Borges, R. Pilatti, C. Almeida, V. d. Nascimento, C. Salle and H. d. S. Moraes (2014). Identification of the capsule type of Pasteurella multocida isolates from cases of fowl cholera by multiplex PCR and comparison with phenotypic methods. *Revista Brasileira de Ciência Avícola* 16: 31-36.

Garvy, B. A. and A. G. Harmsen (1996). The importance of neutrophils in resistance to pneumococcal pneumonia in adult and neonatal mice. *Inflammation* 20(5): 499-512.

Goldblatt, D. (2000). Conjugate vaccines. *Clin Exp Immunol* 119(1): 1-3.

Griffiths, G., N. J. Cook, E. Gottfridson, T. Lind, K. Lidholt and I. S. Roberts (1998). Characterization of the glycosyltransferase enzyme from the *Escherichia coli* K5 capsule gene cluster and identification and characterization of the glucuronyl active site. *J Biol Chem* 273(19): 11752-11757.

Hamilton, H. L., K. J. Schwartz and J. P. Dillard (2001). Insertion-duplication mutagenesis of *Neisseria*: Use in characterization of DNA transfer genes in the gonococcal genetic island. *J Bacteriol* 183(16): 4718-4726.

Harrison, L. H., C. L. Trotter and M. E. Ramsay (2009). Global epidemiology of meningococcal disease. *Vaccine* 27, Supplement 2: B51-B63.

Harrison, O. B., H. Claus, Y. Jiang, J. S. Bennett, H. B. Bratcher, K. A. Jolley, C. Corton, R. Care, J. T. Poolman, W. D. Zollinger, C. E. Frasch, D. S. Stephens, I. Feavers, M. Frosch, J. Parkhill, U. Vogel, M. A. Quail, S. D. Bentley and M. C. J. Maiden (2013). Description and nomenclature of *Neisseria meningitidis* capsule locus. *Emerg Infect Dis* 19(4): 566.

Heiss, C., J. S. Klutts, Z. Wang, T. L. Doering and P. Azadi (2009). The structure of *Cryptococcus neoformans* galactoxylomannan contains beta-D-glucuronic acid. *Carbohyd. Res.* 344: 915-920.

Hendrixson, D., B. Akerley and V. DiRita (2001). Transposon mutagenesis of *Campylobacter jejuni* identifies a bipartite energy taxis system required for motility. *Mol Microbiol* 40(1): 214-224.

Henriksen, S. D. and K. Bovre (1968). *Moraxella kingii* sp.nov., a haemolytic, saccharolytic species of the genus *Moraxella*. *J Gen Microbiol* 51(3): 377-385.

Henriksen, S. D. and K. Bovre (1976). Transfer of *Moraxella-kingae Kingella*-Henriksen and Bovre to Genus Gen-Nov in Family Neisseriaceae. *Int J Syst Bacteriol* 26(4): 447-450.

Jacobs, M. R., R. Dagan, P. C. Appelbaum and D. J. Burch (1998). Prevalence of antimicrobial-resistant pathogens in middle ear fluid: multinational study of 917 children with acute otitis media. *Antimicrob Agents Chemother* 42(3): 589-595.

Jann, B., R. Ahrens, T. Dengler and K. Jann (1988). Structure of the capsular polysaccharide (K19 antigen) from uropathogenic *Escherichia coli* 025:K19: H12. *Carbohydr Res* 177: 273-277.

Jann, B., P. Hofmann and K. Jann (1983). Structure of the 3-deoxy-d-manno-octulosonic acid-(KDO)- containing capsular polysaccharide (K14 antigen) from *Escherichia coli* 06:K14:H31. *Carbohyd. Res.* 120: 131-141.

Jann, K. and B. Jann (1983). The K antigens of *Escherichia coli*. *Prog Allergy* 33: 53-79.

Jeyaseelan, S., S. K. Young, M. Yamamoto, P. G. Arndt, S. Akira, J. K. Kolls and G. S. Worthen (2006). Toll/IL-1R domain-containing adaptor protein (TIRAP) is a critical mediator of antibacterial defense in the lung against *Klebsiella pneumoniae* but not *Pseudomonas aeruginosa*. *J Immunol* 177(1): 538-547.

Kalin, M. (1998). Pneumococcal serotypes and their clinical relevance. *Thorax* 53: 159-162.

Kehl-Fie, T. E., S. E. Miller and J. W. St. Geme III (2008). *Kingella kingae* expresses type IV pili that mediate adherence to respiratory epithelial and synovial cells. *J. Bacteriol.* 190(21): 7157-7163.

Kehl-Fie, T. E., E. A. Porsch, S. E. Miller and J. W. St Geme III (2009). Expression of *Kingella kingae* type IV pili is regulated by sigma 54, PilS, and PilR. *J. Bacteriol.* 191(15): 4976-4986.

Kehl-Fie, T. E., E. A. Porsch, P. Yagupsky, E. A. Grass, C. Obert, D. K. B. Jr. and J. W. St. Geme III (2010). Examination of type IV pilus expression and pilus-associated phenotypes in *Kingella kingae* clinical isolates. *Infect Immun* 78(4): 1692-1699.

Kehl-Fie, T. E. and J. W. St Geme, 3rd (2007). Identification and characterization of an RTX toxin in the emerging pathogen *Kingella kingae*. *J Bacteriol* 189(2): 430-436.

Kelley, L. A., S. Mezulis, C. M. Yates, M. N. Wass and M. J. E. Sternberg (2015). The Phyre2 web portal for protein modeling, prediction and analysis. *Nat. Protocols* 10(6): 845-858.

Kelly, D. F., E. R. Moxon and A. J. Pollard (2004). Haemophilus influenzae type b conjugate vaccines. *Immunology* 113(2): 163-174.

Kiang, K. M., F. Ogunmodede, B. A. Juni, D. J. Boxrud, A. Glennen, J. M. Bartkus, E. A. Cebelinski, K. Harriman, S. Koop, R. Faville, R. Danila and R. Lynfield (2005). Outbreak of osteomyelitis/septic arthritis caused by *Kingella kingae* among child care center attendees. *Pediatrics* 116(2): e206-213.

Kim, J., B. Reuhs, M. M. Rahman, B. Ridley and R. Carlson (1996). Separation of bacterial capsular and lipopolysaccharides by preparative electrophoresis. *Glycobiology* 6(4): 433-437.

Koh, A. Y., G. P. Priebe and G. B. Pier (2005). Virulence of *Pseudomonas aeruginosa* in a murine model of gastrointestinal colonization and dissemination in neutropenia. *Infect Immun* 73(4): 2262-2272.

Kumar, A. S., K. Mody and B. Jha (2007). Bacterial exopolysaccharides – a perception. *J. Basic Microb.* 47(2): 103-117.

Lenter, M., B. Jann and K. Jann (1990). Structure of the K16 antigen from Escherichia coli O7:K16:H-, a Kdo-containing capsular polysaccharide. *Carbohydrate research* 197: 197-204.

Lexau, C. A., R. Lynfield, R. Danila and et al. (2005). CHanging epidemiology of invasive pneumococcal disease among older adults in the era of pediatric pneumococcal conjugate vaccine. *JAMA* 294(16): 2043-2051.

Li, J. and N. Wang (2012). The *gpsX* gene encoding a glycosyltransferase is important for polysaccharide production and required for full virulence in *Xanthomonas citri* subsp. *citri*. *BMC Microbiol* 12(31).

Llull, D., E. Garcia and R. Lopez (2001). Tts, a processive beta-glucosyltransferase of Streptococcus pneumoniae, directs the synthesis of the branched type 37 capsular polysaccharide in Pneumococcus and other gram-positive species. J Biol Chem. United States. 276**:** 21053-21061.

M E Bayer, E. C., and E Kellenberger (1985). Capsule of *Escherichia coli* K29: ultrastructural preservation and immunoelectron microscopy. *J Bacteriol.* 162(3): 985–991.

MacLean, L. L., E. Vinogradov, F. Pagotto, J. M. Farber and M. B. Perry (2009). Characterization of the O-antigen in the lipopolysaccharide of Cronobacter (Enterobacter) malonaticus 3267. *Biochem Cell Biol* 87(6): 927-932.

Maiden, M. C. J. (2013). The impact of protein-conjugate polysaccharide vaccines: an endgame for meningitis? *Philos Trans R Soc Lond B Biol Sci* 368(1623).

Maue, A. C., K. L. Mohawk, D. K. Giles, F. Poly, C. P. Ewing, Y. Jiao, G. Lee, Z. Ma, M. A. Monteiro, C. L. Hill, J. S. Ferderber, C. K. Porter, M. S. Trent and P. Guerry (2013). The Polysaccharide Capsule of Campylobacter jejuni Modulates the Host Immune Response. *Infection and Immunity* 81(3): 665-672.

Merino, S. and J. M. Tomás (2001). Bacterial Capsules and Evasion of Immune Responses. eLS, John Wiley & Sons, Ltd.

Mishra, M., M. S. Byrd, S. Sergeant, A. K. Azad, M. R. Parsek, L. McPhail, L. S. Schlesinger and D. J. Wozniak (2012). *Pseudomonas aeruginosa* Psl polysaccharide reduces neutrophil phagocytosis and the oxidative response by limiting complement-mediated opsonization. *Cell microbiol* 14(1): 95-106.

Morrison, V. A. and K. F. Wagner (1989). Clinical manifestations of *Kingella kingae* infections: Case report and review. *Rev Infect Dis* 11(5): 776-782.

Naumann, M., S. Weßler, C. Bartsch, B. Wieland and T. F. Meyer (1997). *Neisseria gonorrhoeae* epithelial cell interaction leads to the activation of the transcription factors nuclear factor κB and activator protein 1 and the induction of inflammatory cytokines. *J ExpMed* 186(2): 247-258.

Nizet, V. and J. Esko (2009). Bacterial and Viral Infections. Essentials of Glycobiology. A. Varki, R. Cummings and J. Esko. Cold Spring Harbor (NY), Cold Spring Harbor Laboratory Press.

Nwodo, U. U., E. Green and A. I. Okoh (2012). Bacterial Exopolysaccharides: Functionality and Prospects. *Int J Mol Sci* 13(11): 14002-14015.

Orskov, I. F., F. B. Orskov, B. Jann and K. Jann (1977). Serology, chemistry, and genetics of O and K antigens of *Escherichia coli*. *Bacteriol. Rev.* 41: 667-710.

Pan, Y.-J., T.-L. Lin, Y.-H. Chen, C.-R. Hsu, P.-F. Hsieh, M.-C. Wu and J.-T. Wang (2013). Capsular types of *Klebsiella pneumoniae* revisited by wzc sequencing. *PLOS ONE* 8(12).

Peltola, H. (1983). Meningococcal disease: Still with us. *Review of Infectious Diseases* 5(1): 71-91.

Perry, M., E. Altman, J.-R. Brisson, L. Beynon and J. Richards (1990). Structural characteristics of the antigenic capsular polysaccharides and lipopolysaccharides involved in the serological classification of *Actinobacillus* (*Haemophilus*) *pleuromoniae* strains. *Serodiag. Immun. Inf. D.* 4(4): 299-308.

Porsch, E., T. Kehl-Fie and J. W. St. Geme III (2012). Modulation of *Kingella kingae* adherence to human epithelial cells by type IV pili, capsule, and a novel trimeric autotransporter. *mBio* 3: e00372-00312.

Radke, K. L. and E. C. Siegel (1971). Mutation preventing capsular polysaccharide synthesis in *Escherichia coli* K-12 and its effect on bacteriophage resistance. *J Bacteriol* 106(2): 432-437.

Reistad, R., U. Zähringer, K. Bryn, J. Alstad, K. Bøvre and E. Jantzen (1993). A polysaccharide produced by a mucoid strain of *Moraxella nonliquefaciens* with a 2-acetamido-2-deoxy-5-O-(3-deoxy-beta-D-manno-octulopyranosyl)-beta-D-galactopyranosyl repeating unit. *Carbohyd. Res.* 245(1): 129-136.

Riser, E. and P. Noone (1981). *Klebsiella* capsular type versus site of isolation. *J Clin Path* 34: 552-555.

Roberts, I. S. (1996). The biochemistry and genetics of capsular polysaccharide production in bacteria. *Annu. Rev. Microbiol.* 50: 285-315.

Roberts, I. S. (1996). The biochemistry and genetics of capsular polysaccharide production in bacteria. *Annu Rev Microbiol* 50(1): 285-315.

Rose, A., E. Kay, B. Wren and M. Dallman (2011). The Campylobacter jejuni NCTC11168 capsule prevents excessive cytokine production by dendritic cells. *Med Microbiol Immun*.

Sambrook, J., E. F. Fritsch and T. Maniatis (1989). Molecular cloning: a laboratory manual. Cold Spring Harbor, NY, Cold Spring Harbor Laboratory Press.

Schmidt, H., G. Hansen, S. Singh, A. Hanuszkiewicz, B. Lindner, K. Fukase, R. W. Woodard, O. Holst, R. Hilgenfeld, U. Mamat and J. R. Mesters (2012). Structural and

mechanistic analysis of the membrane-embedded glycosyltransferase WaaA required for lipopolysaccharide synthesis. *Proc Natl Acad Sci U S A* 109(16): 6253-6258.

Schuchat, A., K. Robinson, J. D. Wenger, L. H. Harrison, M. Farley, A. L. Reingold, L. Lefkowitz and B. A. Perkins (1997). Bacterial Meningitis in the United States in 1995. *New England Journal of Medicine* 337(14): 970-976.

Siegrist, C.-A. (2008). Vaccine Immunology. New York, Saunders Elsevier.

Slonim, A., M. Steiner and P. Yagupsky (2003). Immune response to invasive *Kingella kingae* infections, age-related incidence of disease, and levels of antibody to outer-membrane proteins. *Clin Infect Dis* 37: 521-527.

Slonim, A., E. S. Walker, E. Mishori, N. Porat, R. Dagan and P. Yagupsky (1998). Person-to-person transmission of *Kingella kingae* among day care center attendees. *J. Infect. Dis.* 178(6): 1843-1846.

Smith, A. B. and R. J. Siebeling (2003). Identification of genetic loci required for capsular expression in *Vibrio vulnificus*. *Infect Immun* 73(1): 1091-1097.

Smyth, K. M. and A. Marchant (2013). Conservation of the 2-keto-3-deoxymanno-octulosonic acid (Kdo) biosynthesis pathway between plants and bacteria. *Carbohydr Res* 380: 70-75.

Stahelin, J., D. Goldenberger, H. E. Gnehm and M. Altwegg (1998). Polymerase chain reaction diagnosis of *Kingella kingae* arthritis in a young child. *Clin Infect Dis* 27(5): 1328-1329.

Starr, K. F., E. A. Porsch, C. Heiss, I. Black, P. Azadi and J. W. St. Geme, III (2013). Characterization of the *Kingella kingae* polysaccharide capsule and exopolysaccharide. *PLoS ONE* 8(9): e75409.

Steenbergen, S. M. and E. R. Vimr (2008). Biosynthesis of the *Escherichia coli* K1 group 2 polysialic acid capsule occurs within a protected cytoplasmic compartment. *Mol Microbiol* 68(5): 1252-1267.

Straus, D. C., M. K. Lonon, D. E. Woods and C. W. Garner (1990). 3-deoxy-D-manno-2-octulosonic acid in the lipopolysaccharide of various strains of *Pseudomonas cepacia*. *J Med Microbiol* 33(4): 265-269.

Strom, M. and S. Lory (1993). Structure-function and biogenesis of the type IV pili. *Annu. Rev. Microbiol.* 47: 565-595.

Studier, F. and B. Moffatt (1986). Use of bacteriophage T7 RNA polymerase to direct selective high-level expression of cloned genes. *J Mol Biol* 189(1): 113-130.

Swartley, J. S., A. A. Marfin, S. Edupuganti, L. J. Liu, P. Cieslak, B. Perkins, J. D. Wenger and D. S. Stephens (1997). Capsule switching of Neisseria meningitidis. *Microbiology* 94(1): 271-276.

Tønjum, T., C. F. Marrs, F. Rozsa and K. Bøvre (1991). The type 4 pilin of Moraxella nonliquefaciens exhibits unique similarities with the pilins of Neisseria gonorrhoeae and Dichelobacter (Bacteroides) nodosus. *Microbiology* 137(10): 2483-2490.

Turk, D. C. (1984). The pathogenicity of *Haemophilus influenzae*. *J Med Microbiol* 18(1): 1-16.

Tzeng, Y., A. Datta, C. Strole, M. Lobritz, R. Carlson and D. Stephens (2005). Translocation and surface expression of lipidated serogroup B capsular polysaccharide in *Neisseria meningitidis*. *Infect Immun* 73(3): 1491-1505.

Virji, M. (2009). Pathogenic neisseriae: Surface modulation, pathogenesis and infection control. *Nat. Rev. Microbiol.* 7: 274-286.

Warren, L. (1959). The thiobarbituric acid assay of sialic acids. *J Biol Chem* 234(8): 1971-1975.

Weinberger, D., Z. Harboe, E. Sanders, M. Ndiritu, K. Klugman, S. Rückinger, R. Dagan, R. Adegbola, F. Cutts, H. Johnson, K. O'Brien, J. Scott and M. Lipsitch (2010). Association of serotype with risk of death due to pneumococcal pneumonia: a meta-analysis. *Clin. Infect. Dis.* 51(6): 692-699.

Weinberger, D. M., K. Trzciński, Y.-J. Lu, D. Bogaert, A. Brandes, J. Galagan, P. W. Anderson, R. Malley and M. Lipsitch (2009). Pneumococcal capsular polysaccharide structure predicts serotype prevalence. *PLOS Pathog* 5(6).

Weiss-Salz, I. and P. Yagupsky (2011). *Kingella kingae* Infections in Children: An Update. *Adv. Exp. Med. Biol.* 719: 67-80.

Whitfield, C. (2006). Biosynthesis and assembly of capsular polysaccharides in *Escherichia coli*. *Annu Rev Biochem* 75: 39-68.

Whitfield, C., P. A. Amor and R. Koplin (1997). Modulation of the surface architecture of Gram-negative bacteria by the action of surface polymer: lipid A–core ligase and by determinants of polymer chain length. *Mol Microbiol* 23(4): 629-638.

Whitfield, C. and I. S. Roberts (1999). Structure, assembly and regulation of expression of capsules in *Escherichia coli*. *Mol Microbiol* 31(5): 1307-1319.

Willis, L. M. and C. Whitfield (2013). KpsC and KpsS are retaining 3-deoxy-d-manno-oct-2-ulosonic acid (Kdo) transferases involved in synthesis of bacterial capsules. *PNAS* 110(51): 20753–20758.

Wilson, R. P., S. E. Winter, A. M. Spees, M. G. Winter, J. H. Nishimori, J. F. Sanchez, S.-P. Nuccio, R. W. Crawford, Ç. Tükel and A. J. Bäumler (2011). The Vi capsular polysaccharide prevents complement receptor 3-mediated clearance of *Salmonella enterica* serotype typhi. *Infect Immun* 79(2): 830-837.

Wishart, D. S., C. G. Bigam, J. Yao, F. Abildgaard, H. J. Dyson, E. Oldfield, J. L. Markley and B. D. Sykes (1995). ^{1}H, ^{13}C, and ^{15}N chemical shift referencing in biomolecular NMR. *J. Biomol. NMR* 6: 135-140.

Wyres, K. L., L. M. Lambertsen, N. J. Croucher, L. McGee, A. von Gottberg, J. Liñares, M. R. Jacobs, K. G. Kristinsson, B. W. Beall, K. P. Klugman, J. Parkhill, R. Hakenbeck, S. D. Bentley and A. B. Brueggemann (2013). Pneumococcal capsular switching: A historical perspective. *J Infect Dis* 207(3): 439-449.

Yagupsky, P. (1999). Diagnosis of *Kingella kingae* arthritis by polymerase chain reaction analysis. *Clin Infect Dis* 29(3): 704-705.

Yagupsky, P. (2004). *Kingella kingae*: from medical rarity to an emerging paediatric pathogen. *Lancet Infect Dis* 4(6): 358-367.

Yagupsky, P. (2014). Outbreaks of *Kingella kingae* infections in daycare facilities. *Emerg Infect Dis* 20(5): 746-753.

Yagupsky, P. (2015). *Kingella kingae*: Carriage, transmission, and disease. *Clin Microbiol Rev* 28(1): 54-79.

Yagupsky, P., R. Dagan, C. W. Howard, M. Einhorn, I. Kassis and A. Simu (1992). High prevalence of *Kingella kingae* in joint fluid from children with septic arthritis revealed by the BACTEC blood culture system. *J. Clin. Microbiol.* 30(5): 1278-1281.

Yagupsky, P., R. Dagan, F. Prajgrod and M. Merires (1995). Respiratory carriage of *Kingella kingae* among healthy children. *Pediatr Infect Dis J* 14(8): 673-678.

Yagupsky, P., Y. Erlich, S. Ariela, R. Trefler and N. Porat (2006). Outbreak of *Kingella kingae* skeletal system infections in children in daycare. *Pediatr Infect Dis J* 25(6): 526-532.

Yagupsky, P., M. Merires, J. Bahar and R. Dagan (1995). Evaluation of novel vancomycin-containing medium for primary isolation of *Kingella kingae* from upper respiratory tract specimens. *J Clin Microbiol* 33(5): 1426-1427.

Yagupsky, P., N. Peled and O. Katz (2002). Epidemiological features of invasive *Kingella kingae* infections and respiratory carriage of the organism. *J Clin Microbiol* 40(11): 4180-4184.

Yagupsky, P., N. Porat and E. Pinco (2009). Pharyngeal colonization by *Kingella kingae* in children with invasive disease. *Pediatr Infect Dis J* 28(2): 155-157.

Yagupsky, P., E. Porsch and J. W. St Geme III (2011). *Kingella kingae*: An emerging pathogen in young children. *Pediatrics* 127(3): 557-565.

Yagupsky, P. and A. Slonim (2005). Characterization and immunogenecity of *Kingella kingae* outer-membrane proteins. *FEMS Immunol Med Mirobiol* 43: 45-50.

Yagupsky, P., I. Weiss-Salz, R. Fluss, L. Freedman, N. Peled, R. Trefler, N. Porat and R. Dagan (2009). Dissemination of *Kingella kingae* in the community and long-term persistence of invasive clones. *Pediatr Infect Dis J* 28(8): 707-710.

Yamamoto, S., K. Miyake, Y. Koike, M. Watanabe, Y. Machida, M. Ohta and S. Iijima (1999). Molecular Characterization of Type-Specific Capsular Polysaccharide Biosynthesis Genes of *Streptococcus agalactiae* Type Ia. *J Bacteriol* 181(17): 5176-5184.

Yazdankhah, S. P. and D. A. Caugant (2004). *Neisseria meningitidis*: an overview of the carriage state. *J Med Microbiol* 53: 821-832.

Yi, H., D. Yong, K. Lee, Y.-J. Cho and J. Chun (2014). Profiling bacterial community in upper respiratory tracts. *BMC Infect Dis* 14: 583.

Zola, T. A., E. S. Lysenko and J. N. Weiser (2009). Natural antibody to conserved targets of *Haemophilus influenzae* limits colonization of the murine nasopharynx. *Infect Immun* 77(8): 3458-3465.

Zughaier, S. M. (2011). Neisseria meningitidis capsular polysaccharides induce inflammatory responses via TLR2 and TLR4-MD-2. *Journal of Leukocyte Biology* 89(3): 469-480.

Biography

Kimberly Freeland Starr was born on October 13, 1985 in Jacksonville, Florida. She attended Auburn University where she graduated cum laude with a B.S. in Microbiology in 2007 and a M.S. in 2010. She moved to Durham, NC following acceptance to Duke University in the department of Molecular Genetics and Microbiology. During her Graduate studies of *K. kingae* she also took the opportunity outside of lab to obtain her Certificate in College Teaching and gain experience as an instructor. She was fortunate to be able to present her work at a national ID Week conference through the Duke Scholars in Infectious Disease Program.

Publications including peer-reviewed works in progress

Starr KF, Porsch EA, Seed P, St. Geme III JW. Genetic and molecular basis of *Kingella kingae* encapsulation. Accepted to Infect Immun.

Starr KF, Porsch EA, Heiss C, Black I, Azadi P, St Geme JW 3rd. Characterization of the *Kingella kingae* polysaccharide capsule and exopolysaccharide. PLoS One. 2013 Sep 30;8(9):e75409. doi: 10.1371/journal.pone.0075409. eCollection 2013.

Porsch E, **Starr KF**, St. Geme III JW. *Kingella kingae.* Feigin and Cherry Textbook of Pediatric Infectious Diseases, 7th Edition. (Eds: Cherry JD, Harrison GJ, Kaplan SL, Steinbach WJ, Hotez P). 2014, Elsevier, Philadelphia, PA.